THERMODYNAMICS OF 3+ METAL CATION CONTAINING SYSTEMS

Michael James Lukacs

B.Sc., University of Lethbridge, 2001

A Thesis
Submitted to the School of Graduate Studies
of the University of Lethbridge
in Partial Fulfilment of the
Requirements for the Degree

MASTER OF SCIENCE

Department of Chemistry and Biochemistry
University of Lethbridge
LETHBRIDGE, ALBERTA, CANADA

June, 2003

ABSTRACT

Measurements of relative densities and relative massic heat capacities have been made for several aqueous rare earth chloride and perchlorate systems.

Densities and relative massic heat capacities of acidified aqueous perchlorates of yttrium, ytterbium, dysprosium, and samarium as well as the chlorides of yttrium, ytterbium, dysprosium, samarium and gadolinium have been measured at the temperatures 288.15, 298.15, 313.15 and 328.15 K. Using the density and massic heat capacity data, apparent molar volumes and apparent molar heat capacities have been calculated. These data have been modeled using the Pitzer ion interaction approach as well as the Helgeson, Kirkham and Flowers equations of state. Apparent molar volumes and apparent molar heat capacities previously presented in the literature have been compared to the data presented here. Single ion apparent molar volume and apparent molar heat capacity contributions were calculated. Infinite dilution properties have been compared to existing models used to predict infinite dilution properties.

Densities of aqueous perchloric acid and ytterbium perchlorate at the temperatures from 348.15 to 423.15 K and at pressures from 10.00 to 30.00 MPa were measured. Apparent molar volumes were calculated from the density measurements. The apparent molar volume data were modeled using Pitzer ion interaction theory as well as HKF equations of state. Models presented are compared to existing models.

ACKNOWLEDGEMENTS

I would like to thank my family, Trina and Emily. You provided me with the encouragement I needed to do this (but not always a quiet place to work). I would also like to thank my parents, Bob and Sharon for putting up with my 19 straight years of school. Thanks to Kendall, Moriah, Keenan and Matt for providing a place to get away to so often. Thank you Rob for telling me that anything is worth trying once. Thanks to Todd for, well...

I would like to thank my supervisor, Dr. Andrew Hakin for putting up with all of my repeat questions and constantly missing reference articles.

I would also like to thank Jin Lian Liu for all of her work that contributed to the completion of this work, mostly in the form of long hours spent with the Picker microcalorimeter and also for her constant worries that I wasn't eating enough.

I have much gratitude to Arlene Nelson for all the help she gave me. You really are a life saver.

TABLE OF CONTENTS

List of Figures

List of Tables

1 INTRODUCTION

1.1 The importance of trivalent metals

The rare earth elements, or lanthanides, have many industrial and scientific uses. For example they are used to make magnets which exhibit unusually strong magnetic fields because of the number of unpaired electrons contained in the partially filled 4f atomic orbitals of the lanthanides. To create permanent magnets at room temperature, rare earth metals must be alloyed with other metals, for example iron, to strengthen the atomic interactions, which are relatively weak in lanthanide metals (Sabot and Maestro,1995).

The magnetic properties of certain lanthanides may also be used in the technique of nuclear magnetic resonance (NMR) spectroscopy to broaden the NMR signals of organic molecules to which they are coordinated (Sabot and Maestro, 1995).

Certain lanthanide compounds also have very strong luminescent and phosphorescent properties. The light emission from lanthanide complexes is characterized by narrow band emissions. Discrete emission bands result in distinct observed colours, making lanthanide complexes ideal as phosphors in the construction of cathode ray tubes (Sabot and Maestro, 1995) and fibre optic applications (Kawa and Frechet, 1998).

In nuclear chemistry research, aqueous solutions of trivalent lanthanide salts are often used as surrogates for the more radioactive actinide salts. Thermodynamic experimentation on aqueous actinide salt solutions is often made impossible, or undesirable, by the danger of radiation exposure, while experimentation on aqueous lanthanide-containing solutions is relatively harmless. Additionally, the predominant ionic state for lanthanides is 3+ while actinides form a mixture of valence states making

measurement of the trivalent property difficult. The results from thermodynamic studies of mixed valence states would result in an average property of the mixture.

Waste produced by high-level liquid nuclear reactors contains a large number of highly radioactive lanthanide isotopes, such as ^{144}Ce, ^{144}Pr, ^{91}Y, ^{141}Ce ^{147}Pr and ^{134}Ce (Marriott, 2001). Proper separation and extraction requires knowledge of the solubility of these dangerous isotopes and their complexes. Thermodynamic and volumetric data can be used to provide this information.

Lanthanides are most often extracted from the minerals monazite ($(Ce,La)PO_4(cr)$), bastnasite ($(Ce,La)(CO_3)F(cr)$), loparite ($(Ce,Na,Ca)(Ti,Nb)O_3(cr)$, and xenotime ($YPO_4(cr)$) (Sabot and Maestro, 1995). Rare earth elements (REEs) are also abundant in the ionic clays of the Chinese provinces of Jiangxi, Nei Mongol and Sichuan. The chemical formulae supplied above only represent the most abundant lanthanides found in each mineral. Due to the similar chemical behaviour along the series, all naturally occurring lanthanides tend to be found together. The ionic clays are the rare earth rich remains of rare earth mineral formations which have been exposed to prolonged erosion and weathering. In most instances, the lighter rare earths are predominant, with the heavier rare earths being found in greater quantities in xenotime and the ionic clays. Separation of individual rare earths is difficult due to the similarity of each rare earth to its neighbours in the periodic table. Separation is thus usually accomplished through repeated fractionation although recently, separation has been achieved through chromatography (Nesterenko and Jones, 1997). Once again, to achieve efficient separation, solubility and thermodynamic data are required.

1.2 Thermochemical investigations of the rare earth chlorides and perchlorates

The wide variety of uses and applications of rare earth compounds illustrates the importance of and need for precise thermochemical data for rare earth species. Extraction and separation of individual lanthanides, the recovery of radioactive isotopes of the lanthanides from nuclear waste, and geochemical modeling all require high quality thermodynamic data over a range of temperature and pressure conditions.

The majority of volumetric and thermochemical studies of REE-containing aqueous solutions have been restricted to p = 0.1 MPa and T = 298.15 K, the only exceptions being the temperature dependent density and heat capacity determinations performed by Xaio and Tremaine (1996, 1997) and the temperature dependent volumetric study of Spedding and coworkers (Gildseth, 1975; Habenschuss, 1976; Spedding, 1975a, 1975b, 1975c, 1966a and 1966b). Predictions of thermochemical and volumetric properties of trivalent metal cation-containing aqueous solutions at elevated temperatures and pressures have been reported by Shock and Helgeson (1988) who used the semi-empirical Helgeson, Kirkham and Flowers (HKF) equations of state to model available partial molar volumes and heat capacities at infinite dilution.

The work presented in this thesis attempts to provide some of the experimental data missing within the literature for aqueous trivalent cation containing solutions. The thesis takes the following form:

Chapter 2 describes the instrumentation and techniques used to acquire thermochemical and volumetric data reported in Chapters 4, 5 and 6. Also covered is the method of standardization for each aqueous rare earth salt solution.

Chapter 3 reports the models that were constructed using experimental data and describes the theoretical basis and development of each model explored within this thesis. In particular, the analyses presented in this thesis focus on modified Pitzer ion interaction equations and the equations developed by Helgeson, Kirkham and Flowers.

Chapter 4 reports apparent molar volumes and heat capacities for aqueous solutions of $Y(ClO_4)_3$, $Yb(ClO_4)_3$, $Dy(ClO_4)_3$ and $Sm(ClO_4)_3$ at p = 0.1MPa and T = (288.15, 298.15, 313.15 and 328.15) K. This chapter also provides a comparison of these data with those previously reported in the literature. Also presented are models of the temperature and composition surfaces of the apparent molar properties created using modified Pitzer ion interaction equations.

Chapter 5 reports apparent molar volumes and heat capacities for aqueous solutions of YCl_3, $YbCl_3$, $DyCl_3$, $SmCl_3$ and $GdCl_3$ at p = 0.1MPa and at temperatures T = (288.15, 298.15, 313.15 and 328.15) K. As with the perchlorates, modified Pitzer ion interaction equations were used to model the reported apparent molar data over extended temperature and composition ranges. All data as well as constructed models are compared with existing literature values.

The final chapter of this thesis, Chapter 6, reports densities and apparent molar volumes for aqueous ytterbium perchlorate solutions at p = (10, 20 and 30) MPa and T = (348.15, 373.15, 398.15 and 423.15) K. Because these measurements were made in solutions containing an excess of perchloric acid, densities and apparent molar volumes are also reported in this chapter for aqueous perchloric acid solutions over an extended temperature and pressure range. The volumetric properties of these systems have been

modeled and apparent molar volumes at infinite dilution have been compared to those which can be estimated using previously reported HKF equations of state.

2 METHODS OF DENSITY AND HEAT CAPACITY COLLECTION

2.1 Heat capacity measurements

2.1.1 The Picker flow microcalorimeter

The Picker Flow Microcalorimeter is used to measure the massic heat capacity of a liquid relative to the massic heat capacity of a reference liquid.

Two solutions will be referred to in this discussion of the instrument: a reference liquid, referred to as A, and the liquid undergoing investigation, referred to as B. In the experiments described in this thesis liquid A is pure water.

Figure 2.1 illustrates the inner workings of the Picker Flow Microcalorimeter. The Picker Flow Microcalorimeter contains two identical cells which are connected in series by a delay loop. The flow rate of liquid through each cell is identical. The cells are isolated within an evacuated chamber which is thermostatted to an initial temperature (T_i). Temperature regulation is provided by a Techneurop Programmable Circulating Thermostat that is capable of maintaining temperature to +/- 0.001K. Each cell is constructed from a length of stainless steel tubing (i.d. 0.020") to which a zener diode is attached. The zener diode serves as a precision heater that is capable of supplying precise amounts of thermal energy to the liquid in the cell. Downstream from the diode is a thermistor that registers any temperature change of the liquid in the cell with a corresponding change in resistance. In this way the thermistor serves as a precise temperature probe. Increased thermal transfer between the liquid within the cell and the heater and thermistor is achieved by flattening the stainless steel tubing at the points of attachment.

Figure 2.1 Diagram of internal workings of the Picker flow microcalorimeter.

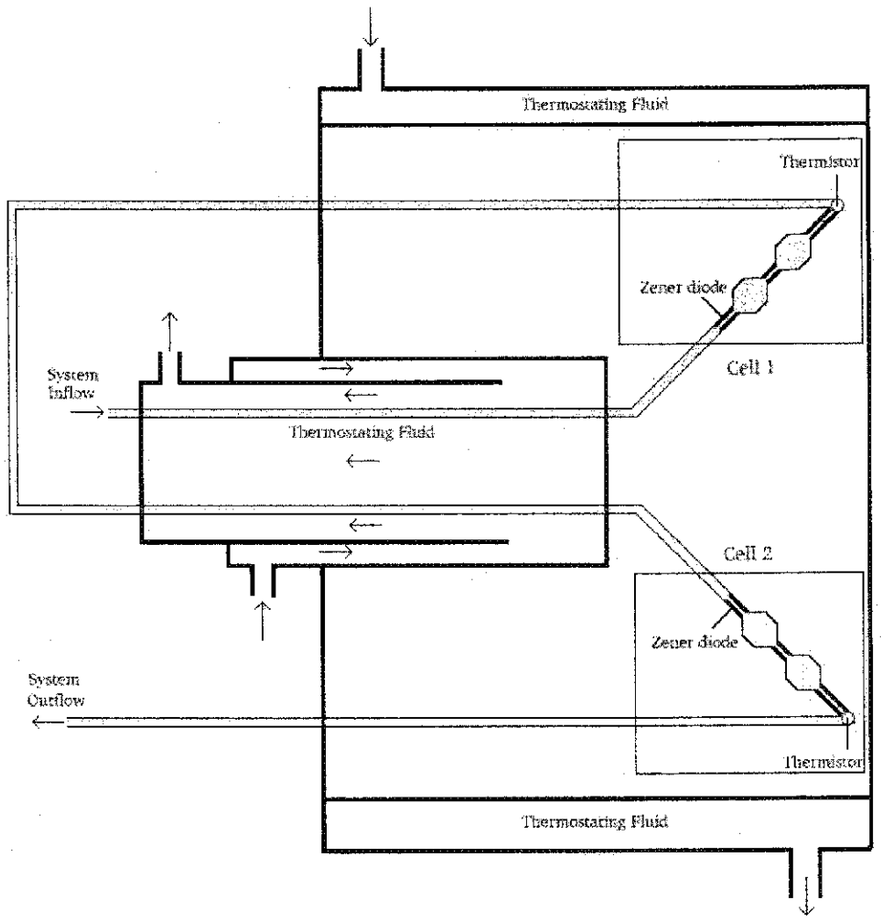

The basic operation of the calorimeter is as follows: a liquid thermostatted to temperature T_i enters cell 1, passes the zener diode and is heated to achieve a temperature increase, ΔT. The liquid then continues past the heater and the liquid's final temperature, T_f ,($\Delta T = T_f - T_i$) is measured using the thermistor. The same ΔT in each of the calorimeter's cells is maintained using a feedback circuit. As the resistance of a thermistor changes, the feedback circuit adjusts the voltage applied to the corresponding zener diode. The resulting input of thermal energy is automatically adjusted to achieve the desired T_f. The difference in voltage applied to the zener diodes is the signal from which all massic heat capacity values are calculated. Voltage differences are recorded as a function of time by an IBM compatible PC which utilizes an "in-house" data collection and storage program.

A single cell flow calorimeter can be constructed to yield absolute volumetric heat capacities the values of which depend on flow rate. The Picker Flow Microcalorimeter can be thought of as two single celled instruments connected in series. This arrangement is suited for the measurement of volumetric heat capacity ratios. Equation 2.1 can be used to calculate the volumetric heat capacity of liquid B, relative to reference liquid A,

$$\frac{\Delta W_{BA}}{W_0} = \frac{\sigma_B - \sigma_A}{\sigma_A}. \qquad (2.1)$$

In this equation, ΔW_{BA} is the difference between the voltage applied to the heater attached to the cell containing liquid B and the voltage applied to the heater attached to the cell containing liquid A. W_0 is the voltage required to produce ΔT in both cells when they are

filled with liquid A. σ_A and σ_B are the volumetric heat capacities of liquids A and B respectively.

Massic heat capacities can be calculated from volumetric heat capacities using the densities of liquids A and B, ρ_A and ρ_B, and equation 2.2:

$$\frac{C_{p,B}}{C_{p,A}} = \frac{\rho_A}{\rho_B}\left(1+\frac{\Delta W_{BA}}{W_0}\right). \tag{2.2}$$

In this equation $C_{p,A}$ and $C_{p,B}$ are the massic heat capacities of liquids A and B respectively. The operation of the Picker Flow Microcalorimeter requires the introduction of different liquids with minimal interruption. This is achieved through the use of a four-way liquid chromatography valve. This valve allows switching between two different liquid reservoirs, one containing liquid A and the other containing liquid B.

Following the first measurement of the massic heat capacity of liquid B relative to liquid A, a second measurement is performed in which the roles of the two calorimeter cells are reversed. A second massic heat capacity can then be determined using the slightly altered equation:

$$\frac{C_{p,A}}{C_{p,B}} = \frac{\rho_B}{\rho_A}\left(1+\frac{\Delta W_{AB}}{W_0}\right). \tag{2.3}$$

Here the difference in power output, ΔW_{AB}, is opposite in sign to the difference in power, ΔW_{BA}, used in equation 2.2. Having two values for $C_{p,B}$, normally the average of the two

Figure 2.2 Example plot of flow rate too fast and too slow for accurate heat capacity measurements

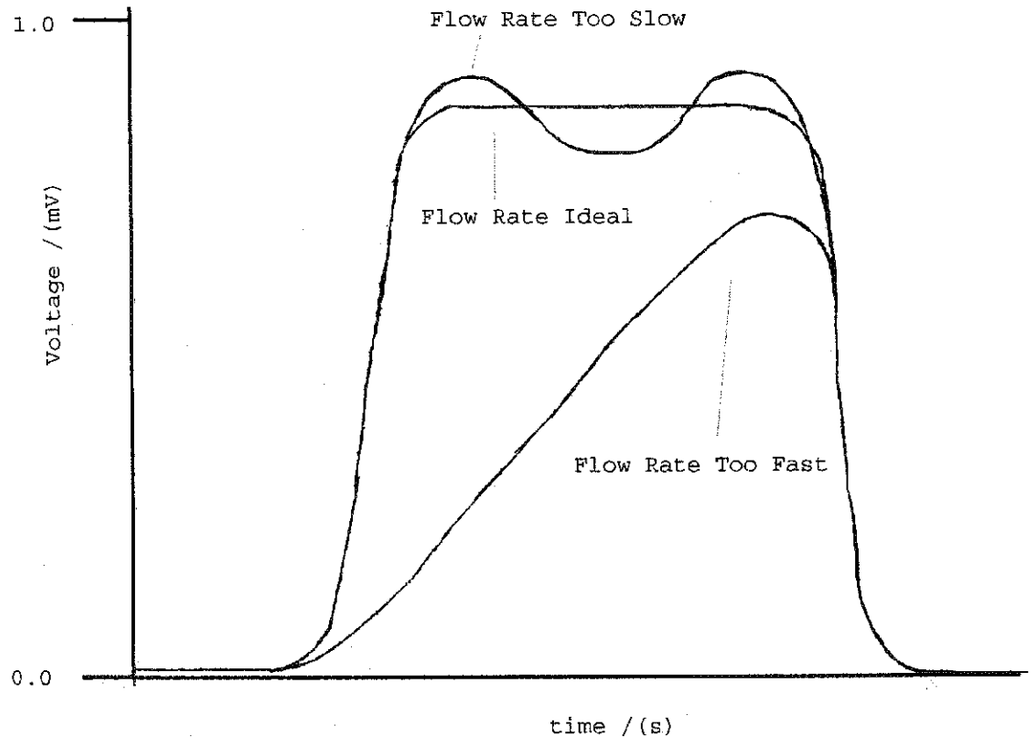

is used in further analysis. If, however, one value of $C_{p,B}$ is subject to large errors the other value of $C_{p,B}$ is normally error free and can be used in place of the average.

The initial set-up of the calorimeter is vital to its operation. For this experimental set-up the flow rate was optimized by adjusting the height of the liquid reservoirs relative to the drain flask. Initially the flow rate must be set to achieve ideal peak shape. This is accomplished by applying a known amount of power to one of the zener diodes and observing the shape of the voltage versus time profile of the resulting signal. Figure 2.2 illustrates how the flow rate affects the voltage versus time profile. Once the flow rate is optimized, ΔT can be determined by measuring the change in

Figure 2.3 Example of output from Picker flow microcalorimeter.

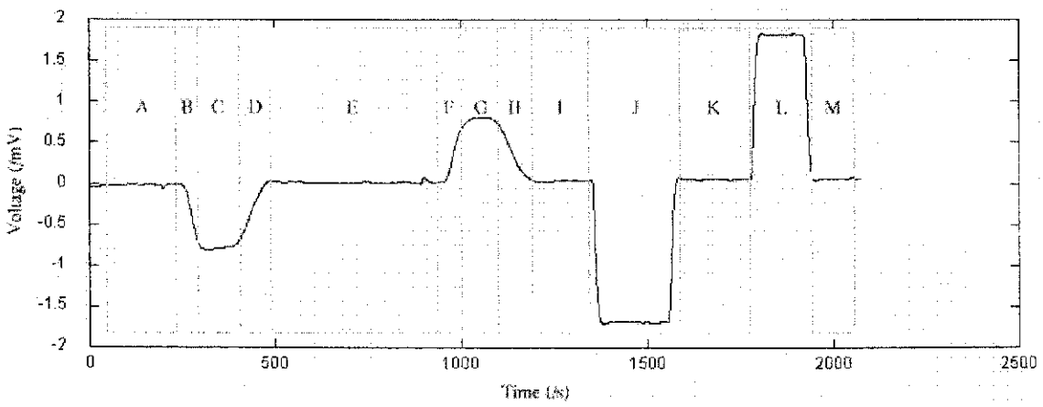

temperature due to heating from the zener diodes. The zener diodes can be supplied with one of three different base power levels, 2, 20 or 100mW. Each setting results in a different ΔT. ΔT must be known precisely so that the thermostatting system can be correctly set. To determine ΔT the thermal regulator unit is first set to the experimental temperature (T^0). The temperature of the system is then measured with no voltage applied to the zener diodes ($T^0\ W_{off}$), and again with the zener diodes energized ($T^0\ W_{on}$). The difference between $T^0\ W_{on}$ and $T^0\ W_{off}$ is the ΔT achieved at the selected base power setting. The thermal regulating unit can now be fixed at the temperature $T^0 - \Delta T/2$ for the duration of the experiment.

Figure 2.3 provides an example of experimental output, which will be referred to in the description of a hypothetical experiment that follows. Prior to any measurements being taken, the calorimeter is filled with pure, deionised, degassed water. The baseline signal in section A of figure 2.3 shows ΔW (ΔW_{AA}) when both cells are filled with liquid A. The difference in voltage applied to the two zener diodes at this point has been nulled.

The four way liquid chromatography valve is then used to introduce liquid B into the calorimeter. As liquid B flows through the calorimeter, it begins to fill cell 1. Figure 2.3, section liquid B shows that as liquid B enters the first cell, ΔW changes. With the first cell entirely filled with liquid B and the second cell filled with liquid A, the difference in power applied to both diodes, ΔW_{BA}, will plateau.

After filling the delay line, liquid B begins to fill cell 2 and the power output to the zener diode attached to cell 2 will change to maintain ΔT. When liquid B has completely filled cells 1 and 2, ΔW (ΔW_{BB}) will again be zero. These changes are illustrated in sections D and E of figure 2.3.

After another section of baseline has been collected (liquid B in both cells), the liquid chromatography valve is switched to reintroduce liquid A into the calorimeter. At this stage, cell 1 will fill with liquid A, leaving the cell 2 filled with liquid B. This introduction provides a second measurement of ΔW, this time ΔW_{AB} (Fig 2.2, Sections F and G). Following the measurements of ΔW_{BA} and ΔW_{AB}, liquid A will once again fill both cells and ΔW (ΔW_{AA}) will return to its original value.

An electrical calibration of both cells can now be performed. Calibration of the cells is performed by applying a known amount of power to one zener diode while the second zener diode maintains a temperature rise of ΔT. Both cells 1 and 2 are calibrated in this way and the resulting change in voltage difference can be seen in sections J and L of figure 2.3. This allows the value of W_0 to be known with great accuracy. No system is perfectly isothermal and the calorimeter used here is not an exception. To compensate for the less than perfect transfer of heat from the thermostatting system to the sample and reference liquids, a heat leak correction factor is used. The correction factor is

determined by measuring the relative volumetric heat capacity of aqueous sodium chloride solutions relative to water. The apparent and massic heat capacities of aqueous sodium chloride solutions are well known. The heat leak correction factor, *f*, is determined by:

$$f = \left(\frac{\sigma_B}{\sigma_A - \sigma_B}\right)\frac{\Delta W_{AB}}{W_0} = \left(\frac{W_0}{\Delta W^*_{AB}}\right)\frac{\Delta W_{AB}}{W_0}, \qquad (2.4)$$

where subscript B now refers to a solution of aqueous sodium chloride of known concentration. For the instrument used in the studies reported in this thesis f=1.010609.

2.2 Density measurements

Densities are needed to convert volumetric heat capacities to massic heat capacities, and are also used in the calculation of apparent molar volumes. Two types of densimeter were used in the research presented in this thesis: a commercial Sodev 02D vibrating tube densimeter for close to ambient temperature and ambient pressure measurements and a "home built" instrument for measurements at elevated temperatures and pressures.

2.2.1 The Sodev 02D vibrating tube densimeter

Most vibrating tube densimeters are comprised of three elements: a vibration sustaining drive, a vibrating tube, and a method of measuring the time period of oscillation of the vibrating tube. The tube in the Sodev densimeter is made from stainless steel and is contained within a thermostatted chamber that is kept at a selected constant

temperature in the range of 283.15<T (/K)<333.15 by a Techneurop Programmable Circulating Thermostat.

Sustained vibration of the tube is achieved magnetically. Current is passed through the tube and induces a magnetic field around the tube. The vibrating tube passes through a magnetic pickup, which is used to both sustain and measure the time period of oscillation. The magnetic pickup is electrically connected to a resistance feedback circuit allowing the oscillation of power applied to the magnetic pickup to correspond to the natural resonance frequency of the vibrating tube. The oscillation of the feedback circuit follows changes in the resonance frequency of the tube due to changes in the density of the liquid within the vibrating tube. Figure 2.4 shows an illustration of the main components of the Sodev instrument.

When filled with a fluid sample the vibrating tube can be regarded as a simple harmonic oscillator for which the undamped resonance frequency, w_u, may be obtained from the equation:

$$w_u = \sqrt{\frac{K'}{m}} \quad . \tag{2.5}$$

In this equation, K' is the spring constant and m is the mass of the vibrating system. This mass is the sum of the mass of the metal tube and the mass of the fluid it contains. The internal volume of the tube does not change, therefore the mass of the fluid within

Figure 2.4 Illustration of the Sodev 02D ambient pressure vibrating tube densimeter

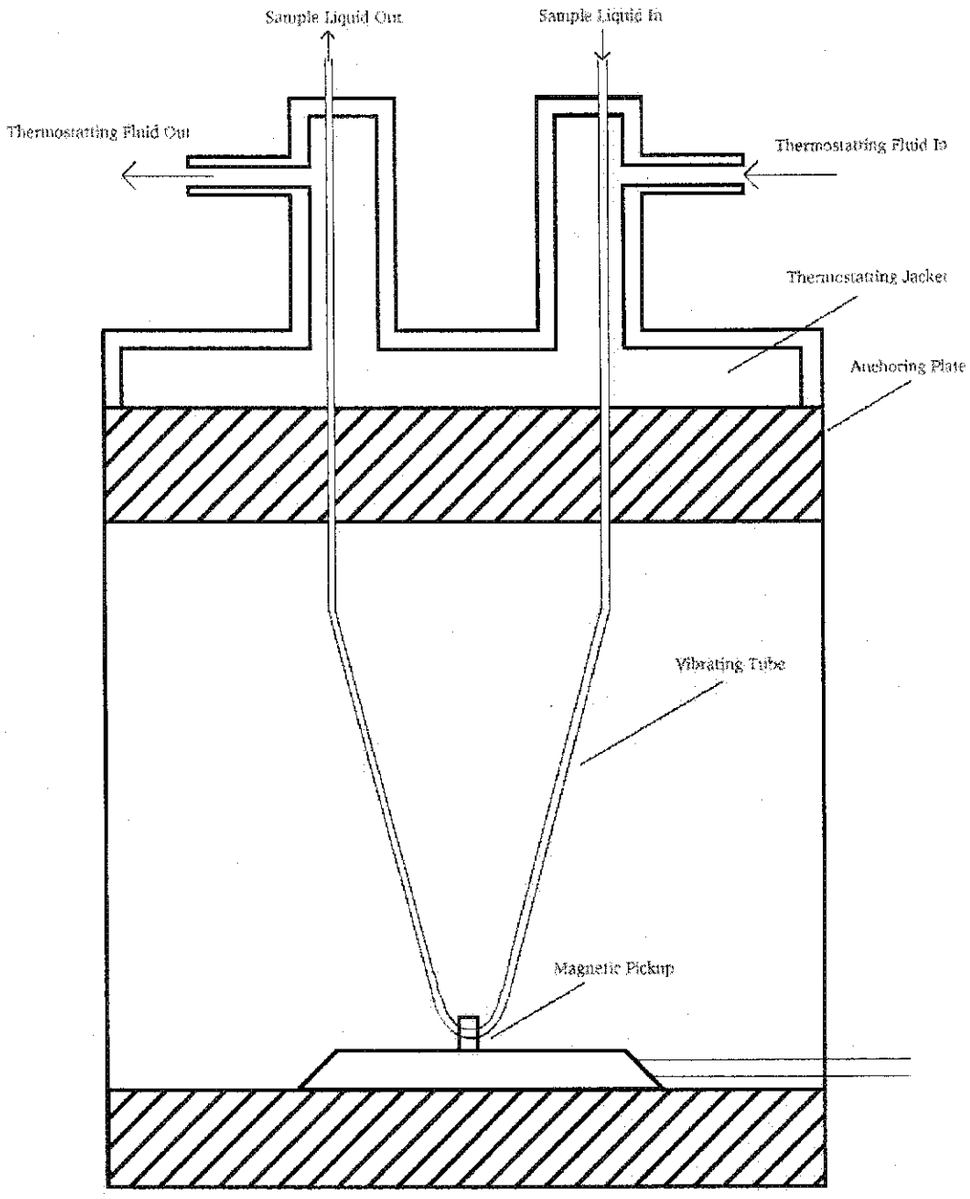

only varies as its density changes. The density of the liquid within the tube, ρ, is related to the time period of oscillation of the tube, τ, by the equation:

$$\rho = c + K\tau^2, \tag{2.6}$$

where c and K are constants which depend on the physical characteristics of the tube, but not on the fluid filling it. The K constant can be determined by measuring the time periods of oscillation of the tube containing substances of known density. Using reference substances 1 and 2 a temperature dependant value of K can be determined by the equation:

$$K = \frac{\rho_1 - \rho_2}{\tau_1^2 - \tau_2^2} \tag{2.7}$$

The reference substances used for calibration are pure degassed water and air. The density of air can be accurately calculated when the temperature, pressure, relative humidity and partial pressure of water at the recorded laboratory temperature are known. The vibrational time period of the tube filled with air along with the time period of the tube filled with pure water are used in equation 2.7 to establish the K constant. Values for the density of pure water were taken from Kell (1967): ρ_1 = (0.9991010, 0.997047, 0.992219 and 0.985696)g/cm3 at T = (288.15, 298.15, 313.15 and 328.15) K. Time periods of oscillation of the vibrating tube were measured with a Phillips PM 6611 Universal Counter and averaged every 10000 counts. The Universal Counter was interfaced to a PC that automatically collected and stored time period data.

Figure 2.5 Example output from the Sodev 02D ambient pressure vibrating tube densimeter.

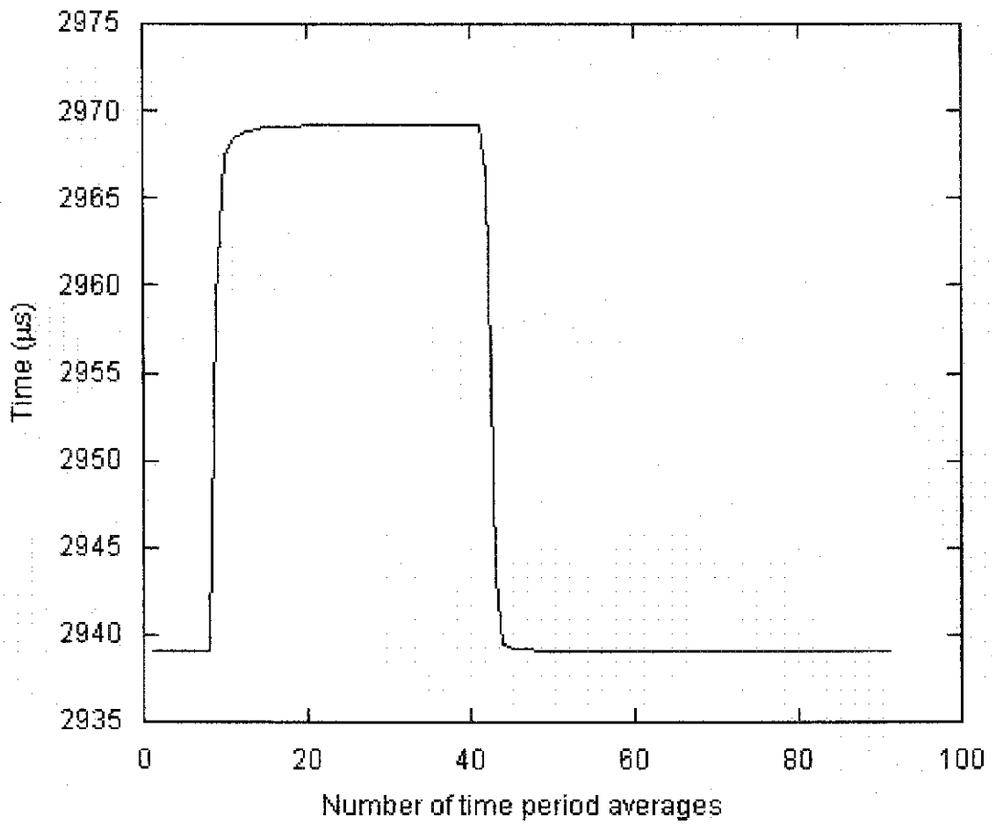

The rearrangement of equation 2.7 gives an expression that can be used to determine the density of a sample solution relative to the density of pure water:

$$\rho_{sol} - \rho_{H_2O} = K\left(\tau_{sol}^2 - \tau_{H_2O}^2\right). \qquad (2.8)$$

Ambient pressure densimetric measurements were performed in series with the

calorimetric measurements, so that the sequence in which solutions are introduced into the instrument follows that described in section 1.1.1. An example plot of time period of oscillation versus time for a typical densimetric measurement is shown as fig 2.5.

2.2.2 The high temperature and pressure vibrating tube densimeter

Figure 2.6 shows a block diagram of the high temperature and pressure vibrating tube densimiter. The operation of this instrument is quite similar to the operation of the Sodev instrument, however there are some differences.

The signal in the high temperature and pressure instrument is achieved through an optically coupled feedback circuit. Light from a small incandescent automotive bulb (part number SL1487) is directed by a 2mm Pyrex glass rod to one side of the vibrating tube. A second Pyrex glass rod leads from the opposite side of the tube to a photocell. With the tube at rest, the path from one glass rod to the other is blocked and the photocell receives no light. When the tube begins to vibrate, it temporarily opens the path from one rod to the other, allowing light to reach the photocell. This square wave signal is received by the photocell and an optically coupled amplified feedback circuit supplies an alternating current to the vibrating tube. A small permanent magnet is positioned near the tube and the combination of the magnetic field and the AC current in the tube forces the tube to oscillate according to the feedback frequency. The signal from the photocell is sent to an Optoelectronics model 8040 multifunction counter timer that averages every 1000 counts. The counter timer is interfaced with a PC which manages data collection and storage.

Figure 2.6 Block diagram of the High Temperature and Pressure Vibrating Tube Densimeter.

1) Pure water reservoir 2) HPLC high pressure pump 3) 6-port HPLC injection valves 4)Delay loop 5)Coiled stainless steel tubing to allow solution to reach equilibrium temperature 6) Fixed metal block, one half electrically insulated from the other. 7)Vibrating tube 8)Fixed magnet 9) Glass rods 10) Light source 11) Photodetector 12)Pressure detector 13) Stepping motor controlled needle valve 14) Pressure control box 15) Electronic counter

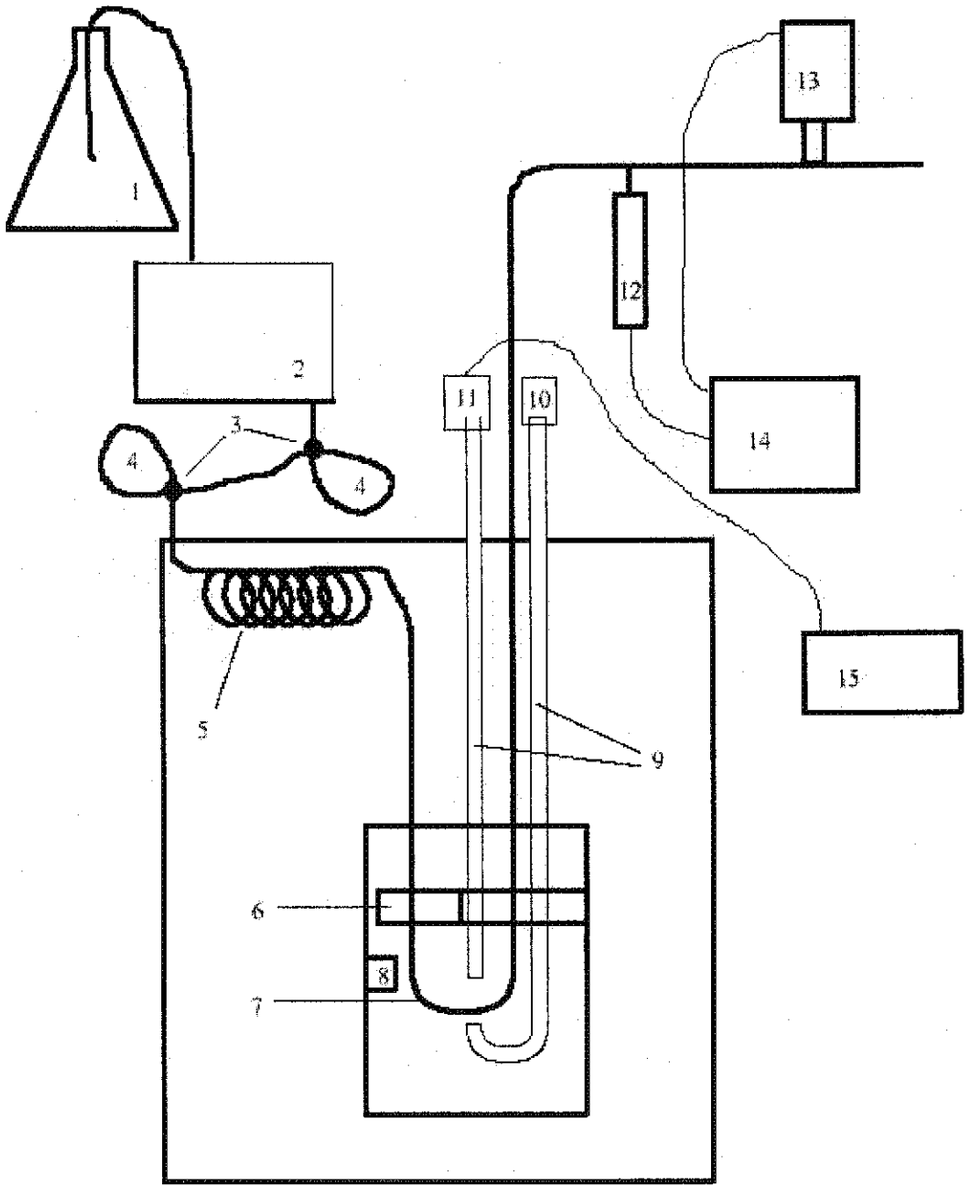

Thermostating for the high temperature and pressure instrument is achieved through several electric heaters controlled by Omega model CN9000A Series Miniature Autotune Temperature Controllers. To reduce temperature fluctuations, several layers of fibreglass insulation separate the thermostatted system from laboratory conditions.

System pressurization is achieved with a Walters 501 HPLC pump which feeds liquid to the system. Pressures are controlled using a Whitey SS-21RS2 high-pressure needle valve connected to a stepping motor. The stepping motor is controlled by a feedback circuit that uses the output from a pressure transducer to maintain a constant pressure. The stepping motor maintains pressure in the system by opening or closing the needle valve thus restricting or increasing fluid flow.

Sample and reference solutions are introduced using two sample loops and six port injection valves. Density measurements of samples were always duplicated, and calibration measurements were performed prior to and following each pair of sample measurements. The calculation of the density of a sample solution utilizes equation 2.8. In the measurements described in this thesis concentrated solutions of aqueous sodium chloride were used as one reference. Pure water was the second reference. The densities of these reference liquids were obtained from a program supplied by Archer (1992).

Figure 2.7 illustrates a typical signal output from the high temperature and pressure vibrating tube densimeter. The high amplitude peaks are the time periods of oscillation of the vibrating tube entirely filled with concentrated aqueous NaCl solution. The time period of these peaks and the time period of oscillation of the baseline allow the calculation of K using equation 2.7. The smaller peaks are due to a sample filling the

Figure 2.7 **Example of output from high temperature and pressure densimeter**

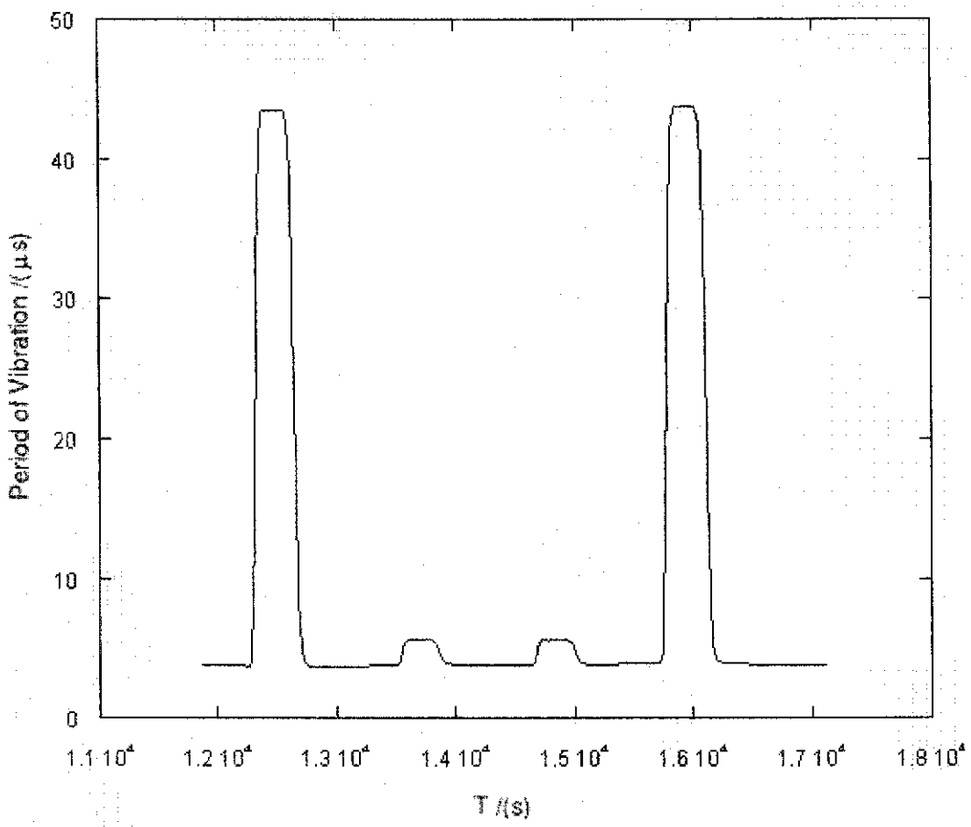

tube. The heights of the peaks were measured using the graphical data analysis program, Spectracalc™.

2.3 Assignment of uncertainties

2.3.1 Uncertainties in apparent molar volumes and heat capacities from Picker flow microcalorimeter and Sodev 02D vibrating tube densimeter

Apparent molar volumes may be defined using the equation:

$$V_\phi = \frac{M_2}{\rho_s} - \frac{\rho_s - \rho_w}{m_2 \rho_s \rho_w}, \tag{2.9}$$

and are therefore a function of ρ_s, the density of the solution, ρ_w, the density of water under the same conditions, m_2, the molality of the solution, and M_2, the molar mass of the solute. The uncertainty, δV_ϕ, can be estimated using the standard propagation of errors method. Contributions to δV_ϕ from uncertainty in the molar mass of solute and uncertainty in the density of pure water are assumed to be negligible, thus the total uncertainty in the apparent molar volume of a solution may be approximated by:

$$\delta V_\phi = \sqrt{\left(\frac{\partial V_\phi}{\partial \rho_s}\right)^2 \delta \rho_s{}^2 + \left(\frac{\partial V_\phi}{\partial m}\right)^2 \delta m^2}$$

$$= \sqrt{\left(\frac{mM+1}{m \rho_s{}^2}\right)^2 \delta \rho_s{}^2 + \left(\frac{\rho - \rho_w}{m^2 \rho_s \rho_w}\right)^2 \delta m^2}. \tag{2.10}$$

In this equation δm is the standard deviation of concentrations resulting from multiple titrations of the stock acidified aqueous rare earth salt solution and $\delta \rho_s$ is the estimated uncertainty in the densities of solutions resulting from measurements using the Sodev 02D vibrating tube densimeter and is equal to 0.00500 kg m^{-3}.

The same approach is used to approximate uncertainties in apparent molar heat capacities, $\delta C_{p,\phi}$, using the equation:

$$C_{p,\phi} = M_2 c_{p,s} + \frac{c_{p,s} - c_{p,w}}{m}, \tag{2.11}$$

where $c_{p,s}$ is the massic heat capacity of the solution and $c_{p,w}$ is the massic heat capacity of pure water under the same temperature and pressure conditions. Again, the contribution to $\delta C_{p,\phi}$ from the molar mass term and the pure solvent property is assumed to be negligible. The uncertainty in the apparent molar heat capacity of a solution is then approximated as:

$$\delta C_{p,\phi} = \sqrt{\left(\frac{\partial C_{p,\phi}}{\partial c_{p,s}}\right)^2 \delta c_{p,s}{}^2 + \left(\frac{\partial C_{p,\phi}}{\partial m}\right)^2 \delta m^2}$$

$$= \sqrt{\left(\frac{mM+1}{m}\right)^2 \delta c_{p,s}{}^2 + \left(\frac{C_{p,s} - C_{p,w}}{m^2}\right)^2 \delta m^2}, \tag{2.12}$$

where δc_{ps} is the uncertainty in massic heat capacity measurements made with the Picker flow microcalorimeter. δC_{ps} is estimated to be 7×10^{-5} J K^{-1} mol^{-1}.

2.3.2 Estimation of uncertainties in apparent molar volumes at high temperatures and pressures

The uncertainty in the densities measured using the high temperature and pressure vibrating tube densimeter (measurements reported in Chapter 6), $\delta\rho$, is determined using the relationship:

$$\delta\rho = \sqrt{\sigma\Delta\rho_e{}^2 + \sigma\Delta\rho_c{}^2}\,, \tag{2.13}$$

where $\sigma\Delta\rho_e$ is the estimated random error associated with experiments and $\sigma\Delta\rho_c$ is the estimated random error from the calibration constant of the instrument, K, which is a function of both temperature and pressure.

The calculation of $\sigma\Delta\rho_c$ is based on the equation:

$$\sigma K = 2\left|\frac{K - K_{avg}}{K_{avg}}\right|, \tag{2.14}$$

where K is the calibration constant of the instrument calculated from one reference solution peak and K_{avg} is the average calibration constant which is used to calculate the density of a given solution. Equation 2.14 gives twice the relative deviation of the calibration constant from the mean of the calibration constants obtained before and after the sample solution densities have been measured. $\sigma\Delta\rho_c$ for a given solution is thus given by the equation:

$$\sigma\Delta\rho_c = \left(\rho_1 - \rho^o\right) - \left\{\left(\sigma K\, K_{avg} + K_{avg}\right)\left(\tau_P{}^2 - \left(\frac{\tau_{B1} + \tau_{B2}}{2}\right)^2\right)\right\}, \tag{2.15}$$

where τ_P is the time period of vibration with the vibrating tube filled with sample solution and τ_{B1} and τ_{B2} are the time period of vibration with the vibrating tube filled with pure water before and after the sample has filled the tube, respectively.

The uncertainty in the density due to the difference between consecutive measurements of identical solutions can then be calculated using the equation:

$$\sigma\Delta\rho_e = \left|\left(\rho_1 - \rho^o\right) - \left(\rho_2 - \rho^o\right)\right|, \tag{2.16}$$

where ρ_1 and ρ_2 are two measured densities of one sample solution.

To arrive at a final expression for δV_ϕ resulting from measurements using the high temperature and pressure vibrating tube densimeter the root mean square of the uncertainty due to density and uncertainty due to concentration is calculated using equation 2.10 where $\delta\rho_s$ is replaced by $\delta\rho$ from equation 2.13.

3 DATA MODELING

Measurements of thermodynamic properties result in data at discrete concentrations, temperatures and pressures. To maximize the utility of a given data set, it is necessary to utilize theoretically based equations to precisely model the surfaces of thermodynamic properties. The most prevalent theories used for the modeling of thermodynamic properties of aqueous electrolyte solutions are arguably the Debye-Hückel theory (1923,1924), Pitzer ion interaction theory (1991) and the equations of state reported by Helgeson, Kirkham and Flowers (HKF) (1976,1981).

3.1 Ionic activity

An understanding of ionic activities is integral to any discussion of Debye-Hückel and Pitzer theories. The activity of a given aqueous species is expressed as the product of its concentration and its activity coefficient. The magnitude of the activity coefficient depends on the concentration scale being used. Although single ion activities are frequently required it is not possible to directly measure them. For an aqueous salt solution, $M_{\nu 1}X_{\nu 2(aq)}$, the mean ionic activity ($a_{\pm}$) is defined as:

$$a_{\pm} = a_{MX}^{\frac{1}{\nu}} = \left(a_M^{\nu 1} a_X^{\nu 2}\right)^{\frac{1}{\nu}} = \left(m_M^{\nu 1} m_X^{\nu 2} \gamma_M^{\nu 1} \gamma_X^{\nu 2}\right)^{\frac{1}{\nu}}, \tag{3.1}$$

where a_M and a_X, m_M and m_X, γ_M and γ_X are the activities, molalities, and activity coefficients of the ions M and X respectively and ν is the sum of the stoichiometric coefficients $\nu 1$ and $\nu 2$. The mean ionic activity coefficient is defined by the equation as:

$$\gamma_{\pm} = \left(\gamma_M^{\nu 1} \gamma_X^{\nu 2}\right)^{\frac{1}{\nu}}, \tag{3.2}$$

and, in a similar fashion the mean ionic molality is given by:

$$m_{\pm} = \left(m_M^{\nu 1} m_X^{\nu 2}\right)^{\frac{1}{\nu}}. \tag{3.3}$$

Activity coefficients are found to depend upon the system ionic strength, I. Ionic strength may be defined using the equation:

$$I = \frac{\sum_i m_i z_i^2}{2} = \varpi m, \tag{3.4}$$

where m_i and z_i are the molality and charge of a given ion i and ϖ is a valency factor.

3.2 Debye-Hückel equations

Debye-Hückel theory relates mean ionic activity coefficients to ionic strength. With respect to a solution of the aqueous salt, $M_{\nu 1}X_{\nu 2(aq)}$, the Debye-Hückel equation takes the form:

$$\ln \gamma_{\pm} = \frac{-A_{\gamma} |z_+ z_-| \sqrt{I}}{1 + \overset{o}{a} B_{\gamma} \sqrt{I}}, \tag{3.5}$$

where z_+ and z_- are the charges on the cation and anion, I is the ionic strength, $\mathring{a}$ is the Debye-Hückel distance of closest approach in angstroms and A_γ and B_γ are constants which depend on the dielectric constant of the solvent at a given temperature and pressure. These constants are defined using the equations:

$$A_\gamma = \frac{\sqrt{2\pi N_A \rho_o e^3}}{\sqrt{1000 \times 2.303 \sqrt{(k\varepsilon T)^3}}}, \tag{3.6}$$

and:

$$B_\gamma = \sqrt{\frac{8\pi N_A e^2}{1000 k \varepsilon T}}, \tag{3.7}$$

where N_A is Avogadro's number, ρ_0 is the density of the solvent, e is the charge of one electron, k is the Boltzmann constant and ε is the dielectric constant of the solvent.

At concentrations approaching infinite dilution, the B_γ term, equation 3.7, becomes negligible, resulting in the Debye-Hückel Limiting Law (DHLL). The DHLL takes the form:

$$\ln \gamma_\pm = -A_\gamma |z_+ z_-| \sqrt{I}, \tag{3.8}$$

and relates the mean ionic activity coefficient directly to the square root of the ionic strength of the solution. A full derivation of the DHLL can be found in Lewis and Randall (1961).

By incorporating the DHLL into mathematical models of measured thermodynamic properties, extrapolation from the experimentally measured region to infinite dilution is aided. Debye-Hückel theory is based on the linear relationship between the mean ionic activity coefficient and the square root of ionic strength ($\sqrt{I}$) at low concentrations.

3.3 Relating Debye-Hückel equations to measured properties

The chemical potential, μ, of a species, i, may also be referred to as the partial molar Gibbs energy;

$$\mu_i = \left(\frac{\partial G}{\partial n_i}\right)_{n_j,T,p}. \tag{3.9}$$

In this equation, G is the Gibbs energy, n_i is the number of moles of species i, n_j is the number of moles of all components within the system except i.

The chemical potential of a given species i in an aqueous solution is defined by the equation:

$$\mu_i = \mu_i^o + RT\ln(a_i), \tag{3.10}$$

where μ_i^o is the chemical potential of species i at any defined standard state, R is the ideal gas constant, and a_i is the activity of species i. As mentioned above, the activity of a single ion in solution cannot be measured, but the chemical potential of a simple salt in solution can be expressed in terms of the mean ionic concentration and mean ionic activity coefficient. The chemical potential of a simple salt becomes:

$$\mu_{MX} = \mu_{MX}^{\circ} + \nu RT \ln(m_{\pm}\gamma_{\pm}) = \mu_{MX}^{\circ} + \nu RT \ln(m_{\pm}) + \nu RT \ln(\gamma_{\pm}). \tag{3.11}$$

The volume of a solution is the partial derivative of the Gibbs energy with respect to pressure under conditions of constant temperature, T:

$$V = \left(\frac{\partial G}{\partial p}\right)_T. \tag{3.12}$$

The partial molar volume of a given ion, V_i, in solution is expressed as:

$$V_i = \left(\frac{\partial \mu_i}{\partial p}\right)_T. \tag{3.13}$$

Combining equations 3.11 and 3.13 gives:

$$V_i = \left(\frac{\partial \mu_{MX}^{\circ}}{\partial p}\right)_T + \nu RT\left(\frac{\partial \ln m_{\pm}}{\partial p}\right)_T + \nu RT\left(\frac{\partial \ln \gamma_{\pm}}{\partial p}\right)_T. \tag{3.14}$$

The molal concentration and the infinite dilution chemical potential do not vary with pressure. Equation 3.14 can thus be simplified to give the partial molar volume of an aqueous salt (*Vi*) in terms of the mean ionic activity coefficient.

$$V_i = V_i^o - \nu RT\left(\frac{\partial \ln \gamma_{\pm}}{\partial p}\right)_{m,T}$$

$$= V_i^o - \nu RT\left(\frac{\partial\left(-A_\gamma \mid z_+ z_- \mid \sqrt{I}\right)}{\partial p}\right)_{m,T}$$

$$= V_i^o - \omega \overline{A}_v \sqrt{I}\ , \qquad (3.15)$$

where V_i^o is the partial molar property at infinite dilution, $\overline{A}_V$ is the Debye-Hückel limiting slope for partial molar volumes and R is the ideal gas constant. $\overline{A}_V$ is defined as:

$$\overline{A}_v = 2RT\left(\frac{\partial A_\gamma}{\partial p}\right)_T . \qquad (3.16)$$

Similarly, the heat capacity of a solution is the partial derivative of the enthalpy of the solution with respect to the temperature at constant pressure, p:

$$C_p = \left(\frac{\partial H}{\partial T}\right)_p . \qquad (3.17)$$

The partial molar heat capacity of an aqueous solution, $C_{p,i}$, is defined by:

$$C_{p,i} = \left(\frac{\partial H_i}{\partial T}\right)_{m,p}$$
$$= C^o_{p,i} - \nu R\left(T^2\left(\frac{\partial^2 \ln \gamma_{\pm}}{\partial T^2}\right)\right) + 2T\left(\frac{\partial \ln \gamma_{\pm}}{\partial T}\right)_{m,p}$$

$$= C^o_{p2} - \omega \bar{A}_J \sqrt{I}\,, \qquad (3.18)$$

In equation 3.18, $\bar{A}_J$ (also commonly referred to as A_C) is the Debye-Hückel limiting slope of partial molar heat capacities defined as:

$$\bar{A}_J = 2RT^2\left(\frac{\delta^2 A_\gamma}{\delta T^2}\right)_p . \qquad (3.19)$$

3.4 Pitzer theory

For very dilute solutions, the DHLL can be used to approximate the behaviour of a partial molar property because interactions between individual ions are small. Assuming a random, uniform distribution of ions in a dielectric medium, the average distance between ions in a dilute solution will be greater than the distance between ions in a more concentrated solution (Robinson and Stokes, 1959). The strength of interactions between charged particles is inversely proportional to the distance between particles squared (Serway, 1996). Thus with increasing concentration interactions

between ions become stronger as the distance between ions decreases. Pitzer theory considers the interactions between individual ions and extends the predictive abilities of Debye-Hückel theory. This is accomplished through the addition of a series of virial concentration terms. A virial equation consists of a base equation followed by a polynomial of one of its variables. The virial equations reported by Pitzer can be seen as a sum of concentration terms, where each term represents ionic interaction one degree higher than the previous term. The first term (B_{MX}) considers interactions between pairs of ions, the second (C_{MX}) considers groups of three ions etc. The expansion could well extend indefinitely, or at least until all ion-ion interactions were considered. Fortunately, for the low ionic strengths investigated in this thesis, the tertiary and higher order terms become insignificant due to relatively large mean interionic distances.

The Gibbs energy of an aqueous electrolyte can be expressed as the sum of the ideal or infinite dilution Gibbs energy and the non-ideal or excess Gibbs energy (Pitzer, 1991). The Gibbs energy of a given electrolyte can be divided into the ideal, G^o, and non-ideal, or excess, G^{EX}, contributions:

$$G = G^o + G^{EX} \tag{3.20}$$

The Pitzer expression for the excess Gibbs energy is:

$$\frac{G^{EX}}{n_w RT} = \frac{-4IA_\gamma}{3b}\ln\left(1+b\sqrt{I}\right) + m^2\left(2\nu_M\nu_X\right)\left[B_{MX} + m\left(\nu_M z_M\right)C_{MX}\right], \tag{3.21}$$

where b is a universal parameter with $b = 1.2 kg^{1/2} mol^{-1/2}$. B_{MX} and C_{MX} are the second and third virial coefficients.

The volume of an ionic species is equal to the standard state volume plus the partial derivative of the excess Gibbs energy with respect to pressure at constant temperature and solution composition:

$$V = V^o + \left(\frac{\partial G^{EX}}{\partial p} \right)_{T,m} \tag{3.22}$$

An apparent molar volume for a solution containing only solute i is defined by the equation:

$$V_{\phi,i} = \frac{V - n_{solvent} V^o_{solvent}}{n_i} \tag{3.23}$$

For some thermodynamic parameter Y, the relationship between partial, Y_i, and apparent, $Y_{\phi i}$, molar properties of solute i is given as:

$$Y_i = Y_{\phi,i} + n_i \left(\frac{\partial Y_{\phi,i}}{\partial n_i} \right)_{T,p,n_j} \tag{3.24}$$

The Pitzer equation for apparent molar volumes then becomes:

$$V_{\phi,2} = V^o_{\phi,2} + \left\{ \frac{\nu(z_M z_X) A_v \ln\left(1 + b\sqrt{I}\right)}{2b} \right\} + 2|\nu_M \nu_X| RT\left(mB^V_{MX} + m^2 (\nu_M z_M) C^V_{MX} \right), \tag{3.25}$$

where $V^o_{\phi,2}$ is the apparent molar volume at infinite dilution, B^V_{MX} and C^V_{MX} are the second and third volumetric virial coefficients. Note also that the Debye-Hückel limiting slope for apparent molar volumes, A_v, is used. Apparent molar limiting slopes relate to partial molar limiting slopes by:

$$A_Y = \frac{2}{3}\overline{A}_Y \tag{3.26}$$

Heat capacity relates to the excess Gibbs energy as the second partial derivative of the excess Gibbs energy with respect to temperature, holding pressure and solution composition constant:

$$C_p = C_p^o + \left(\partial\left\{-T^2\left[\partial\left(G^{ex}/T\right)/\partial T\right]_{p,m}\right\}/\partial T\right)_{p,m} \tag{3.27}$$

An apparent molar heat capacity is defined in an analogous manner to the apparent molar volume.

$$C_{p,\phi,2} = C^o_{p2} + \frac{v|z_M z_X|A_J \ln(1+b\sqrt{I})}{2b} - 2v_M v_X RT^2\left[mB^J_{MX} + m^2(v_M z_M)C^J_{MX}\right] \tag{3.28}$$

The equation for apparent molar heat capacities therefore takes the form:

$$C_{p,\phi,2} = C^o_{p,2} + \left\{v(z_M z_X)\left(\frac{A_J}{2b}\right)\ln\left(1+b\sqrt{I}\right)\right\}$$

$$-2v_M v_X RT^2\left[B^J_{MX} - m^2(v_M v_X)C^J_{MX}\right], \tag{3.29}$$

Where R is the ideal gas constant, and $C^o_{p,2}$ is the apparent molar heat capacity at infinite dilution. In addition B^J_{MX} and C^J_{MX} are the second and third thermochemical virial coefficients. The volumetric and thermochemical virial coefficients are related to temperature and pressure derivatives of the activity virial coefficients and complete derivations can be found in the compilation by Pitzer (1991).

3.5 Helgeson Kirkham and Flowers equations

The HKF equations are semi-empirical equations that are comprised of structural and electrostatic contributions. For a given thermodynamic property, Y, the partial molar property at infinite dilution (equal to the apparent molar property) may be expressed in the form:

$$Y^o = Y^o_S + Y^o_E \tag{3.30}$$

where Y^o_S is the structural contribution and Y^o_E is the electrostatic contribution. For partial molar volumes, the structural contribution, V^o_S, is given by the equation:

$$\Delta V^o_S = a_1 + \frac{a_2}{(\Psi + p)} + \frac{a_3}{(T - \Theta)} + \frac{a_4}{((\Psi + p)(T - \Theta))}, \tag{3.31}$$

where Θ and Ψ are arbitrary solvent dependent parameters and are assigned values of Θ = 228 K and Ψ = 2600 bar (Helgeson, *et al.*, 1981) for water. a_i (i=1-4) are fitting coefficients. The electrostatic contribution to the volume, V^o_E, is given by the equation:

$$V_E^o = -\omega Q \tag{3.32}$$

where ω is an effective Born coefficient specific to the salt under study and Q is a Born function that is related to the derivative of the dielectric constant of the solvent with respect to pressure. Values of ω were calculated from the compilation of single ion values reported by Shock and Helgeson (1988).

The structural contribution to the partial molar heat capacity is given by the equation:

$$\Delta C_{p,S}^o = c_1 + \frac{c_2}{(T-\Theta)^2} + \frac{2T}{(T-\Theta)^3}\left\{a_3(p-p_r) + \frac{a_4 \ln(\Psi+p)}{(\Psi+p_r)}\right\}, \tag{3.33}$$

where p_r is a reference pressure of 1 bar. The electrostatic contribution to the partial molar heat capacity is given by:

$$C_{p,E}^o = \omega T X\ , \tag{3.34}$$

where X is a Born function that is related to the derivative of the dielectric constant of the solvent with respect to temperature.

At constant pressure, the structural contribution to the partial molar volume takes the form:

$$V_S^o = v_1 + \frac{v_2}{T - \Theta}, \tag{3.35}$$

where:

$$v_1 = a_1 + \frac{a_2}{\Psi + p}, \tag{3.36}$$

and

$$v_2 = a_3 + \frac{a_4}{\Psi + p}. \tag{3.37}$$

Similarly, under the condition of $p = p_r$, structural contributions to partial molar heat capacities may be represented by the equation:

$$C_{p,S}^o = c_1 + \frac{c_2}{(T - \Theta)^2} \tag{3.38}$$

3.6 Application of data modeling

Volumetric and thermochemical data reported in Chapters 4 and 5 have been modeled using Pitzer equations previously used by Xaio and Tremaine (1997). Xaio and Tremaine showed that these equations adequately represent the ionic strength dependence of apparent molar volumes and heat capacities of aqueous trivalent metal chlorides and

perchlorates at a constant temperature, T. The equation used to model apparent molar volumes in Chapters 4 and 5 takes the form:

$$V_{\phi,2} = V_2^o + \frac{6A_V \ln\left(1+b\sqrt{I}\right)}{b} + 2\nu_M \nu_X RTm_2 B_{MX}^V \tag{3.39}$$

where:

$$B_{MX}^V = \beta^{(0)V} + 2\beta^{(1)V} f(I). \tag{3.40}$$

$f(I)$ is a function of ionic strength defined as:

$$f(I) = \left[1 - \left\{\left(1+a\sqrt{I}\right)e^{-a\sqrt{I}}\right\}\right] a^2 I\,. \tag{3.41}$$

The equation used to model apparent molar heat capacities in Chapters 4 and 5 is:

$$C_{p\phi,2} = C_{p,2}^o + \frac{6A_J \ln\left(1+b\sqrt{I}\right)}{b} - 2\nu_M \nu_X RT^2 m_2 B_{MX}^J\,, \tag{3.42}$$

where:

$$B_{MX}^J = \beta^{0J} + 2\beta^{1J} f(I). \tag{3.43}$$

As will be seen in later chapters, these equations have been successfully used to model the volumetric and thermochemical properties of rare earth perchlorate and chloride systems. Values for the Debye-Hückel limiting slopes were taken from the compilations reported by Archer and Wang (1990).

Modified Pitzer equations have been used to model the temperature and concentration dependences of volumetric and thermochemical properties. These modified equations use the Helgeson, Kirkham and Flowers equations that were utilized by Tanger and Helgeson (1988) to model the temperature dependences of apparent molar properties at infinite dilution. These equations take the same general form as equations 3.37 and 3.39 where:

$$V_2^o = v_1 + \frac{v_2}{T-\Theta} - \omega Q \tag{3.44}$$

$$\beta^{0V} = v_3 + v_4 T \tag{3.45}$$

$$\beta^{1V} = \frac{v_5}{T} + v_6 + v_7 T \tag{3.46}$$

$$C_{p,2}^o = c_1 + \frac{c_2}{(T-\Theta)^2} + \omega T X \tag{3.47}$$

$$\beta^{0J} = \frac{c_3}{T} + c_4 + c_5 T \tag{3.48}$$

$$\beta^{1J} = \frac{c_6}{T} + c_7 + c_8 T \qquad (3.49)$$

Values for Q and X were calculated using the equations for the dielectric constant of water provided by Johnson and Norton (1991). Values for the fitting constants c_i (i = 1 through 7) and v_i (i=1 through 8) were obtained through regression analyses.

For the high temperature and pressure volumetric measurements of $HClO_4$ and $Yb(ClO_4)_3$, pressure dependent terms were added to equations 3.43, 3.44, 3.46 and 3.47. The specific equations are presented in Chapter 6.

4 RARE EARTH PERCHLORATE STUDY

4.1 Previous studies

Nearly all thermodynamic studies of the rare earth perchlorates reported in the literature have been performed at close to ambient temperature and pressure conditions (T=298.15K, p=0.1MPa). Much of this work was completed by Spedding and co-workers (1975) using pycnometric measurements to obtain density and volume data and an adiabatic single-can solution calorimeter to determine massic heat capacities. More recently Xaio and Tremaine (1997) have investigated temperature dependences of the apparent molar volumes and heat capacities of several aqueous rare earth perchlorate systems. Babakulov and Latysheva (1974) have also made heat capacity measurements using a double adiabatic calorimeter on aqueous solutions of the Group III metal perchlorate $Y(ClO_4)_3$. These authors reported values for the apparent molar heat capacities of $Y(ClO_4)_3$ at T = 298.15K at various concentrations in the range 0.1-4.05 M.

Work described in this chapter addresses the lack of high precision volumetric and thermochemical data in the literature for trivalent metal cations by probing the temperature dependences of the apparent molar volumes and heat capacities of selected aqueous rare earth perchlorate systems. This work also yields single ion volumes and heat capacities for the selected trivalent metal cation containing systems.

4.2 Experimental

4.2.1 Stock solution preparation

The procedure used to prepare stock solutions of aqueous rare earth perchlorate solutions followed that previously described by Spedding *et al.* (1966) with several minor variations. Stock solutions of the rare earth perchlorates were prepared by adding slightly more than equivalent pure rare earth oxide to approximately 1.2M aqueous perchloric acid at approximately T = 353K. A cloudy solution was obtained on the addition of the metal oxide sample. The solution was allowed to cool, and the pH was measured. Additional 0.1 M perchloric acid was added to achieve pH <3. The solution was heated again until further dissolution of the metal oxide could not be observed. At this stage, the solution was cooled and the pH measured again. If the pH was above 3, additional dilute perchloric acid was added to further decrease the pH to below 3. This process was repeated until the heating, dissolution, cooling cycle, produced no change in the pH of the system. Keeping the pH below 3 ensured that there was no formation of rare earth hydroxide species. At this stage the solution was vacuum filtered through a fine, sintered glass filter funnel and stored in a sealed volumetric flask. The filtrates were found to be free of colloidal particles. The time required to prepare the acidified aqueous rare earth perchlorate solutions varied depending upon which rare earth oxide was used and ranged from several days to less than 30 minutes.

The oxides used were $Y_2O_{3(s)}$ (99.99 mol%), $Yb_2O_{3(s)}$ (99.9 mol%), $Dy_2O_{3(s)}$ (99.9 mol%), and $Sm_2O_{3(s)}$ (99.9 mol%) from Aldrich Chemical Company (Cat. No. 20,516-8, 24,699-9, 28,926-4, and 22,867-2 respectively). The perchloric acid was obtained from

BDH Chemicals. All water used was distilled then further purified by an Osmonics model Aries High-Purity D.I. Loop that polishes water to a resistance of 18.3MΩ.

4.2.2 Stock solution standardization

Stock solutions created by the above description contained only rare earth perchlorate salt and a slight excess of perchloric acid. The molarities of the perchloric acid in the stock solutions were determined by titration with tris(hydroxymethyl)aminomethane (99.94±0.01 mol%, obtained from US Department of Commerce, National Bureau of Standards) using xylenol orange as the indicator. The molarities of rare earth perchlorate salts were determined by titration with the disodium salt of ethylenediaminetetraacetic acid (EDTA) (obtained from BDH, 99.0-101.0% assay) buffered to pH=5.5 using an acetic acid sodium acetate buffer solution. Methyl-red was used as the indicator in the EDTA titrations. Solutions of EDTA used in the titrations were prepared according to the procedure outlined by Skoog *et al.* (2000) The densities of the stock acidified aqueous rare earth perchlorate solutions were measured at the temperatures at which the titrations were performed. These densities were used to convert the molar concentrations to molal concentrations.

4.2.3 Sample preparation

To obtain both the concentration and temperature dependences of both the apparent molar volumes and apparent molar heat capacities of the perchlorate salts, four sets of ten solutions ranging in concentration (0.0264 to 0.3974m, 0.0162 to 0.2155m,

0.0221 to 0.3968m and 0.0350 to 0.4182m for $Y(ClO_4)_3$, $Yb(ClO_4)_3$, $Dy(ClO_4)_3$ and $Sm(ClO_4)_3$, respectively) were prepared. Solutions were prepared by mass by dilution of the stocks of each salt with pure, degassed water. Relative densities and massic heat capacities were measured at T=(288.15, 298.15, 313.15, and 328.15) K and p = 0.1 MPa.

4.2.4 Measurements

All volumetric and heat capacity data were collected as described in Chapter 3 of this thesis. The determination of apparent molar heat capacities and apparent molar volumes of the aqueous rare earth perchlorates required several additional calculations.

Measured relative massic heat capacities (C_p-C_p^o) of the acidified rare earth perchlorate solutions may be used to calculate experimental apparent molar heat capacities of the acidified rare earth perchlorate solution ($C_{p,\phi,\mathrm{exp}}$) using the equation:

$$C_{p,\phi,\mathrm{exp}} = \left(\frac{C_p \{1 + (m_2 M_2) + (m_3 M_3)\} - C_p^o}{m_2 + m_3} \right). \qquad (4.1)$$

In this equation, C_p is the massic heat capacity of the sample solution and C_p^o is the massic heat capacity of pure water (Stimson, 1955). m_2, m_3, M_2 and M_3 are the molalities and molar masses of the salt and the excess acid, respectively. In a similar manner, experimental apparent molar volumes ($V_{\phi,exp}$) may be calculated from measured relative densities (ρ-ρ^o) using the equation:

$$V_{\phi,\exp} = \left(\frac{1 + (m_2 M_2) + (m_3 M_3)}{\rho} - \frac{1}{\rho^o} \right) \Bigg/ m_2 + m_3 , \qquad (4.2)$$

where ρ is the measured density of the solution and ρ^o is the density of pure water (Kell, 1967).

The calculated experimental apparent molar properties ($V_{\phi\,\exp}$ and $C_{p,\,\phi\,\exp}$) may be represented using Young's rule as the sum of the apparent molar contributions of the rare earth perchlorate salts and perchloric acid in water. Young's rule takes the generic form:

$$Y_{\phi,\exp} = \frac{m_2}{m_2 + m_3} Y_{\phi,2} + \frac{m_3}{m_2 + m_3} Y_{\phi,3} + \delta . \qquad (4.3)$$

In equation 4.3, Y is the thermodynamic property of interest and δ is an excess mixing term. This term is defined by the equation:

$$\delta = k_{2,3} \left[\frac{m_2 m_3}{(m_2 + m_3)^2} \right] I , \qquad (4.4)$$

where $k_{2,3}$ is the binary interaction coefficient and I is the ionic strength of the system. For all acidified aqueous rare earth perchlorate solutions in this study, the contribution of δ is assumed to be negligible. Values for δ tend towards zero when the concentration of one species is much higher than the concentration of the other in a given mixture. This

condition applies to nearly all the solutions investigated in this study. By assuming the contribution of δ to be zero, any real contribution will affect the apparent molar property of the aqueous salt solution (values of $Y_{\phi,3}$ for $HClO_4$ being those previously reported by Hovey (1988)). Solutions of $Y(ClO_4)_3$ investigated at 288.15 and 328.15 K are the only systems in which perchloric acid concentrations in the mixtures were not significantly lower than those of the salt. No irregularities were observed in the apparent molar properties of this system at 288.15 and 328.15 K when compared with those obtained at other temperatures.

The calculation of the required apparent molar properties of the aqueous perchlorate salt solutions can be obtained by rearranging equation 4.3:

$$Y_{\phi,2} = \left(Y_{\phi,\exp} - \frac{m_3}{m_2 + m_3} Y_{\phi,3} \right) \left(\frac{m_2 + m_3}{m_2} \right) \tag{4.5}$$

Tables 4.1-4.4 list the concentrations, relative densities, relative massic heat capacities, apparent molar volumes and apparent molar heat capacities along with uncertainties for the solutions investigated. Uncertainties were calculated using the procedure described in Chapter 2.

4.3 Data modeling

As indicated in Chapter 3, two forms of data modeling were performed. The concentration dependences of isothermal apparent molar volume and heat capacity values for each aqueous perchlorate salt were modeled using Pitzer ion interaction equations. For apparent molar volumes this equation takes the form:

Table 4.1 The concentration dependences of relative densities, relative massic heat capacities, apparent molar volumes and apparent molar heat capacities of aqueous solutions of $Y(ClO_4)_3$, component 2, in $HClO_4$ (component 3) at T = (288.15, 298.15, 313.15, and 328.15) K. Uncertainties are given in parentheses.

m_2 /mol kg^{-1}	m_3 /mol kg^{-1}	$\rho_{expt} - \rho^o$ /kg m^{-3}	$V_{\phi,expt}$ /cm^3 mol^{-1}	$V_{\phi,2}$ /cm^3 mol^{-1}	$c_{p\ expt} - c_p^o$ /J K^{-1} g^{-1}	$C_{p,\phi,expt}$ /J K^{-1} mol^{-1}	$C_{p,\phi,2}$ /J K^{-1} mol^{-1}
				T = 288.15 K			
0.02642	0.02636	9.389	65.43 (1.73)	87.79 (1.74)	-0.05782	-88.1 (11.0)	-144.4 (11.2)
0.04317	0.04307	15.295	65.58 (1.71)	87.98 (1.72)	-0.09313	-81.2 (10.7)	-135.6 (10.8)
0.07194	0.07177	25.337	65.96 (1.68)	88.65 (1.69)	-0.15178	-71.7 (10.3)	-123.8 (10.5)
0.10150	0.10125	35.566	66.16 (1.65)	89.00 (1.67)	-0.20969	-64.0 (10.1)	-114.4 (10.3)
0.12980	0.12949	45.262	66.37 (1.63)	89.39 (1.64)	-0.26316	-57.7 (9.9)	-106.9 (10.1)
0.15565	0.15528	54.020	66.60 (1.61)	89.82 (1.62)	-0.30992	-51.0 (9.7)	-97.6 (9.9)
0.18852	0.18807	65.061	66.83 (1.58)	90.26 (1.60)	-0.36705	-42.8 (9.5)	-85.9 (9.7)
0.22752	0.22698	78.006	67.07 (1.55)	90.75 (1.57)	-0.43184	-34.1 (9.3)	-73.3 (9.5)
0.27511	0.27445	93.601	67.31 (1.52)	91.24 (1.53)	-0.50710	-25.0 (9.0)	-60.2 (9.2)
0.30683	0.30610	103.867	67.47 (1.50)	91.56 (1.51)	-0.55489	-19.3 (8.8)	-51.5 (9.1)
				T = 298.15 K			
0.03616	0.00025	10.583	93.08 (1.13)	93.41 (1.15)	-0.06065	-78.8 (6.7)	-79.3 (7.0)
0.07259	0.00050	21.118	93.79 (1.11)	94.12 (1.12)	-0.11900	-63.8 (6.4)	-64.2 (6.7)
0.10907	0.00075	31.579	94.20 (1.09)	94.54 (1.11)	-0.17497	-50.4 (6.2)	-50.7 (6.5)
0.14517	0.00099	41.818	94.67 (1.07)	95.01 (1.09)	-0.22857	-41.5 (6.1)	-41.9 (6.4)
0.18453	0.00126	52.891	95.04 (1.05)	95.38 (1.07)	-0.28479	-32.3 (6.0)	-32.5 (6.3)
0.22290	0.00153	63.580	95.39 (1.04)	95.74 (1.06)	-0.33768	-24.4 (5.8)	-24.6 (6.2)
0.26599	0.00182	75.489	95.66 (1.02)	96.01 (1.04)	-0.39501	-16.8 (5.7)	-17.0 (6.1)
0.30140	0.00206	85.164	95.95 (1.01)	96.30 (1.03)	-0.44029	-10.2 (5.6)	-10.4 (6.0)
0.35266	0.00241	98.998	96.41 (0.99)	96.76 (1.01)	-0.50365	-2.2 (5.5)	-2.4 (5.9)
0.39744	0.00272	111.027	96.59 (0.97)	96.94 (0.99)	-0.55683	4.2 (5.4)	4.1 (5.8)
				T = 313.15 K			
0.03534	0.00024	10.139	97.92 (1.12)	98.27(1.14)	-0.05775	-35.2 (6.6)	-35.4 (6.9)
0.08089	0.00055	23.008	99.09 (1.09)	99.45 (1.11)	-0.12830	-14.7 (6.2)	-14.9 (6.5)
0.11884	0.00081	33.614	99.60 (1.07)	99.96 (1.09)	-0.18461	-4.1 (6.0)	-4.3 (6.3)
0.16199	0.00111	45.543	100.10 (1.05)	100.47 (1.07)	-0.24628	5.0 (5.9)	4.9 (6.2)
0.20487	0.00140	57.312	100.31 (1.03)	100.68 (1.05)	-0.30519	12.8 (5.7)	12.7 (6.1)
0.24231	0.00166	67.474	100.56 (1.02)	100.93 (1.04)	-0.35511	17.5 (5.6)	17.5 (6.0)
0.28709	0.00196	79.535	100.76 (1.00)	101.14 (1.02)	-0.41282	22.7 (5.5)	22.7 (5.9)
0.39744	0.00272	108.718	101.27 (0.96)	101.64 (0.98)	-0.54531	37.1 (5.3)	37.1 (5.7)
				T = 328.15 K			
0.03003	0.02996	10.062	74.17 (1.67)	100.21 (1.69)	-0.06108	-12.7 (10.2)	-35.4 (10.4)
0.05425	0.05412	18.069	74.58 (1.65)	100.94 (1.66)	-0.10766	0.7 (9.8)	-12.4 (10.0)
0.08435	0.08415	27.937	74.80 (1.62)	101.34 (1.63)	-0.16402	7.1 (9.5)	-3.9 (9.7)
0.11216	0.11189	36.956	75.00 (1.60)	101.74 (1.61)	-0.21411	12.7 (9.3)	4.5 (9.6)
0.14090	0.14056	46.175	75.20 (1.57)	102.18 (1.59)	-0.26486	14.9 (9.2)	6.5 (9.4)
0.17405	0.17363	56.707	75.37 (1.55)	102.57 (1.56)	-0.32094	19.2 (9.0)	12.5 (9.2)
0.20563	0.20514	66.642	75.48 (1.53)	102.88 (1.54)	-0.37318	21.0 (8.9)	14.1 (9.1)
0.24458	0.24340	78.788	75.56 (1.50)	103.13 (1.51)	-0.43456	25.1 (8.7)	19.9 (8.9)
0.27566	0.27501	88.404	75.56 (1.48)	103.23 (1.49)	-0.48184	28.0 (8.5)	24.0 (8.8)
0.30683	0.30610	97.948	75.58 (1.46)	103.37 (1.47)	-0.52717	31.8 (8.4)	30.2 (8.6)

Table 4.2 The concentration dependences of relative densities, relative massic heat capacities, apparent molar volumes and apparent molar heat capacities of aqueous solutions of $Yb(ClO_4)_3$, component 2, in $HClO_4$ (component 3) at T = (288.15, 298.15, 313.15, and 328.15) K. Uncertainties are given in parentheses.

m_2 /mol kg^{-1}	m_3 /mol kg^{-1}	$\rho_{expt} - \rho^o$ /kg m^{-3}	$V_{\phi,expt}$ /cm^3 mol^{-1}	$V_{\phi,2}$ /cm^3 mol^{-1}	$c_{p\,expt} - c_p^o$ /J K^{-1} g^{-1}	$C_{p,\phi,expt}$ /J K^{-1} mol^{-1}	$C_{p,\phi,2}$ /J K^{-1} mol^{-1}
			T = 288.15 K				
0.01624	0.00614	6.600	74.04 (1.42)	85.81 (1.44)	-0.03669	-105.7 (8.9)	-132.1 (9.1)
0.04141	0.01567	16.747	74.71 (1.38)	86.67 (1.39)	-0.09203	-99.5 (7.8)	-126.5 (8.1)
0.05786	0.02190	23.349	74.88 (1.36)	86.89 (1.38)	-0.12732	-96.5 (7.7)	-123.9 (7.9)
0.07618	0.02883	30.656	75.12 (1.35)	87.19 (1.36)	-0.16529	-88.2 (7.5)	-114.0 (7.8)
0.10229	0.03871	41.024	75.32 (1.33)	87.45 (1.34)	-0.21822	-81.4 (7.4)	-106.6 (7.6)
0.12062	0.04564	48.239	75.57 (1.31)	87.79 (1.33)	-0.25410	-75.4 (7.3)	-99.4 (7.5)
0.14704	0.05564	58.599	75.80 (1.30)	88.10 (1.31)	-0.30495	-70.4 (7.2)	-94.1 (7.4)
0.16633	0.06294	66.195	75.64 (1.29)	87.87 (1.30)	-0.34102	-66.6 (7.1)	-90.0 (7.3)
0.19509	0.07383	77.398	75.70 (1.27)	87.95 (1.28)	-0.39321	-60.6 (6.9)	-83.1 (7.2)
0.21549	0.08155	85.223	75.98 (1.26)	88.33 (1.27)	-0.42894	-55.7 (6.9)	-77.4 (7.1)
			T = 298.15 K				
0.01974	0.00747	7.914	77.48 (1.40)	89.93 (1.41)	-0.04345	-68.4 (8.4)	-89.0 (8.6)
0.04036	0.01527	16.110	78.11 (1.36)	90.77 (1.38)	-0.08723	-55.6 (7.6)	-73.2 (7.9)
0.06006	0.02273	23.893	78.47 (1.35)	91.24 (1.36)	-0.12785	-47.1 (7.4)	-62.8 (7.7)
0.08326	0.03151	33.004	78.75 (1.33)	91.62 (1.34)	-0.17437	-39.4 (7.3)	-53.6 (7.5)
0.10180	0.03852	40.255	78.89 (1.32)	91.81 (1.33)	-0.21055	-33.8 (7.1)	-46.8 (7.4)
0.12286	0.04649	48.441	79.07 (1.30)	92.06 (1.32)	-0.25097	-30.2 (7.1)	-42.9 (7.3)
0.14413	0.05454	56.643	79.35 (1.29)	92.44 (1.30)	-0.29053	-25.2 (7.0)	-37.0 (7.2)
0.16848	0.06376	66.014	79.45 (1.27)	92.58 (1.29)	-0.33464	-20.2 (6.8)	-31.1 (7.1)
0.18972	0.07179	74.160	79.48 (1.26)	92.63 (1.27)	-0.37258	-17.9 (6.8)	-28.8 (7.1)
			T = 313.15 K				
0.02464	0.00932	9.657	82.82 (1.37)	96.54 (1.39)	-0.05253	-22.0 (7.9)	-31.7 (8.1)
0.04156	0.01573	16.250	82.99 (1.35)	96.75 (1.36)	-0.08731	-12.1 (7.4)	-19.2 (7.7)
0.08425	0.03188	32.732	83.42 (1.31)	97.33 (1.33)	-0.17208	-1.2 (7.1)	-6.2 (7.4)
0.10104	0.03824	39.154	83.61 (1.30)	97.58 (1.32)	-0.20422	2.4 (7.0)	-1.9 (7.3)
0.11796	0.04464	45.605	83.70 (1.29)	97.72 (1.31)	-0.23569	7.5 (6.9)	4.5 (7.2)
0.13677	0.05176	52.746	83.80 (1.28)	97.86 (1.30)	-0.27051	9.3 (6.8)	6.4 (7.1)
0.16529	0.06255	63.523	83.89 (1.26)	97.99 (1.28)	-0.32183	12.6 (6.7)	10.2 (7.0)
0.18599	0.07038	71.291	83.96 (1.25)	98.11 (1.27)	-0.35814	14.8 (6.6)	12.6 (6.9)
0.21549	0.08155	82.290	84.07 (1.23)	98.28 (1.25)	-0.40813	19.3 (6.5)	17.9 (6.8)
			T = 328.15 K				
0.01658	0.00628	6.424	85.13 (1.40)	99.20 (1.41)	-0.03533	-12.9 (8.5)	-20.2 (8.7)
0.04105	0.01553	15.841	85.40 (1.35)	99.52 (1.36)	-0.08587	-3.8 (7.4)	-9.6 (7.7)
0.05810	0.02199	22.352	85.70 (1.33)	99.90 (1.35)	-0.12009	1.5 (7.2)	-3.2 (7.5)
0.07530	0.02849	28.926	85.57 (1.32)	99.72 (1.34)	–	–	-
0.10134	0.03835	38.739	86.12 (1.30)	100.47 (1.32)	-0.20415	8.7 (7.0)	4.8 (7.2)
0.11999	0.04541	45.757	86.18 (1.29)	100.55 (1.31)	-0.23880	13.4 (6.9)	10.7 (7.2)
0.14712	0.05567	55.866	86.48 (1.27)	100.98 (1.29)	-0.28787	19.6 (6.7)	18.4 (7.0)
0.16387	0.06201	62.102	86.51 (1.26)	101.02 (1.28)	-0.31804	20.0 (6.7)	18.5 (7.0)
0.19439	0.07356	73.374	86.63 (1.24)	101.21 (1.26)	-0.37043	26.1 (6.6)	26.2 (6.9)
0.21549	0.08155	81.129	86.67 (1.23)	101.29 (1.25)	-0.40602	28.6 (6.5)	29.7 (6.8)

Table 4.3 The concentration dependences of relative densities, relative massic heat capacities, apparent molar volumes and apparent molar heat capacities of aqueous solutions of $Dy(ClO_4)_3$, component 2, in $HClO_4$ (component 3) at T = (288.15, 298.15, 313.15, and 328.15) K. Uncertainties are given in parentheses.

m_2 /mol kg^{-1}	m_3 /mol kg^{-1}	$\rho_{expt} - \rho^o$ /kg m^{-3}	$V_{\phi,expt}$ /cm^3 mol^{-1}	$V_{\phi,2}$ /cm^3 mol^{-1}	$c_{p\,expt} - c_p^{\,o}$ /J K^{-1} g^{-1}	$C_{p,\phi,expt}$ /J K^{-1} mol^{-1}	$C_{p,\phi,2}$ /J K^{-1} mol^{-1}
			T = 288.15 K				
0.03067	0.01409	12.106	75.81 (1.18)	90.87 (1.20)	-0.06838	-95.9 (7.1)	-125.7 (7.4)
0.06230	0.02862	24.484	76.06 (1.16)	91.16 (1.17)	-0.13573	-85.9 (6.6)	-114.9 (6.9)
0.09216	0.04234	36.031	76.59 (1.14)	91.91 (1.15)	-0.19637	-74.0 (6.4)	-100.4 (6.7)
0.12840	0.05899	49.936	76.90 (1.11)	92.34 (1.13)	-0.26725	-64.9 (6.3)	-90.0 (6.6)
0.15970	0.07337	61.815	77.23 (1.10)	92.81 (1.11)	-0.32605	-58.1 (6.1)	-82.3 (6.5)
0.18742	0.08610	72.268	77.42 (1.08)	93.09 (1.10)	-0.37567	-49.8 (6.0)	-71.9 (6.4)
0.23068	0.10598	88.432	77.69 (1.06)	93.47 (1.08)	-0.45087	-41.8 (5.9)	-62.6 (6.2)
0.26765	0.12296	102.061	77.99 (1.04)	93.91 (1.06)	-0.51115	-32.0 (5.7)	-50.1 (6.1)
0.30446	0.13987	115.574	78.10 (1.02)	94.08 (1.04)	-0.56993	-26.5 (5.6)	-43.6 (6.0)
0.34677	0.15931	130.895	78.34 (1.00)	94.43 (1.02)	-0.63431	-19.6 (5.5)	-35.1 (5.8)
			T = 298.15 K				
0.02211	0.01016	8.632	78.89 (1.19)	94.65 (1.21)	-0.04826	-60.3 (7.3)	-81.9 (7.6)
0.06052	0.02780	23.477	79.23 (1.15)	95.08 (1.16)	-0.12818	-44.0 (6.5)	-61.8 (6.8)
0.09235	0.04242	35.618	79.64 (1.13)	95.67 (1.14)	-0.19121	-33.3 (6.3)	-48.5 (6.6)
0.12632	0.05803	48.470	80.09 (1.11)	96.32 (1.12)	-0.25588	-25.0 (6.1)	-38.3 (6.4)
0.15832	0.07273	60.406	80.49 (1.09)	96.92 (1.10)	-0.31433	-17.8 (6.0)	-29.5 (6.3)
0.18202	0.08362	69.219	80.72 (1.07)	97.25 (1.09)	-0.35671	-14.9 (5.9)	-26.4 (6.2)
0.22864	0.10504	86.433	80.86 (1.05)	97.49 (1.07)	-0.43679	-8.9 (5.7)	-19.7 (6.1)
0.26707	0.12270	100.258	81.46 (1.03)	98.39 (1.05)	-0.49790	1.5 (5.6)	-6.2 (5.9)
			T = 313.15 K				
0.03141	0.01443	11.978	83.68 (1.16)	100.80 (1.18)	-0.06650	-22.4 (6.7)	-35.1 (7.0)
0.09373	0.04306	35.399	84.25 (1.11)	101.51 (1.13)	-0.18927	2.0 (6.1)	-3.1 (6.4)
0.12549	0.05765	47.183	84.41 (1.09)	101.76 (1.11)	-0.24875	6.8 (6.0)	2.6 (6.3)
0.15858	0.07285	59.341	84.62 (1.08)	101.98 (1.10)	-0.30856	11.1 (5.9)	7.6 (6.2)
0.19432	0.08927	72.346	84.82 (1.06)	102.40 (1.08)	-0.37008	18.0 (5.7)	16.4 (6.1)
0.23177	0.10648	85.865	84.93 (1.04)	102.60 (1.06)	-0.43257	22.4 (5.6)	21.6 (6.0)
0.26614	0.12265	98.140	85.06 (1.02)	102.84 (1.04)	-0.48786	26.0 (5.5)	25.8 (5.9)
0.30702	0.14104	112.594	85.21 (1.00)	103.10 (1.02)	-0.55117	29.9 (5.4)	30.2 (5.8)
			T = 328.15 K				
0.03033	0.01393	11.432	85.64 (1.16)	102.91 (1.18)	-0.06398	-14.7 (6.7)	-25.9 (7.0)
0.05839	0.02682	21.873	86.34 (1.14)	103.87 (1.15)	-0.12015	1.2 (6.3)	-4.9 (6.6)
0.09059	0.04162	33.767	86.61 (1.11)	104.26 (1.13)	-0.18201	13.0 (6.1)	10.6 (6.4)
0.12163	0.05588	45.106	86.93 (1.10)	104.72 (1.11)	-0.24006	17.1 (6.0)	15.3 (6.3)
0.15873	0.07292	58.508	87.31 (1.08)	105.30 (1.09)	-0.30636	23.9 (5.8)	24.0 (6.1)
0.19856	0.09122	72.773	87.50 (1.05)	105.62 (1.07)	-0.37582	25.3 (5.7)	24.8 (6.0)
0.22556	0.10362	82.368	87.58 (1.04)	105.98 (1.04)	-0.42086	28.2 (5.6)	28.2 (6.0)
0.26247	0.12058	95.370	87.70 (1.02)	106.03 (1.03)	-0.47909	35.7 (5.5)	38.3 (5.8)
0.30224	0.13885	109.289	87.70 (1.00)	106.00 (1.01)	-0.54067	39.3 (5.4)	42.6 (5.7)
0.34677	0.15931	124.747	87.65 (0.98)	102.91 (1.18)	-0.60709	42.4 (5.3)	46.1 (5.6)

Table 4.4 The concentration dependences of relative densities, relative massic heat capacities, apparent molar volumes and apparent molar heat capacities of aqueous solutions of $Sm(ClO_4)_3$, component 2, in $HClO_4$ (component 3) at T = (288.15, 298.15, 313.15, and 328.15) K. Uncertainties are given in parentheses.

m_2 /mol kg^{-1}	m_3 /mol kg^{-1}	$\rho_{expt} - \rho^o$ /kg m^{-3}	$V_{\phi,expt}$ /cm^3 mol^{-1}	$V_{\phi,2}$ /cm^3 mol^{-1}	$c_{p\,expt} - c_p^o$ /J K^{-1} g^{-1}	$C_{p,\phi,expt}$ /J K^{-1} mol^{-1}	$C_{p,\phi,2}$ /J K^{-1} mol^{-1}
			T = 288.15 K				
0.03501	0.00102	12.628	87.01 (1.23)	88.30 (1.24)	–	–	–
0.07204	0.00211	25.822	88.04 (1.20)	89.34 (1.21)	-0.14292	-154.3 (6.9)	-158.2 (7.1)
0.10848	0.00317	38.680	88.71 (1.18)	90.04 (1.19)	-0.21094	-145.1 (6.7)	-148.9 (7.0)
0.14535	0.00425	51.576	89.22 (1.15)	90.56 (1.17)	-0.27582	-127.9 (6.5)	-131.5 (6.8)
0.19184	0.00561	67.673	89.77 (1.13)	91.13 (1.15)	-0.35300	-117.3 (6.3)	-120.7 (6.6)
0.23202	0.00679	81.462	90.12 (1.11)	91.48 (1.13)	-0.42085	-109.7 (6.2)	-113.0 (6.5)
0.27656	0.00809	96.574	90.56 (1.09)	91.94 (1.11)	-0.48829	-92.9 (6.0)	-95.9 (6.4)
0.32349	0.00946	112.351	90.93 (1.07)	92.32 (1.09)	-0.55778	-83.2 (5.9)	-86.0 (6.2)
0.37015	0.01083	127.837	91.36 (1.05)	92.76 (1.07)	-0.62345	-73.3 (5.8)	-75.9 (6.1)
0.41822	0.01223	143.658	91.69 (1.03)	93.10 (1.05)	-0.68889	-65.9 (5.6)	-68.4 (6.0)
			T = 298.15 K				
0.03542	0.00104	12.552	92.59 (1.21)	93.99 (1.23)	–	–	–
0.07376	0.00216	26.013	92.98 (1.18)	94.39 (1.20)	-0.14166	-94.3 (6.6)	-96.9 (6.9)
0.11131	0.00326	39.076	93.34 (1.16)	94.76 (1.18)	-0.20895	-80.0 (6.4)	-82.4 (6.7)
0.15052	0.00440	52.573	93.81 (1.14)	95.25 (1.16)	-0.27594	-68.2 (6.3)	-70.4 (6.6)
0.19182	0.00561	66.643	94.26 (1.12)	95.71 (1.14)	-0.34382	-58.4 (6.1)	-60.4 (6.5)
0.23340	0.00683	80.700	94.53 (1.10)	95.99 (1.12)	-0.40933	-49.6 (6.0)	-51.5 (6.3)
0.27750	0.00812	95.519	94.63 (1.08)	96.09 (1.10)	-0.47671	-41.8 (5.9)	-43.6 (6.2)
0.32201	0.00942	110.160	95.23 (1.06)	96.72 (1.08)	-0.54084	-35.3 (5.7)	-36.9 (6.1)
0.36945	0.01081	125.709	95.52 (1.04)	97.01 (1.06)	-0.60700	-28.7 (5.6)	-30.3 (6.0)
0.41822	0.01223	141.534	95.76 (1.02)	97.27 (1.04)	-0.67170	-21.3 (5.5)	-22.7 (5.8)
			T = 313.15 K				
0.03613	0.00106	12.567	97.76 (1.24)	99.25 (1.25)	-0.06955	-67.2 (7.1)	-69.3 (7.3)
0.11289	0.00330	38.874	98.56 (1.19)	100.08 (1.20)	-0.20636	-33.1 (6.5)	-34.4 (6.8)
0.15014	0.00439	51.454	98.92 (1.17)	100.46 (1.18)	-0.26874	-23.5 (6.3)	-24.6 (6.6)
0.19211	0.00562	65.487	99.29 (1.14)	100.84 (1.16)	-0.33628	-14.8 (6.2)	-15.7 (6.5)
0.23219	0.00679	78.770	99.55 (1.13)	101.11 (1.14)	-0.39840	-8.4 (6.1)	-9.3 (6.4)
0.27781	0.00812	93.738	99.83 (1.10)	101.40 (1.12)	-0.46690	-4.3 (5.9)	-5.1 (6.3)
0.32111	0.00939	107.839	99.96 (1.08)	101.54 (1.10)	-0.52902	0.7 (5.8)	0.0 (6.1)
0.36772	0.01075	122.828	100.21 (1.06)	101.80 (1.08)	-0.59315	6.0 (5.7)	5.4 (6.0)
0.41822	0.01223	138.938	100.35 (1.04)	101.94 (1.06)	-0.65940	12.2 (5.6)	11.7 (5.9)
			T = 328.15 K				
0.03665	0.00107	12.580	100.62 (1.24)	102.16 (1.25)	-0.07003	-52.4 (7.0)	-54.1 (7.3)
0.07269	0.00213	24.813	101.29 (1.21)	102.85 (1.23)	-0.13503	-28.8 (6.6)	-30.0 (6.9)
0.11101	0.00325	37.674	101.91 (1.19)	103.49 (1.20)	-0.20112	-13.4 (6.4)	-14.2 (6.7)
0.15092	0.00441	50.956	102.27 (1.16)	103.86 (1.18)	-0.26782	-6.5 (6.3)	-7.1 (6.6)
0.19122	0.00559	64.236	102.58 (1.14)	104.18 (1.16)	-0.33246	0.1 (6.1)	-0.5 (6.5)
0.23313	0.00682	77.916	102.83 (1.12)	104.45 (1.14)	-0.39760	3.6 (6.0)	3.1 (6.3)
0.27777	0.00812	92.354	103.05 (1.10)	104.67 (1.12)	-0.46339	11.0 (5.9)	10.6 (6.2)
0.32202	0.00942	106.560	103.13 (1.08)	104.76 (1.10)	-0.52607	17.1 (5.8)	16.9 (6.1)
0.37001	0.01082	121.757	103.35 (1.06)	104.99 (1.08)	-0.59141	22.7 (5.6)	22.6 (6.0)
0.41822	0.01223	136.877	103.52 (1.04)	105.17 (1.06)	-0.65469	26.9 (5.1)	26.9 (5.9)

$$V_{\phi,2} - \left\{\frac{6A_V \ln\left(1+b\sqrt{I}\right)}{b}\right\} = V_2^o + RTI\beta^{0V} + 2RTI\beta^{1V} f(I). \qquad (4.6)$$

For apparent molar heat capacities equation 4.7 was utilized:

$$C_{p,\phi,2} - \left\{\frac{6A_J \ln\left(1+b\sqrt{I}\right)}{b}\right\} = C_{p,2}^o - RT^2 I\beta^{0J} - 2RT^2 I\beta^{1J} f(I). \qquad (4.7)$$

The coefficients and constants used in these equations have been defined in Chapter 3. Values for V_2^o, β^{0V}, β^{1V}, $C_{p,2}^o$, β^{0J} and β^{1J} were obtained through regression analyses and are reported in table 4.5.

The temperature and concentration dependences of the apparent molar volumes and the apparent molar heat capacities of the investigated salts were modeled using modified Pitzer ion interaction equations. In these equations, the β^{0V}, β^{1V}, β^{0J} and β^{1J} constants from equations 4.6 and 4.7 were modeled as a function of temperature. HKF equations of state (Shock and Helgeson, 1988) were used to model the temperature dependences of V_2^o and $C_{p,2}^o$ values. These equations take the forms:

$$V_2^o = v_1 + \frac{v_2}{T-\Theta} - \omega Q \qquad (4.8)$$

$$\beta^{0V} = v_3 + v_4 T \qquad (4.9)$$

Table 4.5 Estimates of parameters to the Pitzer ion interaction model equations, shown as equations (4.6) and (4.7), for aqueous solutions of $Y(ClO_4)_3$, $Yb(ClO_4)_3$, $Dy(ClO_4)_3$, and $Sm(ClO_4)_3$ at T = (288.15, 298.15, 313.15, and 328.15) K and p = 0.1 MPa.

T /K	V°_2 /cm^3 mol^{-1}	$10^4\beta^{(0)V}$ /cm^3 kg mol^{-1}J^{-1}	$10^3\beta^{(1)V}$ /cm^3 kg mol^{-1}J^{-1}	$C_{p,2}^{\circ}$ /J K^{-1} mol^{-1}	$10^5\beta^{(0)}$ /kg mol^{-1} K^{-2}	$10^4\beta^{(1)}$ /kg mol^{-1} K^{-2}
			$Y(ClO_4)_3$			
288.15	85.12±0.14	4.095±0.618	-4.331±0.424	-188.08±1.73	4.658±0.265	-2.589±0.181
298.15	90.32±0.09	1.077±0.307	-3.531±0.237	-140.49±1.12	1.019±0.126	-1.341±0.973
313.15	94.45±0.11	-2.693±0.372	-2.190±0.277	-101.68±1.46	–0.3545 ± 0.1563	-1.464±0.116
328.15	96.08±0.18	-1.545±0.659	-4.042±0.470	-105.57±6.20	-1.648±0.676	-1.337 ± 0.482
			$Yb(ClO_4)_3$			
288.15	83.46±0.22	-2.933±1.978	-1.961±0.942	-166.79±4.00	5.633±1.243	-3.553±0.601
298.15	87.12±0.13	-2.476±1.272	-1.727±0.568	-141.65±1.32	-0.8389 ±0.4434	-0.5571 ±0.2009
313.15	93.57±0.13	-3.881±1.008	-4.990±0.490	-89.44±2.45	-1.100 ±0.606	-1.557±0.299
328.15	96.29±0.30	3.557±2.405	-7.577±1.146	-68.79±2.31	2.218±0.581	-3.662±0.277
			$Dy(ClO_4)_3$			
288.15	87.98±0.27	2.285±1.075	-3.677±0.779	-171.58±4.84	3.891±0.657	-2.719±0.476
298.15	92.20±0.37	7.425±2.226	-6.221±1.272	-133.19±4.03	1.199±0.807	-1.523±0.461
313.15	97.99±0.13	-1.773±0.528	-6.390±0.353	-101.61±3.06	1.013 ±0.400	-1.183 ±0.267
328.15	98.53±0.22	-3.987±0.793	-2.558 ±0.568	-95.26±5.45	-1.222 ±0.587	-1.525±0.421
			$Sm(ClO_4)_3$			
288.15	85.00±0.07	0.9315 ±0.2192	-1.402±0.173	-234.67±9.08	3.001 ±0.756	-1.057±0.715
298.15	91.16±0.21	2.142±0.662	-4.758±0.524	-187.01±1.39	0.1222 ±0.1062	-0.2829 ±0.1013
313.15	95.92±0.16	-0.4445 ±0.4439	-4.547 ±0.3549	-142.93±2.23	-1.096±0.201	-0.6303 ±0.1634
328.15	97.95 ±0.09	-2.625 ±0.269	-3.744 ±0.214	-131.58 ±4.62	-1.288 ±0.399	-0.9746 ±0.3219

$$\beta^{1V} = \frac{v_5}{T} + v_6 + v_7 T \tag{4.10}$$

$$C^{o}_{p,2} = c_1 + \frac{c_2}{(T-\Theta)^2} + \omega T X \tag{4.11}$$

$$\beta^{0J} = \frac{c_3}{T} + c_4 + c_5 T \tag{4.12}$$

$$\beta^{1J} = \frac{c_6}{T} + c_7 + c_8 T \tag{4.13}$$

The fitting parameters v_i (i=1-7) and c_i (i=1-8) for all perchlorate salts analysed were also obtained through regression analyses and are reported in Tables 4.6 and 4.7. Values for V^{o}_{2} and $C^{o}_{p,2}$ calculated from the HKF equations differ slightly from those obtained from equations 4.6 and 4.7. The single temperature fits do not include temperature dependent terms, and predict the infinite dilution values using only the concentration dependent measurements at a particular temperature. The global fits, on the other hand, place emphasis on changes in the thermodynamic properties as a function of temperature and concentration. The emphasis on a larger data set causes the rapidly changing values of $V_{\phi,2}$ and $C_{p\phi,2}$ at low molalities to be less well modeled. For this reason both modeling techniques were used.

Table 4.6 Estimates of parameters to equations (9), (10), and (11) which model the temperature dependences of $V_{\phi,2}$ values for aqueous solutions of $Y(ClO_4)_3$, $Yb(ClO_4)_3$, $Dy(ClO_4)_3$, and $Sm(ClO_4)_3$ at p = 0.1 MPa.

Parameter	$Y(ClO_4)_3$	$Yb(ClO_4)_3$	$Dy(ClO_4)_3$	$Sm(ClO_4)_3$
υ_1 /(cm^3 mol^{-1})	135.90 ± 0.98	135.18 ± 0.70	137.11 ± 1.42	139.35 ± 0.68
υ_2 /(cm^3 K mol^{-1})	-2198 ± 71	-2220 ± 46	-2096 ±105	-2393 ± 50
10^3 υ_3 /(kg mol^{-1} MPa^{-1})	2.550 ± 1.393	4.913 ± 1.274	5.804 ± 2.036	3.028 ± 0.780
10^5 υ_4 /(kg mol^{-1} K^{-1} MPa^{-1})	-0.8381 ± 0.4534	-1.580 ± 0.380	-1.874 ± 0.657	-0.9856 ± 0.2525
υ_5 /(kg mol^{-1} K MPa^{-1})	-81.59 ± 10.17	-1.412 ± 0.395	30.23 ± 15.14	52.26 ± 6.50
υ_6 /(kg mol^{-1} MPa^{-1})	0.5378 ± 0.0607	–	-0.2115 ± 0.0901	-0.3292 ± 0.0386
10^4 υ_7 /(kg mol^{-1} K^{-1} MPa^{-1})	-8.946 ± 0.914	–	3.547 ± 1.353	5.044 ± 0.577

Table 4.7 Estimates of parameters to equations (12), (13), and (14) which model the temperature dependences of $C_{p,\phi,2}$ values for aqueous solutions of $Y(ClO_4)_3$, $Yb(ClO_4)_3$, $Dy(ClO_4)_3$, and $Sm(ClO_4)_3$ at p = 0.1 MPa.

Parameter	$Y(ClO_4)_3$	$Yb(ClO_4)_3$	$Dy(ClO_4)_3$	$Sm(ClO_4)_3$
c_1 /(J K^{-1} mol^{-1})	198.47 ± 5.60	228.33 ± 6.33	200.36 ± 7.06	171.69 ± 5.72
$10^{-5}c_2$ /(J K mol^{-1})	-6.636 ± 0.280	-7.123 ± 0.322	-6.274 ± 0.361	-7.542 ± 0.359
c_3 /(kg mol^{-1} K^{-1})	-1.991 ± 0.264	-1.640 ± 0.687	-1.532 ± 0.392	-1.377 ±0.196
10^2 c_4 /(kg mol^{-1} K^{-2})	1.254 ± 0.170	1.034 ± 0.444	0.9636 ± 0.2536	0.8654 ± 0.1263
10^5 c_5 /(kg mol^{-1} K^{-3})	-1.969 ± 0.273	-1.629 ± 0.715	-1.511 ± 0.409	-1.355 ± 0.203
c_6 /(kg mol^{-1} K^{-1})	11.40 ± 1.31	6.824 ± 2.480	7.728 ± 1.821	4.995 ± 1.153
c_7 /(kg mol^{-1} K^{-2})	-0.07355 ±0.00831	-0.04405 ± 0.01588	-0.04970 ± 0.01164	-0.03253 ± 0.00726
10^5 c_8 /(kg mol^{-1} K^{-3})	11.88 ±1.32	7.173 ± 2.537	8.022 ± 1.856	5.309 ± 1.142

4.4 Comparison of our experimental data with existing experimental data

The limited data existing for these systems agrees favourably with the data collected in this study. Figure 4.1 describes the apparent molar volumes of $Yb(ClO_4)_3$ measured at T = 298.15K and compares the values obtained in this study to those reported by Xaio and Tremaine (1997). The $V_{\phi,2}$ values reported by Spedding, Baker and Walters (1975) are also shown in this plot. Values for $V_{\phi,2}$ obtained in this study deviate from those of Xaio and Tremaine (1997) by less than 1 cm^3mol^{-1}. Even better agreement is achieved with the $V_{\phi,2}$ data of Spedding *et al.* (1966). $C_{p,\phi,2}$ values for $Yb(ClO_4)_3$ at T = 298.15K are compared in figure 4.2. Again, good agreement is found for experimental data presented here and the data collected by Xaio and Tremaine (1997). The heat capacity data collected by Spedding *et al.* (1975) agreed with the data from this study at higher concentrations, but at lower concentrations there is significant deviation. This is most likely due to the differing measurement techniques used in the two studies. The batch calorimetry technique used by Spedding *et al.* (1975) does not produce massic heat capacities with the precision achieved by the flow calorimetry technique used in this study. Figure 4.3 compares the data presented here to the apparent molar heat capacity data collected by Babakulov and Latysheva (1974). It can be seen that, like the comparison with Spedding's $Yb(ClO_4)_3$ data (1975), good agreement is found for higher concentrations but at lower concentrations the agreement is poor.

4.5 Comparison with existing HKF models

Shock and Helgeson (1988) have compiled thermodynamic data for many different ionic systems and used the HKF equations of state to predict single ion

Figure 4.1 Comparison of $V_{\phi,2}$ values for $Yb(ClO_4)_3$ at T=298.15K and p=0.1 MPa to available literature values.

(•) data reported in this study, (+) Spedding (1966), (×) Xaio and Tremaine (1997)

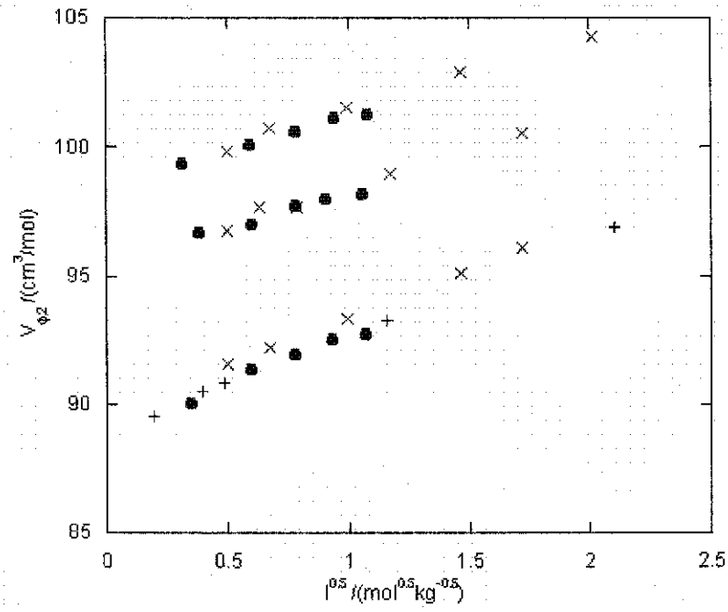

Figure 4.2 Comparison of $C_{p,\phi,2}$ collected at T=(298.15, 328.15) K and p=0.1 MPa in this study to literature data.

Spedding and co-workers (1975), Xaio and Tremaine (1997). (•) data collected in this study, (+) Spedding *et al.*, (×) Xaio and Tremaine.

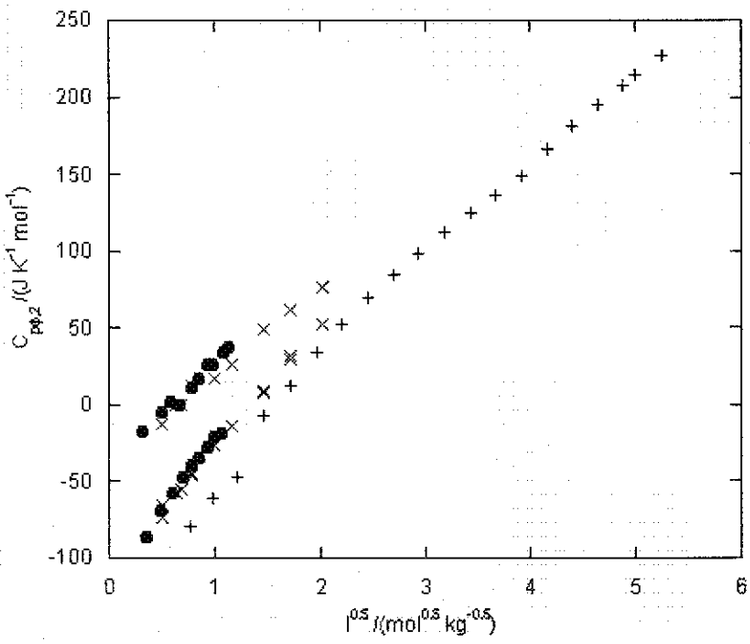

Figure 4.3 Comparison of $C_{p\phi,2}$ data for $Y(ClO_4)_{3(aq)}$ at T=298.15K and p=0.1 MPa collected in this study to that reported by Babakulov and Latysheva (1974). (•) this study, (+) Babakulov and Latysheva.

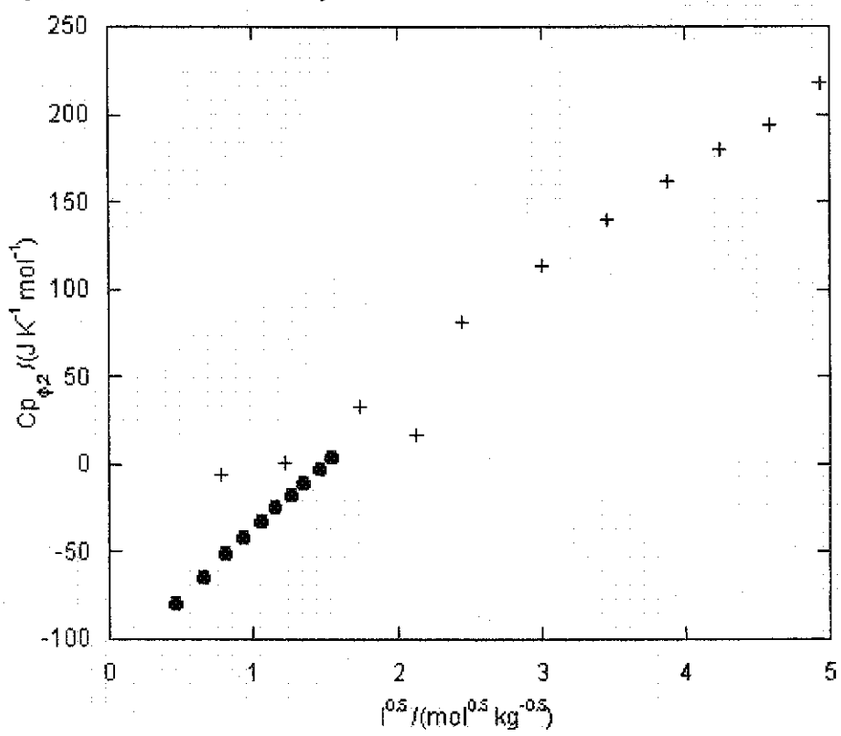

thermodynamic property values, including values for apparent molar volume and apparent molar heat capacity for a large number of ions. Among the systems compiled were several trivalent cations, including Y^{3+}, Yb^{3+}, Dy^{3+} and Sm^{3+}, as well as the perchlorate anion, ClO_4^-. The majority of rare earth thermodynamic data available at the time of the Shock and Helgeson study was reported by Spedding and co-workers (1966, 1975). Table 4.8 compares infinite dilution apparent molar volumes and heat capacities to those reported in the literature. Figures 4.4-4.7 compare the infinite dilution apparent molar volumes predicted by Shock and Helgeson (1988) to the single temperature and temperature-dependent infinite dilution apparent molar heat capacities obtained in this study while Figures 4.8-4.11 compare the apparent molar heat capacities at infinite

Table 4.8 Comparison of our calculated V^{o}_{2} and $C_{p,2}^{o}$ values with those previously reported in the literature for aqueous solutions of $Y(ClO_4)_3$, $Yb(ClO_4)_3$, $Dy(ClO_4)_3$, and $Sm(ClO_4)_3$ at T = 298.15 K and p = 0.1 MPa.

Species	V^{o}_{2} / cm^3 mol^{-1}	$C_{p,2}^{o}$ / J K^{-1} mol^{-1}
$Y(ClO_4)_3$	90.32 (0.09), 91.91[c]	–140.49 (1.12), –150.5[c],
$Yb(ClO_4)_3$	87.12 (0.22), 88.325[a], 87.88	–141.65 (1.32), –137.7[c], –
	(0.10)[b], 87.70[c]	280.3[d], `–137.9 (2.0)[b], -137.65[e]
$Dy(ClO_4)_3$	92.20 (0.37), 91.593[a], 91.42[c]	–133.19 (4.03), –150.1[c], –
		212.0[d], –150.02[e]
$Sm(ClO_4)_3$	91.16 (0.21), 90.393[a], 89.87[c]	–187.01 (1.39), –197.2[c], –
		251.6[d], –197.13[e]

[a] – (Spedding, Shiers, Brown, Derer, Swanson, Habenschuss, 1975), [b] – (Xaio, Tremaine, 1997), [c] – (Sabot, Maestro, 1995), [d] – (Spedding, Baker, Walters, 1975), [e] – (Criss, Millero, 1999) Uncertainties of our values are reported in parentheses

Figure 4.4 Comparison plot of infinite dilution apparent molar volumes of $Y(ClO_4)_3$ at p=0.1 MPa.

(•) equation 4.6, - - - - - - - - Equation 4.8, _____ – Shock and Helgeson (1988).

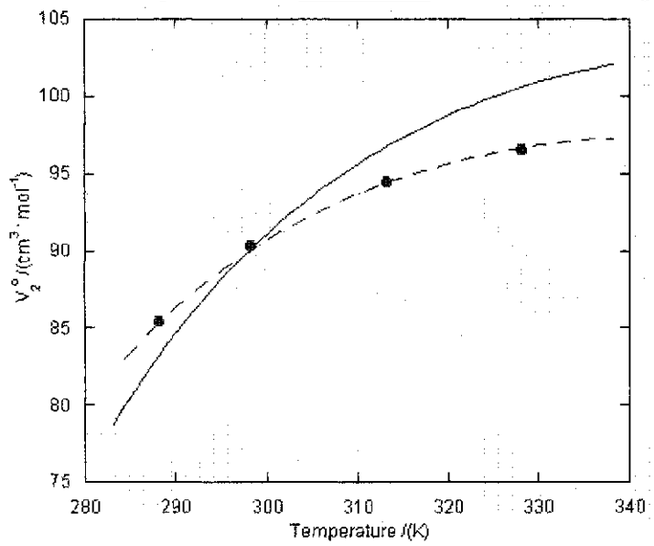

Figure 4.5 Comparison plot of infinite dilution apparent molar volumes of $Yb(ClO_4)_3$ at p=0.1 MPa.

(•) Equation 4.6, (+) Xaio and Tremaine (1997), - - - - - - - - – Equation 4.6, _____ – Shock and Helgeson (1988).

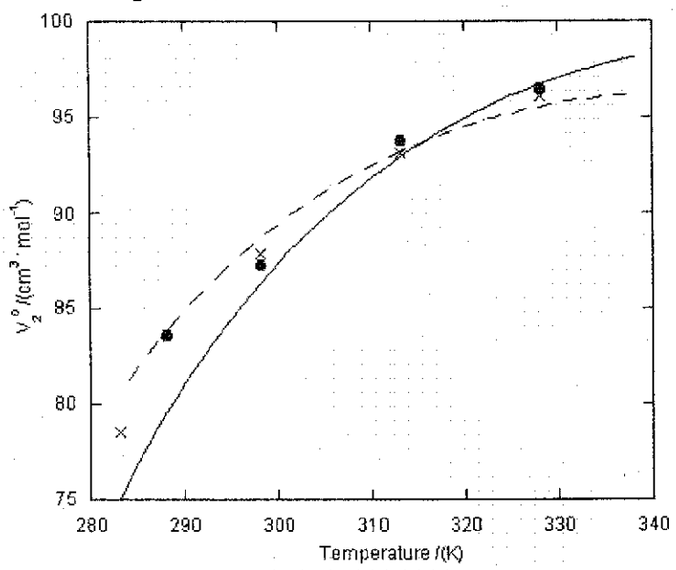

Figure 4.6 Comparison plot of infinite dilution apparent molar volumes values of $Dy(ClO_4)_3$ at p=0.1 MPa.

(•) Equation 4.6, - - - - - - - Equation 4.8, _____ – Shock and Helgeson (1988).

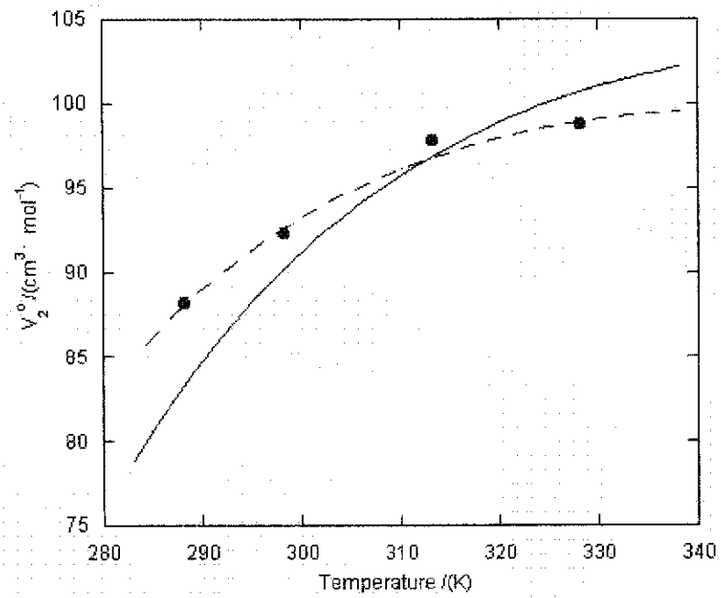

Figure 4.7 Comparison plot of infinite dilution apparent molar volumes values of $Sm(ClO_4)_3$ at p=0.1 MPa.

(•) Equation 4.6, - - - - - - - - Equation 4.8, _____ – Shock and Helgeson (1988).

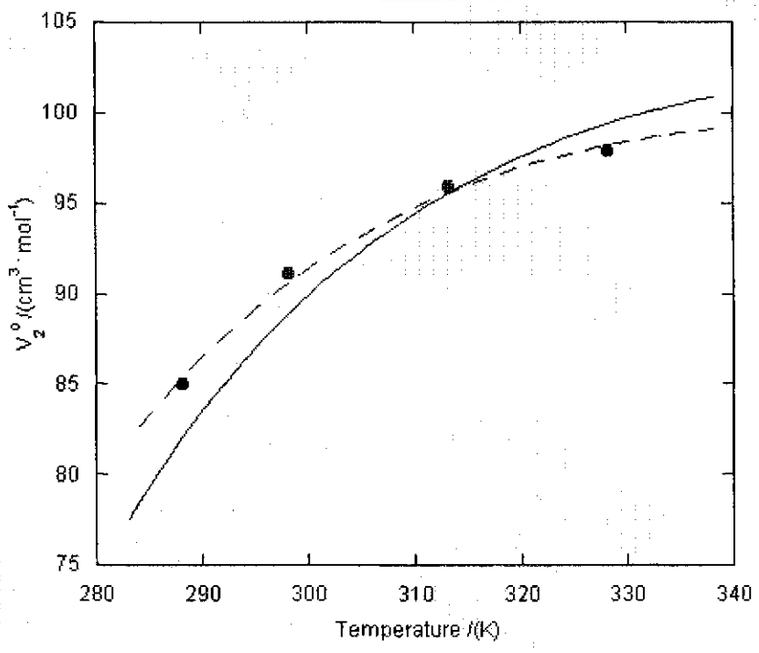

Figure 4.8 Comparison plot of infinite dilution apparent molar heat capacities of $Y(ClO_4)_3$ at p=0.1 MPa.

(•) Equation 4.7, - - - - - - - - Equation 4.11, _____ – Shock and Helgeson (1988).

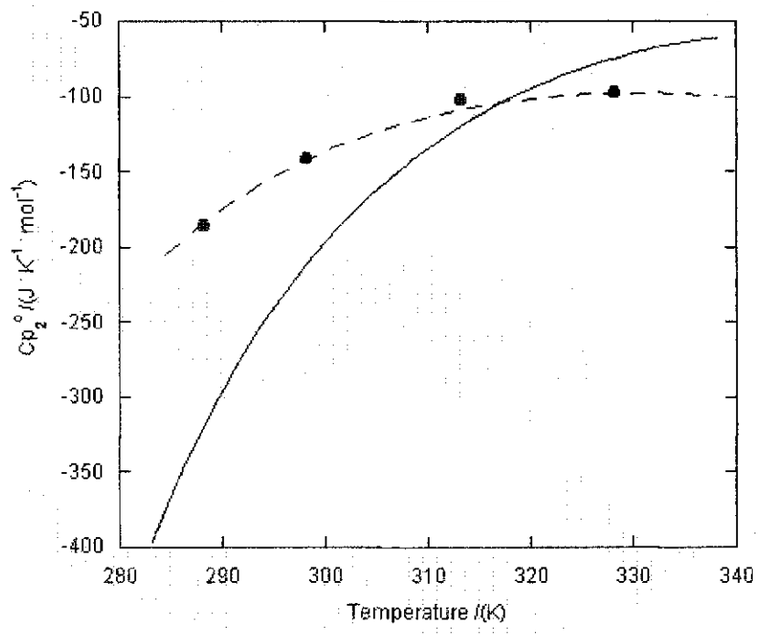

Figure 4.9 Comparison plot of infinite dilution apparent molar heat capacities of $Yb(ClO_4)_3$ at p=0.1 MPa.

(•) Equation 4.7, (+) Xaio and Tremaine (1997), - - - - - - - – Equation 4.11, _____ – Shock and Helgeson (1988).

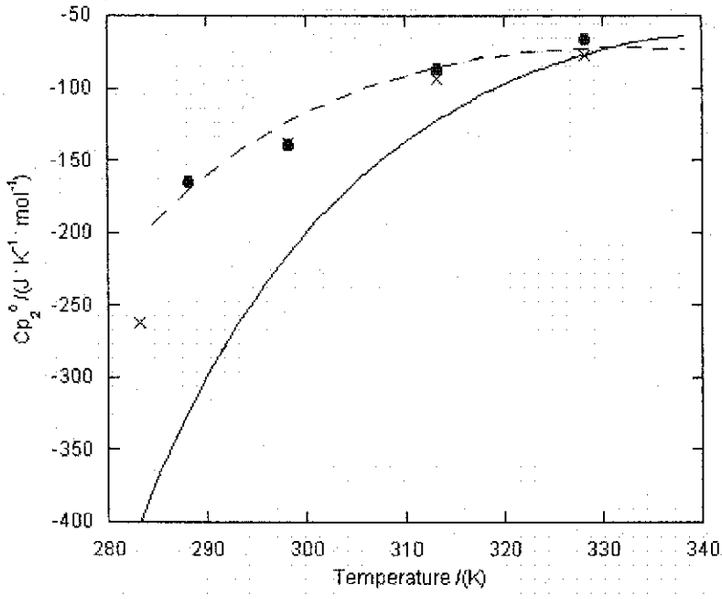

Figure 4.10 Comparison plot of infinite dilution apparent molar heat capacities of $Dy(ClO_4)_3$ at p=0.1 MPa.

(•) Equation 4.7, Broken line – Equation 4.11, Solid line – Shock and Helgeson (1988).

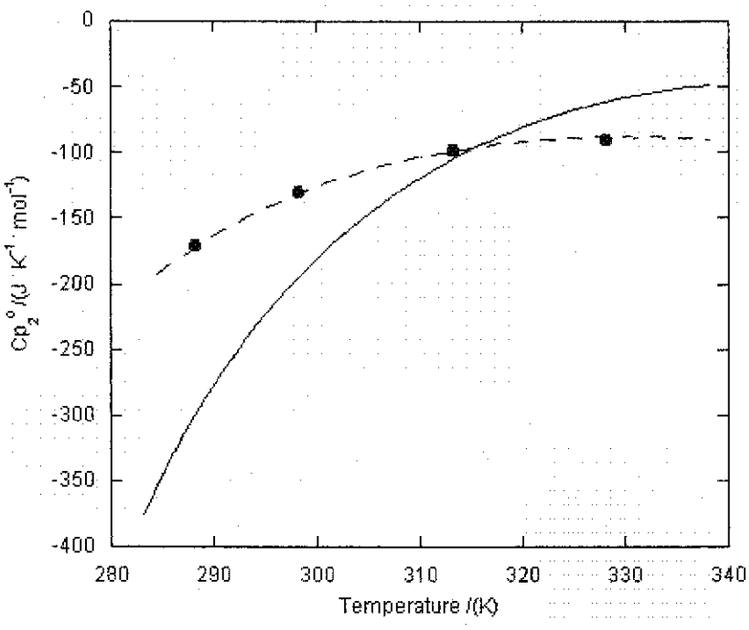

Figure 4.11 Comparison plot of infinite dilution apparent molar heat capacities of $Sm(ClO_4)_3$ at p=0.1 MPa.

(•) Equation 4.7, - - - - - - - – Equation 4.11, _____ –Shock and Helgeson (1988).

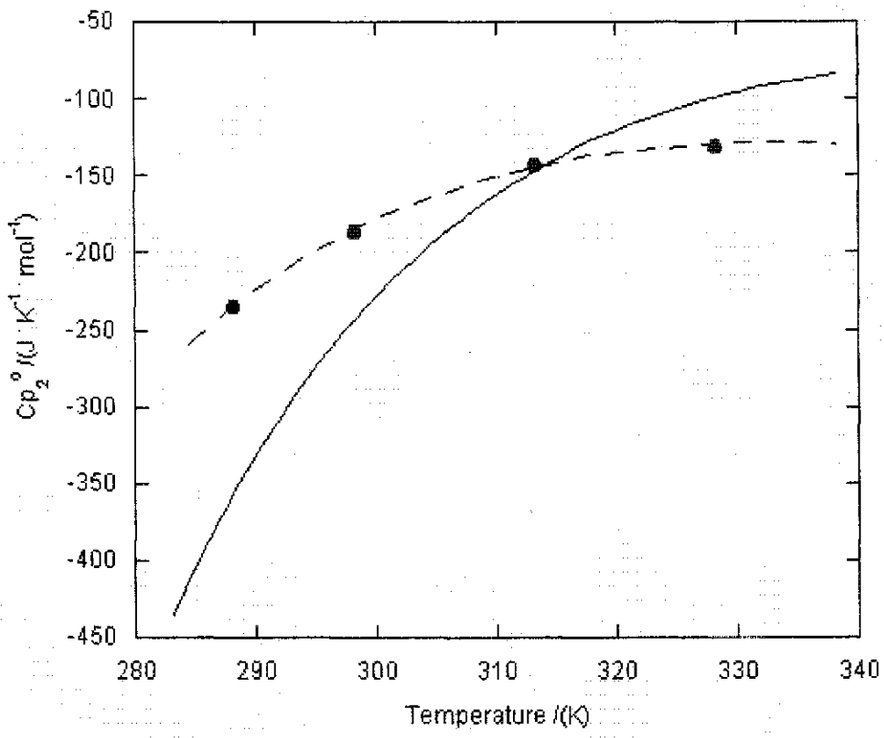

dilution. In each plot, although the infinite dilution curves produced by each model intersect at one temperature, the overall temperature dependences predicted by Shock and Helgeson (1988) deviate from the empirically determined temperature-dependent apparent molar volumes and apparent molar heat capacities. There is greater deviation in the infinite dilution apparent molar heat capacity predictions. For the $Dy(ClO_4)_3$ system this difference reaches a maximum of 100 $JK^{-1}mol^{-1}$.

Batch calorimetry necessitates solutions of high concentrations relative to the more sensitive Picker flow technique utilized in this study. For accurate prediction of

infinite dilution properties, experimental heat capacity values at low solution concentrations are required.

In addition, the temperature dependences of the apparent molar properties of the trivalent rare earth cations were modeled by Shock and Helgeson (1988) using only data collected at 298.15 K. The measurements made in this study were taken at T=(288.15, 298.15, 313.15 and 328.15) K, allowing empirical modeling of the infinite dilution apparent molar volumes and apparent molar heat capacities.

4.6 Single ion values

The thermodynamic properties of an aqueous salt solution can be represented as the sum of the contributions made by its constituent ions. Using the convention that $Y^{o}_{(H+)} = 0$, the infinite dilution apparent molar heat capacity and volume values of the trivalent cations investigated in this study can be determined. Single ion values for the perchlorate anion can be obtained from the apparent molar volume and apparent molar heat capacity data reported by Hovey (1988) for aqueous perchloric acid solutions. Using the convention identified above:

$$Y^{o}_{ClO_4^-} = Y^{o}_{HClO_4} \tag{4.14}$$

The infinite dilution values of the investigated trivalent metal cations can be obtained from the equation:

$$Y^{o}_{R^{3+}} = Y^{o}_{R(ClO_4)_3} - 3Y^{o}_{ClO_4^-}, \tag{4.15}$$

where R identifies the trivalent metals examined in this study. The single ion values calculated in this manner are reported in table 4.9 along with those previously reported by Marriott *et al* (2001). Marriott's values of $V^{o}_{\phi,R^{3+}}$ were calculated from experimental V_{ϕ} data reported by Xaio and Tremaine (1997) and Spedding *et al.* (1966, 1975), while Marriott's values of $C^{o}_{p,\phi,R^{3+}}$ were taken directly from the compilation of Criss and Millero (1999).

Criss and Millero (1999) compiled data reported by Spedding (1975) and Xaio and Tremaine (1997), fitting all reported data for all salts (Cl^-, ClO_4^-, and NO_3^-) with a common cation to a single Pitzer equation. The calculations used by Criss and Millero (1999) do not mention any correction to compensate for the differing amounts of complex formation resulting from different anions. Modeling data in this way does not lead to the most precise values for single ion heat capacities. Instead, average values resulting from the dissociated salts and any complexes present are obtained. In addition, as mentioned earlier, the heat capacities reported by Spedding *et al.* (1975) are of lower precision than those reported here at low salt concentrations.

In spite of the above, the single ion apparent molar data reported here and those reported by Marriott agree well, with a maximum difference of $1.7 cm^3 mol^{-1}$ for volumes and $14.6 JK^{-1}mol^{-1}$ for heat capacities.

4.7 Conclusions

The literature is far from complete with respect to thermodynamic data for aqueous salts of the trivalent rare earth cations. Many systems have not been studied and

Table 4.9 A comparison of literature and calculated $V_2^o(R^{3+})$ and $C_{p2}^o(R^{3+})$ values for R^{3+} = (Y^{3+}, Yb^{3+}, Dy^{3+}, and Sm^{3+}) at T = (288.15, 298.15, 313.15, and 328.15) K.

T /K			$V_2^o(R^{3+})$ /cm^3mol^{-1}		
	Y^{3+}	Yb^{3+}	Dy^{3+}	Sm^{3+}	ClO_4^-
288.15	-42.38 (0.4)	-44.0 (0.4)	-39.5 (0.4)	-42.5 (0.4)	42.5 (0.2)
298.15	-42.0 (0.4), -40.21[a]	-45.2 (0.4), -44.425 (0.3)[a]	-40.0 (0.5), –40.70 (0.3)[a]	-41.1 (0.4), -42.25 (0.3)[a]	44.1 (0.2)
313.15	-43.6 (0.4)	-44.4 (0.4)	-40.1 (0.4)	-42.1 (0.4)	46.0 (0.2)
328.15	-47.0 (0.4)	-45.9 (0.5)	-43.7 (0.4)	-44.3 (0.4)	47.4 (0.2)
			$C_{p2}^o(R^{3+})$ /$JK^{-1}mol^{-1}$		
	Y^{3+}	Yb^{3+}	Dy^{3+}	Sm^{3+}	ClO_4^-
288.15	-47 (4)	-26 (5)	-31 (6)	-94 (10)	-47 (2)
298.15	-65 (4), –70 (10)[a]	-67 (4), –57.2 (5)[a]	-58 (5), –69.6 (10)[a]	-112 (4), –116.7 (10)[a]	-25 (2)
313.15	-78 (4)	-65 (4)	-78 (4)	-119 (4)	-8 (2)
328.15	-91 (7)	-54 (4)	-80 (6)	-117 (6)	-5 (2)

[a] – Marriott , 2001.

nearly all that have were investigated by Spedding and co-workers at T = 298.15K. The calorimetric techniques used by Spedding and co-workers were not suited to low concentration measurements and thus extrapolations to infinite dilution were not precise. The data presented here achieve greater precision at low molalities than those of Spedding and co-workers, and thus can be used with greater confidence for infinite dilution extrapolations.

The only temperature dependent measurements of apparent molar heat capacities thus far are the experiments performed by Xaio and Tremaine (1997) which are limited to six perchlorates and one chloride. Further, the predominant model used by geochemists

for calculation of elevated temperature and pressure apparent molar volumes and heat capacities (HKF equations of state reported by Shock and Helgeson (1988)) are based on what we have identified as less precise thermodynamic data than those reported in this study. The data reported in this chapter provide some of the temperature dependent information required to fully characterize the thermodynamics of the trivalent rare earth salts.

5 RARE EARTH CHLORIDE STUDY

The previous chapter reported volumetric and thermochemical properties for aqueous solutions of several perchlorate salts containing trivalent metal cations. To complement the perchlorate salt investigation, this chapter reports volumetric and thermochemical properties of aqueous solutions of the corresponding trivalent metal chlorides. Relative densities and massic heat capacities have been measured at four temperatures and apparent molar volumes and heat capacities have been calculated. The concentration and temperature dependences of the apparent molar volumes and heat capacities have been modeled using the Pitzer ion interaction equations discussed previously in Chapters 3 and 4. Calculated infinite dilution apparent molar properties of the aqueous chloride salts provide an independent check of the single ion thermodynamic data calculated in the previous chapter.

This chapter also considers the effects of complex ion formation within the aqueous chloride salt systems and provides qualitative evidence in support of the earlier complex formation studies reported by Wood (1990a, 1990b).

5.1 Previous studies

Spedding and co-workers (Spedding, 1966b, 1975; Habenschuss, 1976; Gildseth, 1975) have reported the apparent molar volumes of many aqueous rare earth chloride systems. The required densities were measured using a variety of techniques including a magnetically controlled float (Spedding 1966b), dilatometry (Habenschuss, 1975; Gildseth, 1976) and pycnometry (Spedding, 1975). The dilatometry studies comprised measurements at temperatures ranging from T = 278.15K to T = 353.15K while the

magnetically controlled float and pycnometric experiments were performed at T = 298.15K. All studies were performed at p = 0.1MPa. Spedding and coworkers (Spedding, 1966a, 1975c) also reported the apparent molar heat capacities of many aqueous rare earth chloride systems at T = 298.15K and p = 0.1MPa. These measurements were invariably made using an adiabatic batch calorimeter (Spedding et al., 1975c). Pitzer *et al.* (1978) used a single equation to reevaluate the apparent molar volumes reported by Spedding *et al.* (1975b) which resulted in revised infinite dilution values. Shock and Helgeson also utilized the volumetric and thermochemical data reported by Spedding and coworkers (Spedding, 1966b, 1975b, 1975c, 1979, 1975d) to construct HKF equations of state for the aqueous trivalent metal cations and the chloride anion. The apparent molar volumes and apparent molar heat capacities reported by Karapet'yants *et al.* (1976) for aqueous solutions of YCl_3 at T = 298.15 and p = 0.1MPa provide a useful comparison for the values reported by Spedding and coworkers (1975b, 1966a).

5.2 Experimental

The preparation of stock acidified metal chloride solutions follows the procedure detailed in Chapter 4, the only significant change to the procedure being the replacement of perchloric acid with hydrochloric acid.

5.2.1 Stock solution preparation

Samples of pure rare earth oxide were dissolved in less than equivalent hydrochloric acid (BDH 36.5-38.0% assay). Excess hydrochloric acid was added to the

stock metal chloride solutions after all the oxide had dissolved to ensure a final pH less than pH = 3. The acidified stock solutions were filtered through fine sintered glass crucibles and subsequently found to be free of colloidal particles by shining a light through the solution and observing that no cone of light formed.

5.2.2 Stock solution standardization

Standardizations of the rare earth chloride stock solutions were performed according to the procedure detailed for the rare earth perchlorates in Chapter 4.

The concentrations of the trivalent metal cations in the various stock solutions were determined by titrating aliquots of each stock solution with EDTA. Xylenol orange was used as the indicator and the system was buffered to pH 5.5 using an acetic acid/sodium acetate buffer.

The acid concentration in each stock solution was determined by titration with the standard reference material tris(hydroxymethyl)aminomethane (THAM, 99.94±0.01 mol%, obtained from US Department of Commerce, National Bureau of Standards) using methyl red as the indicator.

The density of each stock solution was measured at the temperature at which the titrations were performed allowing conversion from the molar concentration scale to molal concentration scale.

5.2.3 Sample preparation

Sample solutions of the aqueous rare earth chloride were prepared by diluting portions of the stock solutions with pure, degassed water. For each investigated system,

four sets of ten solutions that ranged in concentration (0.05489 to 0.69779 mol kg^{-1} for YCl_3, 0.04560 to 0.46912 mol kg^{-1} for $YbCl_3$, 0.03274 to 0.35480 mol kg^{-1} for $DyCl_3$, 0.03659 to 0.39817 mol kg^{-1} for $SmCl_3$, and 0.03523 to 0.38566 mol kg^{-1} for $GdCl_3$) were prepared by mass using a Mettler Toledo AT201 balance. Solutions were stored in glass 25mL volumetric flasks and used within 24 hours of preparation.

5.2.4 Measurements

Relative densities and relative massic heat capacities of acidified aqueous yttrium chloride and four rare earth chlorides ($YbCl_3$, $DyCl_3$, $SmCl_3$ and $GdCl_3$) were measured using the Sodev model 02D vibrating tube densimeter and the Picker flow microcalorimeter. Measurement details have been described in Chapter 2. Experimental apparent molar volumes and heat capacities were calculated from the measured relative properties using equations 4.1 and 4.2. The apparent molar properties of the aqueous trivalent metal salts were calculated using equations 4.3 and 4.4. The required apparent molar properties of aqueous hydrochloric acid, utilized in the calculation of values of $V_{\phi,2}$ and $C_{p\phi,2}$, were calculated from equations reported by Sharygin and Wood (1997) and Ballerat-Busserolles *et al.* (1999) respectively. Concentration and temperature dependences of the measured and calculated properties are reported in tables 5.1 through 5.5 for YCl_3, $YbCl_3$, $DyCl_3$, $SmCl_3$, and $GdCl_3$ respectively.

Figures 5.1-5.10 illustrate that the apparent molar volumes, $V_{\phi,2}$, reported in tables 5.1 through 5.5, at T = 298.15 K, differ by a maximum of approximately 1.5 cm^3mol^{-1} from those reported by Spedding *et al.* (Spedding, 1966b,

Table 5.1 The concentration dependences of relative densities, relative heat capacities, apparent molar volumes and apparent molar heat capacities for acidified aqueous solutions YCl_3, component 2, in HCl (component 3) at T = (288.15, 298.15, 313.15, and 328.15) K.

m_2 /mol kg^{-1}	m_3 /mol kg^{-1}	$\rho_{expt} - \rho^o$ /kg m^{-3}	$V_{\phi,\,expt}$ /cm^3 mol^{-1}	$V_{\phi,2}$ /cm^3 mol^{-1}	$c_{p\,expt} - c_p^o$ /J K^{-1} g^{-1}	$C_{p,\phi,expt}$ /J K^{-1} mol^{-1}	$C_{p,\phi,2}$ /J K^{-1} mol^{-1}
			T = 288.15 K				
0.12499	0.00655	21.897	16.33(0.19)	16.21 (0.49)	-0.14387	-362.7(1.4)	-376.3 (4.5)
0.18489	0.00993	32.997	17.11(0.19)	17.03 (0.49)	-0.21269	-348.1(1.3)	-361.2 (4.5)
0.25162	0.01352	44.677	17.74(0.18)	17.69 (0.49)	-0.28207	-333.2(1.2)	-345.8 (4.5)
0.31833	0.01710	56.194	18.47(0.18)	18.45 (0.48)	-0.34956	-324.1(1.2)	-336.4 (4.5)
0.37944	0.02038	66.682	18.99(0.17)	19.00 (0.48)	-0.40777	-312.7(1.2)	-324.6 (4.5)
0.45799	0.02460	80.005	19.68(0.17)	19.72 (0.48)	-0.47987	-300.7(1.1)	-312.2 (4.4)
0.52598	0.02825	91.465	20.17(0.17)	20.23 (0.48)	-0.54016	-292.2(1.1)	-303.4 (4.4)
0.58615	0.03149	101.534	20.56(0.17)	20.64 (0.48)	-0.59141	-284.8(1.1)	-295.7 (4.4)
0.06005	0.00323	10.867	15.12(0.21)	14.96 (0.49)	-	-	-
0.67834	0.03644	116.908	21.03(0.17)	21.12 (0.48)	-0.66644	-273.6(1.1)	-284.1 (4.4)
			T = 298.15 K				
0.05651	0.00010	10.140	15.25(0.77)	15.24 (0.89)	-0.06594	-362.7(5.2)	-363.1 (6.7)
0.10005	0.00017	17.860	16.03(0.76)	16.02 (0.88)	-0.11427	-347.5(4.9)	-347.9 (6.6)
0.14260	0.00025	25.347	16.65(0.75)	16.64 (0.87)	-0.16004	-336.6(4.8)	-337.0 (6.5)
0.18912	0.00033	33.485	17.20(0.74)	17.19 (0.87)	-0.20876	-327.7(4.7)	-328.1 (6.4)
0.24214	0.00042	42.671	17.85(0.73)	17.85 (0.86)	-0.26244	-318.2(4.7)	-318.4 (6.3)
0.29200	0.00051	51.266	18.32(0.72)	18.32 (0.85)	-0.31169	-311.4(4.6)	-311.7 (6.3)
0.34351	0.00060	60.083	18.79(0.71)	18.79 (0.84)	-0.36024	-302.2(4.5)	-302.4 (6.2)
0.39636	0.00069	69.064	19.26(0.70)	19.26 (0.83)	-0.40925	-295.6(4.4)	-295.8 (6.2)
0.45211	0.00079	78.495	19.68(0.69)	19.68 (0.83)	-0.45901	-288.1(4.4)	-288.2 (6.1)
0.50807	0.00088	87.908	20.06(0.69)	20.06 (0.82)	-0.50722	-280.6(4.3)	-280.7 (6.1)
			T = 313.15 K				
0.05490	0.00010	9.786	15.63(0.78)	15.62 (0.90)	-0.06224	-329.1 (5.0)	-329.5 (6.6)
0.09782	0.00017	17.372	16.16(0.77)	16.15 (0.89)	-0.10876	-316.4 (4.9)	-316.8 (6.5)
0.14228	0.00025	25.134	16.97(0.76)	16.97 (0.88)	-0.15536	-305.6 (4.8)	-305.9 (6.4)
0.19151	0.00033	33.687	17.57(0.75)	17.56 (0.88)	-0.20536	-295.7 (4.7)	-296.0 (6.3)
0.24154	0.00042	42.324	18.08(0.74)	18.07 (0.87)	-0.25454	-286.9 (4.6)	-287.1 (6.3)
0.29343	0.00051	51.192	18.66(0.73)	18.66 (0.86)	-0.30394	-278.5 (4.5)	-278.8 (6.2)
0.34322	0.00060	59.685	19.05(0.72)	19.04 (0.85)	-0.34970	-270.6 (4.4)	-270.7 (6.2)
0.39683	0.00069	68.735	19.54(0.71)	19.54 (0.84)	-0.39852	-265.5 (4.4)	-265.6 (6.1)
0.44726	0.00078	77.210	19.93(0.71)	19.93 (0.84)	-0.44228	-258.7 (4.3)	-258.8 (6.1)
0.50807	0.00088	87.365	20.37(0.70)	20.37 (0.83)	-0.49394	-252.1 (4.2)	-252.1 (6.0)
			T = 328.15 K				
0.06126	0.00329	10.928	15.48(0.21)	15.29 (0.50)	-0.06948	-306.5 (1.7)	-317.4 (4.6)
0.12007	0.00645	21.286	16.34(0.20)	16.22 (0.49)	-0.13148	-281.0 (1.3)	-292.5 (4.5)
0.21243	0.01141	37.336	17.55(0.19)	17.45 (0.49)	-0.22435	-261.5 (1.2)	-268.6 (4.5)
0.35387	0.01901	61.460	19.06(0.18)	19.02 (0.49)	-0.35647	-239.9 (1.1)	-244.4 (4.4)
0.48080	0.02583	82.728	20.13(0.18)	20.15 (0.48)	-0.46669	-225.7 (1.1)	-227.9 (4.4)
0.57535	0.03091	98.361	20.82(0.17)	20.87 (0.48)	-0.53344	-215.2 (1.0)	-215.6 (4.4)
0.28333	0.01522	49.539	18.19(0.19)	18.12 (0.49)	-0.29245	-251.5 (1.2)	-257.4 (4.5)
0.67834	0.03644	115.173	21.53(0.17)	21.61 (0.48)	-0.62332	-205.9 (1.0)	-202.0 (4.4)

Table 5.2 The concentration dependences of relative densities, relative heat capacities, apparent molar volumes and apparent molar heat capacities for acidified aqueous solutions $YbCl_3$, component 2, in HCl (component 3) at T = (288.15, 298.15, 313.15, and 328.15) K.

m_2 /mol kg^{-1}	m_3 /mol kg^{-1}	$\rho_{expt} - \rho^o$ /kg m^{-3}	$V_{\phi,expt}$ /cm^3 mol^{-1}	$V_{\phi,2}$ /cm^3 mol^{-1}	$c_{p\,expt} - c_p^o$ /J K^{-1} g^{-1}	$C_{p,\phi,expt}$ /J K^{-1} mol^{-1}	$C_{p,\phi,2}$ /J K^{-1} mol^{-1}
			T = 288.15 K				
0.04560	0.03721	12.374	14.71(0.64)	11.90 (0.78)	-0.07769	-262.7 (4.1)	-369.4 (5.9)
0.08643	0.07052	23.321	15.37(0.62)	12.97 (0.77)	-0.14373	-251.1 (4.0)	-341.6 (5.9)
0.12814	0.10455	34.419	15.85(0.61)	13.74 (0.76)	-0.20875	-243.1 (3.9)	-319.3 (5.8)
0.17891	0.14598	47.829	16.33(0.60)	14.49 (0.75)	-0.28506	-236.0 (3.7)	-296.0 (5.7)
0.21863	0.17838	58.183	16.79(0.59)	15.57 (0.74)	-0.40542	-222.9 (3.6)	-253.8 (5.6)
0.26436	0.21570	70.152	17.00(0.58)	16.04 (0.73)	-0.47482	-216.8 (3.6)	-231.1 (5.6)
0.31617	0.25797	83.581	17.30(0.57)	16.47 (0.72)	-0.53889	-211.0 (3.5)	-209.2 (5.5)
0.36607	0.29868	96.427	17.57(0.56)	16.78 (0.71)	-0.60294	-205.8 (3.4)	-188.0 (5.5)
0.41765	0.34077	109.656	17.79(0.55)	17.39 (0.71)	-0.66253	-198.4 (3.3)	-162.3 (5.4)
0.46912	0.38277	122.616	18.16(0.55)	11.90 (0.78)	-0.07769	-262.7 (4.1)	-369.4 (5.9)
			T = 298.15 K				
0.04700	0.03835	12.644	15.70(0.63)	13.34 (0.78)	-0.07115	-234.3 (4.0)	-328.6 (5.9)
0.08696	0.07096	23.299	16.13(0.62)	13.98 (0.76)	-0.13397	-224.3 (3.9)	-304.6 (5.8)
0.12877	0.10507	34.351	16.59(0.61)	14.69 (0.76)	-0.19751	-217.7 (3.7)	-285.3 (5.7)
0.17299	0.14114	45.948	17.00(0.60)	15.35 (0.75)	-0.26176	-209.8 (3.7)	-262.6 (5.6)
0.21789	0.17778	57.686	17.27(0.59)	15.75 (0.74)	-0.32515	-204.4 (3.6)	-243.8 (5.6)
0.26646	0.21741	70.252	17.64(0.58)	16.34 (0.73)	-0.39042	-197.2 (3.5)	-220.7 (5.5)
0.31144	0.25411	81.836	17.90(0.57)	16.75 (0.73)	-0.45024	-194.4 (3.4)	-205.8 (5.5)
0.36232	0.29563	94.860	18.17(0.56)	17.17 (0.72)	-0.51442	-189.1 (3.4)	-185.0 (5.5)
0.41247	0.33655	107.639	18.38(0.55)	17.49 (0.71)	-0.57617	-185.4 (3.3)	-167.1 (5.4)
0.46912	0.38277	122.059	18.53(0.55)	17.67 (0.71)	-0.64206	-179.7 (3.2)	-143.8 (5.4)
			T = 313.15 K				
0.04627	0.03776	12.390	15.76(0.64)	13.23 (0.78)	-0.07460	-213.0 (3.9)	-298.6 (5.8)
0.09019	0.07359	24.043	16.23(0.62)	14.09 (0.77)	-0.14208	-203.8 (3.8)	-276.4 (5.7)
0.12947	0.10564	34.330	16.83(0.61)	14.86 (0.76)	-0.19955	-194.5 (3.6)	-253.2 (5.6)
0.17340	0.14149	45.789	17.23(0.60)	15.48 (0.75)	-0.26247	-189.6 (3.6)	-236.6 (5.6)
0.22124	0.18052	58.178	17.61(0.59)	16.08 (0.74)	-0.32715	-181.0 (3.5)	-212.0 (5.5)
0.26686	0.21774	69.927	17.90(0.58)	16.53 (0.74)	-0.38769	-176.7 (3.4)	-195.1 (5.5)
0.31404	0.25623	81.994	18.18(0.57)	16.98 (0.73)	-0.44796	-172.1 (3.3)	-177.1 (5.4)
0.36287	0.29607	94.391	18.47(0.56)	17.44 (0.72)	-0.50810	-167.6 (3.3)	-158.6 (5.4)
0.41602	0.33944	107.840	18.70(0.56)	17.79 (0.71)	-0.57269	-165.2 (3.2)	-142.8 (5.4)
0.46912	0.38277	121.192	18.92(0.55)	18.11 (0.71)	-0.63352	-160.8 (3.2)	-123.2 (5.3)
			T = 328.15 K				
0.04571	0.03729	12.242	14.83(0.65)	11.56 (0.79)	-0.07319	-206.2 (3.9)	-289.9 (5.8)
0.08617	0.07031	22.939	15.58(0.63)	12.71 (0.77)	-0.13472	-195.5 (3.8)	-266.2 (5.7)
0.13030	0.10632	34.474	16.31(0.62)	13.89 (0.76)	-0.19882	-185.2 (3.6)	-241.3 (5.6)
0.17343	0.14151	45.674	16.78(0.61)	14.65 (0.76)	-0.25903	-177.4 (3.5)	-220.0 (5.6)
0.21880	0.17852	57.410	17.11(0.60)	15.16 (0.75)	-0.32044	-171.5 (3.4)	-201.3 (5.5)
0.26908	0.21955	70.310	17.48(0.59)	15.74 (0.74)	-0.38653	-166.9 (3.4)	-183.5 (5.5)
0.36496	0.29778	94.666	18.07(0.57)	16.69 (0.73)	-0.50697	-160.6 (3.3)	-153.0 (5.4)
0.41892	0.34181	108.222	18.39(0.56)	17.20 (0.72)	-0.57014	-155.5 (3.2)	-132.6 (5.4)

Table 5.3 The concentration dependences of relative densities, relative heat capacities, apparent molar volumes and apparent molar heat capacities for acidified aqueous solutions $DyCl_3$, component 2, in HCl (component 3) at T = (288.15, 298.15, 313.15, and 328.15) K.

ν	m_3 /mol kg^{-1}	$\rho_{expt} - \rho^o$ /kg m^{-3}	$V_{\phi,\,expt}$ /cm^3 mol^{-1}	$V_{\phi,2}$ /cm^3 mol^{-1}	$c_{p\,expt} - c_p^o$ /J K^{-1} g^{-1}	$C_{p,\phi,expt}$ /J K^{-1} mol^{-1}	$C_{p,\phi,2}$ /J K^{-1} mol^{-1}
			T = 288.15 K				
0.03274	0.00494	8.365	16.10(0.38)	15.81 (0.59)	-0.05064	-358.1 (3.0)	-392.6 (5.3)
0.06584	0.00993	16.755	16.80(0.35)	16.59 (0.57)	-0.10043	-351.6 (2.4)	-384.3 (4.9)
0.10470	0.01579	26.539	17.50(0.34)	17.37 (0.56)	-0.15690	-341.7 (2.2)	-371.8 (4.8)
0.12878	0.01942	32.566	17.90(0.34)	17.82 (0.56)	-0.19085	-335.3 (2.1)	-363.7 (4.8)
0.17066	0.02574	42.988	18.54(0.33)	18.55 (0.56)	-0.24821	-325.1 (2.0)	-350.6 (4.8)
0.19712	0.02973	49.572	18.76(0.33)	18.79 (0.56)	-0.28372	-320.5 (2.0)	-344.4 (4.7)
0.23135	0.03489	58.033	19.14(0.33)	19.21 (0.56)	-0.32820	-313.1 (2.0)	-334.6 (4.7)
0.26314	0.03968	65.896	19.34(0.32)	19.44 (0.55)	-0.36846	-306.7 (1.9)	-326.1 (4.7)
0.29242	0.04410	73.091	19.60(0.32)	19.72 (0.55)	-0.40462	-300.9 (1.9)	-318.4 (4.7)
0.35480	0.05351	88.322	20.14(0.31)	20.33 (0.55)	-0.48039	-293.2 (1.9)	-307.2 (4.7)
			T = 298.15 K				
0.03522	0.00531	8.948	16.91(0.37)	16.67 (0.58)	-0.05297	-323.1 (2.9)	-354.2 (5.3)
0.06653	0.01003	16.823	17.77(0.35)	17.63 (0.57)	-0.09866	-315.8 (2.3)	-345.2 (4.9)
0.10066	0.01518	25.359	18.42(0.34)	18.37 (0.56)	-0.14666	-304.7 (2.1)	-331.5 (4.8)
0.13367	0.02016	33.575	18.92(0.34)	18.92 (0.56)	-0.19215	-298.5 (2.0)	-323.5 (4.8)
0.16746	0.02526	41.949	19.33(0.33)	19.39 (0.56)	-0.23711	-290.5 (2.0)	-313.2 (4.7)
0.20339	0.03067	50.816	19.71(0.33)	19.81 (0.56)	-0.28366	-283.2 (1.9)	-303.6 (4.7)
0.24018	0.03622	59.882	19.98(0.32)	20.11 (0.55)	-0.33048	-278.0 (1.9)	-296.5 (4.7)
0.27469	0.04143	68.321	20.31(0.32)	20.48 (0.55)	-0.37226	-270.0 (1.9)	-286.0 (4.7)
0.31488	0.04749	78.111	20.66(0.32)	20.87 (0.55)	-0.42164	-267.7 (1.8)	-282.0 (4.7)
0.35480	0.05351	87.864	20.81(0.31)	21.03 (0.55)	-0.46806	-261.6 (1.8)	-273.5 (4.7)
			T = 313.15 K				
0.03483	0.00525	8.820	16.64(0.38)	16.32 (0.59)	-0.05146	-299.9 (2.9)	-329.0 (5.3)
0.06254	0.00943	15.756	17.62(0.35)	17.41 (0.57)	-0.09110	-291.4 (2.3)	-318.9 (4.9)
0.09454	0.01426	23.727	18.31(0.34)	18.19 (0.57)	-0.13501	-277.4 (2.1)	-302.1 (4.8)
0.13519	0.02039	33.786	19.05(0.34)	19.02 (0.56)	-0.18944	-266.6 (2.0)	-288.6 (4.7)
0.16974	0.02560	42.298	19.49(0.33)	19.51 (0.56)	-0.23479	-261.8 (1.9)	-282.1 (4.7)
0.19682	0.02968	48.927	19.89(0.33)	19.96 (0.56)	-0.26849	-253.2 (1.9)	-271.4 (4.7)
0.22077	0.03329	54.785	20.13(0.33)	20.23 (0.56)	-0.29867	-250.7 (1.9)	-267.7 (4.7)
0.25676	0.03872	63.554	20.49(0.32)	20.64 (0.55)	-0.34318	-247.1 (1.9)	-262.4 (4.7)
0.30399	0.04585	74.947	21.07(0.32)	21.30 (0.55)	-0.39876	-238.8 (1.8)	-251.3 (4.7)
0.35480	0.05351	87.128	21.63(0.31)	21.92 (0.55)	-0.45629	-230.2 (1.8)	-239.6 (4.7)
			T = 328.15 K				
0.06587	0.00993	16.576	16.52(0.38)	16.15 (0.59)	-0.09500	-278.8 (2.8)	-304.3 (5.3)
0.09683	0.01460	24.278	17.19(0.36)	16.90 (0.57)	-0.13712	-266.2 (2.3)	-289.9 (4.9)
0.13300	0.02006	33.220	17.87(0.35)	17.67 (0.57)	-0.18487	-254.9 (2.1)	-276.1 (4.8)
0.16902	0.02549	42.101	18.30(0.34)	18.15 (0.57)	-0.23105	-245.9 (2.0)	-264.8 (4.7)
0.19955	0.03010	49.560	18.80(0.34)	18.71 (0.56)	-0.26966	-241.5 (1.9)	-258.8 (4.7)
0.23763	0.03584	58.848	19.24(0.33)	19.20 (0.56)	-0.31616	-234.4 (1.8)	-249.6 (4.7)
0.27472	0.04143	67.903	19.46(0.33)	19.45 (0.56)	-0.36094	-230.7 (1.8)	-243.7 (4.7)
0.31113	0.04692	76.741	19.73(0.32)	19.75 (0.55)	-0.40299	-224.5 (1.8)	-235.9 (4.7)
0.35480	0.05351	87.239	20.17(0.32)	20.24 (0.55)	-0.45232	-218.6 (1.8)	-232.3 (4.7)

Table 5.4 The concentration dependences of relative densities, relative heat capacities, apparent molar volumes and apparent molar heat capacities for acidified aqueous solutions $SmCl_3$, component 2, in HCl (component 3) at T = (288.15, 298.15, 313.15, and 328.15) K.

m_2 /mol kg^{-1}	m_3 /mol kg^{-1}	$\rho_{expt} - \rho^o$ /kg m^{-3}	$V_{\phi,\,expt}$ /cm^3 mol^{-1}	$V_{\phi,2}$ /cm^3 mol^{-1}	$c_{p\,expt} - c_p^{\,o}$ /J K^{-1} g^{-1}	$C_{p,\phi,expt}$ /J K^{-1} mol^{-1}	$C_{p,\phi,2}$ /J K^{-1} mol^{-1}
			T = 288.15 K				
0.03689	0.00004	8.975	13.17(0.52)	13.16 (0.69)	-0.05584	-452.9 (3.7)	-453.2 (5.7)
0.07422	0.00008	17.968	14.19(0.50)	14.18 (0.67)	-0.10985	-433.0 (3.2)	-433.4 (5.4)
0.11163	0.00012	26.933	14.88(0.49)	14.87 (0.67)	-0.16214	-418.9 (3.1)	-419.2 (5.3)
0.14948	0.00015	35.966	15.38(0.49)	15.38 (0.66)	-0.21362	-408.8 (3.0)	-409.1 (5.3)
0.19111	0.00020	45.839	15.95(0.48)	15.94 (0.66)	-0.26851	-398.8 (3.0)	-399.0 (5.2)
0.22988	0.00024	55.043	16.21(0.48)	16.20 (0.65)	-0.31795	-389.6 (2.9)	-389.8 (5.2)
0.27007	0.00028	64.465	16.76(0.47)	16.75 (0.65)	-0.36814	-382.5 (2.9)	-382.8 (5.2)
0.31188	0.00032	74.283	17.10(0.46)	17.10 (0.65)	-0.41873	-375.0 (2.8)	-375.2 (5.1)
0.35522	0.00037	84.403	17.45(0.46)	17.45 (0.64)	-0.46936	-366.7 (2.8)	-366.9 (5.1)
0.39854	0.00041	94.504	17.74(0.45)	17.74 (0.64)	-0.51912	-360.7 (2.7)	-360.9 (5.1)
			T = 298.15 K				
0.03840	0.00004	9.256	14.85(0.55)	14.85 (0.71)	-0.05646	-411.5 (3.7)	-411.8 (5.7)
0.07533	0.00008	18.115	15.32(0.53)	15.31 (0.70)	-0.10781	-385.5 (3.3)	-385.8 (5.4)
0.11217	0.00012	26.891	15.92(0.52)	15.92 (0.69)	-0.15772	-373.1 (3.2)	-373.4 (5.3)
0.15111	0.00016	36.102	16.53(0.51)	16.53 (0.68)	-0.20904	-363.5 (3.1)	-363.8 (5.3)
0.18978	0.00020	45.241	16.93(0.51)	16.93 (0.68)	-0.25882	-356.8 (3.0)	-357.0 (5.3)
0.22702	0.00023	53.992	17.32(0.50)	17.32 (0.67)	-0.30533	-349.9 (3.0)	-350.1 (5.2)
0.26599	0.00028	63.115	17.69(0.50)	17.68 (0.67)	-0.35261	-342.8 (2.9)	-343.0 (5.2)
0.30393	0.00031	71.960	18.03(0.49)	18.03 (0.67)	-0.39740	-336.1 (2.9)	-336.3 (5.2)
0.34574	0.00036	81.676	18.35(0.49)	18.36 (0.66)	-0.44546	-329.4 (2.9)	-329.5 (5.2)
0.39817	0.00041	93.804	18.75(0.48)	18.75 (0.66)	-0.50412	-322.1 (2.8)	-322.3 (5.1)
			T = 313.15 K				
0.03712	0.00004	8.912	14.73(0.52)	14.73 (0.69)	-0.05283	-363.7 (3.5)	-364.0 (5.5)
0.07495	0.00008	17.919	15.64(0.50)	15.64 (0.67)	-0.10431	-345.3 (3.1)	-345.6 (5.3)
0.11101	0.00011	26.451	16.29(0.49)	16.29 (0.67)	-0.15180	-333.3 (2.9)	-333.5 (5.2)
0.15040	0.00016	35.711	16.96(0.49)	16.96 (0.66)	-0.20247	-325.0 (2.9)	-325.2 (5.2)
0.18978	0.00020	44.940	17.44(0.48)	17.43 (0.66)	-0.25147	-316.5 (2.8)	-316.7 (5.1)
0.22985	0.00024	54.293	17.84(0.48)	17.84 (0.65)	-0.30004	-309.3 (2.7)	-309.5 (5.1)
0.26960	0.00028	63.529	18.23(0.47)	18.23 (0.65)	-0.34649	-301.1 (2.7)	-301.2 (5.1)
0.31276	0.00032	73.516	18.61(0.46)	18.61 (0.65)	-0.39596	-294.6 (2.7)	-294.7 (5.1)
0.35496	0.00037	83.241	18.96(0.46)	18.95 (0.64)	-0.44283	-288.2 (2.6)	-288.3 (5.0)
0.39854	0.00041	93.255	19.26(0.45)	19.26 (0.64)	-0.49307	-283.2 (2.6)	-283.3 (5.0)
			T = 328.15 K				
0.03753	0.00004	8.997	13.60(0.53)	13.60 (0.69)	-0.05306	-353.3 (3.5)	-353.6 (5.5)
0.07398	0.00008	17.646	14.72(0.51)	14.71 (0.68)	-0.10207	-331.8 (3.0)	-332.0 (5.3)
0.11156	0.00012	26.517	15.41(0.50)	15.41 (0.67)	-0.15082	-316.5 (2.9)	-316.7 (5.2)
0.15097	0.00016	35.763	16.08(0.49)	16.07 (0.67)	-0.20021	-303.4 (2.8)	-303.6 (5.1)
0.18826	0.00019	44.452	16.68(0.49)	16.68 (0.66)	-0.24588	-295.2 (2.8)	-295.3 (5.1)
0.22964	0.00024	54.068	17.19(0.48)	17.19 (0.66)	-0.29489	-285.8 (2.7)	-285.9 (5.1)
0.27003	0.00028	63.414	17.62(0.47)	17.62 (0.65)	-0.34144	-278.1 (2.7)	-278.2 (5.1)
0.31278	0.00032	73.268	18.02(0.47)	18.02 (0.65)	-0.38874	-268.6 (2.6)	-268.8 (5.0)
0.35363	0.00037	82.619	18.45(0.46)	18.45 (0.65)	-0.43290	-261.3 (2.6)	-261.4 (5.0)
0.39854	0.00041	92.877	18.83(0.46)	18.83 (0.64)	-0.47998	-253.5 (2.5)	-253.6 (5.0)

Table 5.5 The concentration dependences of relative densities, relative heat capacities, apparent molar volumes and apparent molar heat capacities for acidified aqueous solutions $GdCl_3$, component 2, in HCl (component 3) at T = (288.15, 298.15, 313.15, and 328.15) K.

m_2 /mol kg^{-1}	m_3 /mol kg^{-1}	$\rho_{expt} - \rho^o$ /kg m^{-3}	$V_{\phi,\,expt}$ /cm^3 mol^{-1}	$V_{\phi,2}$ /cm^3 mol^{-1}	$c_{p\,expt} - c_p^o$ /J K^{-1} g^{-1}	$C_{p,\phi,expt}$ /J K^{-1} mol^{-1}	$C_{p,\phi,2}$ /J K^{-1} mol^{-1}
			T = 288.15 K				
0.03018	0.00064	8.640	16.75(0.31)	16.88 (0.53)	-0.10761	-398.4 (2.0)	-403.1 (4.7)
0.07254	0.00132	17.892	16.91(0.29)	17.53 (0.53)	-0.16140	-386.3 (1.8)	-390.8 (4.7)
0.11079	0.00201	27.222	17.55(0.28)	17.83 (0.53)	-0.19285	-379.5 (1.7)	-383.7 (4.6)
0.13377	0.00243	32.815	17.84(0.28)	18.52 (0.53)	-0.26037	-367.6 (1.7)	-371.4 (4.6)
0.18445	0.00334	45.074	18.52(0.27)	18.93 (0.52)	-0.31093	-360.0 (1.6)	-363.5 (4.6)
0.22361	0.00405	54.504	18.93(0.27)	19.28 (0.52)	-0.35827	-352.6 (1.6)	-355.8 (4.6)
0.26142	0.00474	63.578	19.27(0.26)	19.65 (0.52)	-0.40685	-346.2 (1.6)	-349.1 (4.6)
0.30112	0.00546	73.056	19.63(0.26)	19.97 (0.52)	-0.45802	-339.3 (1.5)	-341.9 (4.6)
0.34422	0.00624	83.325	19.95(0.26)	20.23 (0.52)	-0.50572	-332.7 (1.5)	-335.0 (4.6)
0.38566	0.00699	93.169	20.21(0.25)	16.88 (0.53)	-0.10761	-398.4 (2.0)	-403.1 (4.7)
			T = 298.15 K				
0.03523	0.00064	8.678	16.85(0.32)	16.82 (0.55)	-0.04860	-387.2 (2.6)	-392.1 (5.0)
0.07209	0.00131	17.690	17.58(0.29)	17.56 (0.53)	-0.10085	-366.5 (1.9)	-370.9 (4.7)
0.10917	0.00198	26.686	18.28(0.28)	18.27 (0.53)	-0.15175	-353.9 (1.8)	-358.0 (4.6)
0.14680	0.00266	35.783	18.82(0.27)	18.82 (0.53)	-0.20172	-342.3 (1.7)	-346.0 (4.6)
0.18567	0.00337	45.137	19.28(0.27)	19.28 (0.52)	-0.25204	-333.7 (1.6)	-337.2 (4.6)
0.22295	0.00404	54.059	19.70(0.27)	19.71 (0.52)	-0.29887	-326.0 (1.6)	-329.2 (4.6)
0.26000	0.00471	62.901	20.05(0.26)	20.06 (0.52)	-0.34429	-319.3 (1.6)	-322.2 (4.6)
0.30344	0.00550	73.219	20.43(0.26)	20.45 (0.52)	-0.39608	-312.2 (1.5)	-314.8 (4.6)
0.34212	0.00620	82.371	20.74(0.26)	20.76 (0.52)	-0.44092	-306.3 (1.5)	-308.6 (4.6)
0.38566	0.00699	92.642	21.04(0.25)	21.07 (0.52)	-0.49011	-300.2 (1.5)	-302.2 (4.6)
			T = 313.15 K				
0.03555	0.00064	8.714	16.76(0.32)	16.72 (0.55)	-0.05158	-353.8 (2.6)	-358.3 (5.0)
0.07090	0.00129	17.319	17.69(0.29)	17.67 (0.53)	-0.10065	-335.9 (1.9)	-340.0 (4.7)
0.10727	0.00195	26.168	17.75(0.28)	18.94 (0.53)	-0.20008	-308.6 (1.6)	-311.9 (4.6)
0.14653	0.00266	35.540	18.95(0.28)	19.38 (0.53)	-0.24573	-300.8 (1.6)	-304.0 (4.6)
0.18262	0.00331	44.180	19.38(0.27)	19.87 (0.52)	-0.29598	-292.8 (1.6)	-295.7 (4.6)
0.22352	0.00405	53.919	19.87(0.27)	20.21 (0.52)	-0.34213	-287.1 (1.5)	-289.7 (4.6)
0.26194	0.00475	63.044	20.20(0.27)	20.56 (0.52)	-0.38878	-281.8 (1.5)	-284.1 (4.6)
0.30175	0.00547	72.457	20.54(0.26)	20.84 (0.52)	-0.43632	-277.8 (1.5)	-279.9 (4.5)
0.34308	0.00622	82.208	20.82(0.26)	21.08 (0.52)	-0.48276	-270.3 (1.5)	-272.0 (4.5)
0.38566	0.00699	92.228	21.06(0.26)	16.72 (0.55)	-0.05158	-353.8 (2.6)	-358.3 (5.0)
			T = 328.15 K				
0.03641	0.00066	8.935	15.10(0.32)	15.03 (0.55)	-0.05194	-329.3 (2.5)	-333.4 (5.5)
0.07211	0.00131	17.579	16.28(0.29)	16.23 (0.54)	-0.10072	-312.6 (1.9)	-316.3 (4.7)
0.10958	0.00199	26.643	17.08(0.28)	17.05 (0.53)	-0.15033	-300.9 (1.7)	-304.4 (4.6)
0.14761	0.00268	35.754	17.83(0.28)	17.81 (0.53)	-0.19925	-292.0 (1.6)	-295.1 (4.6)
0.18825	0.00341	45.498	18.30(0.27)	18.28 (0.53)	-0.25013	-284.4 (1.6)	-287.4 (4.6)
0.22282	0.00404	53.706	18.72(0.27)	18.71 (0.53)	-0.29215	-278 .1 (1.5)	-280.8 (4.6)
0.26063	0.00473	62.652	19.11(0.27)	19.11 (0.52)	-0.33682	-271.2 (1.5)	-273.6 (4.6)
0.30075	0.00545	72.192	19.26(0.27)	19.26 (0.52)	-0.38320	-265.4 (1.5)	-267.6 (4.6)
0.34182	0.00620	81.795	19.79(0.26)	19.79 (0.52)	-0.42899	-258.5 (1.5)	-260.4 (4.5)
0.38566	0.00699	92.102	20.04(0.26)	20.04 (0.52)	-0.47717	-253.6 (1.4)	-255.2 (4.5)

Figure 5.1 A comparison of $V_{\phi 2}$ values for YCl_3 at T = 298.15 K reported by Spedding to those reported by Karapet'yants and those reported here.

(•) Data reported here, (+) Karapet'yants *et al.* (1976), (X) Spedding *et al.* (1975b)

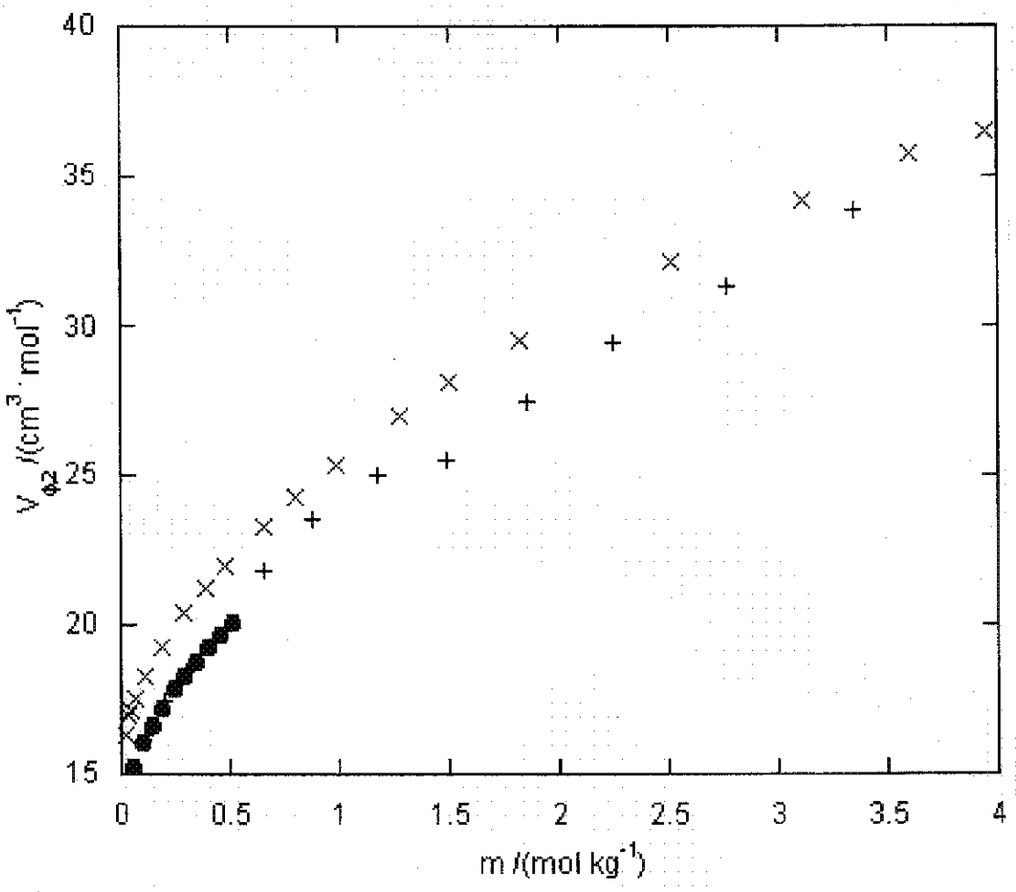

Figure 5.2 Comparison of experimental $C_{p\phi 2}$ values for YCl_3 at T = 298.15 K reported here to those reported by Karapet'yants et al.
(•) Data reported here, (X) Karapet'yants *et al.* (1976)

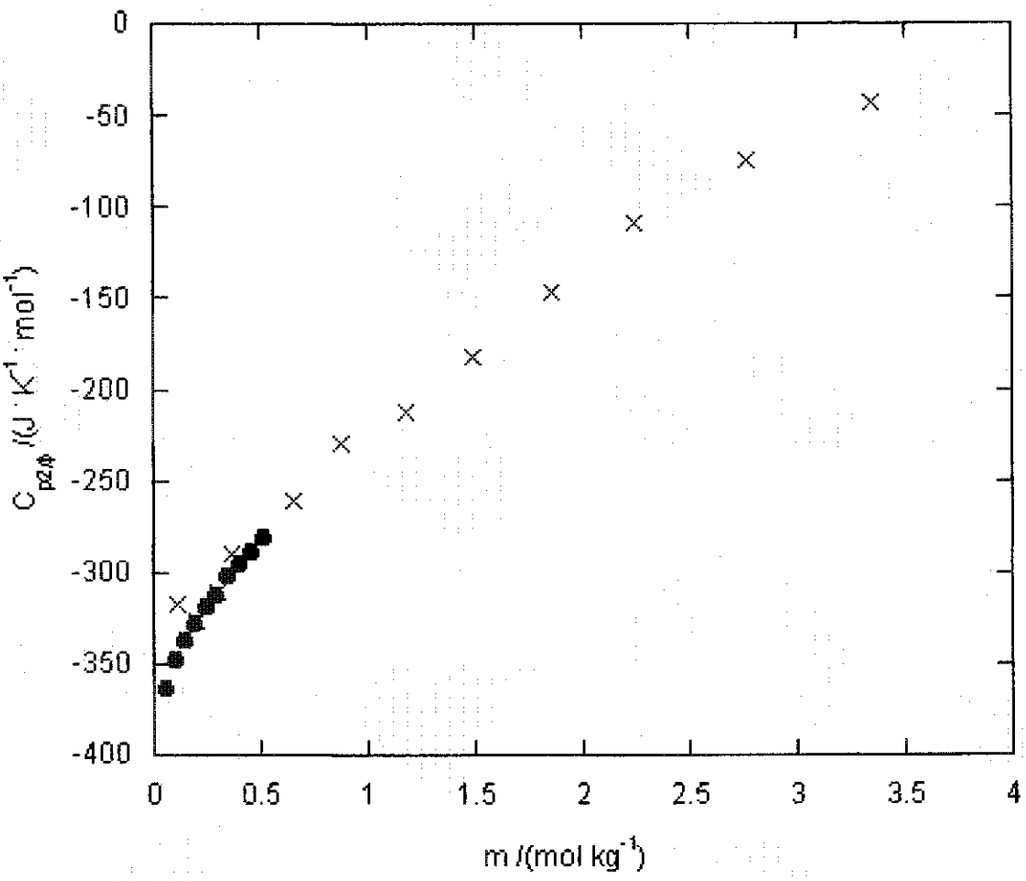

Figure 5.3 Comparison between experimental $V_{\phi 2}$ values for $YbCl_3$ at T = 298.15K.

(•) Data reported here, (+) Spedding *et al.*, 1966b, (X) Spedding *et al.*, 1975b, and (◊) Habenschuss and Spedding, 1976

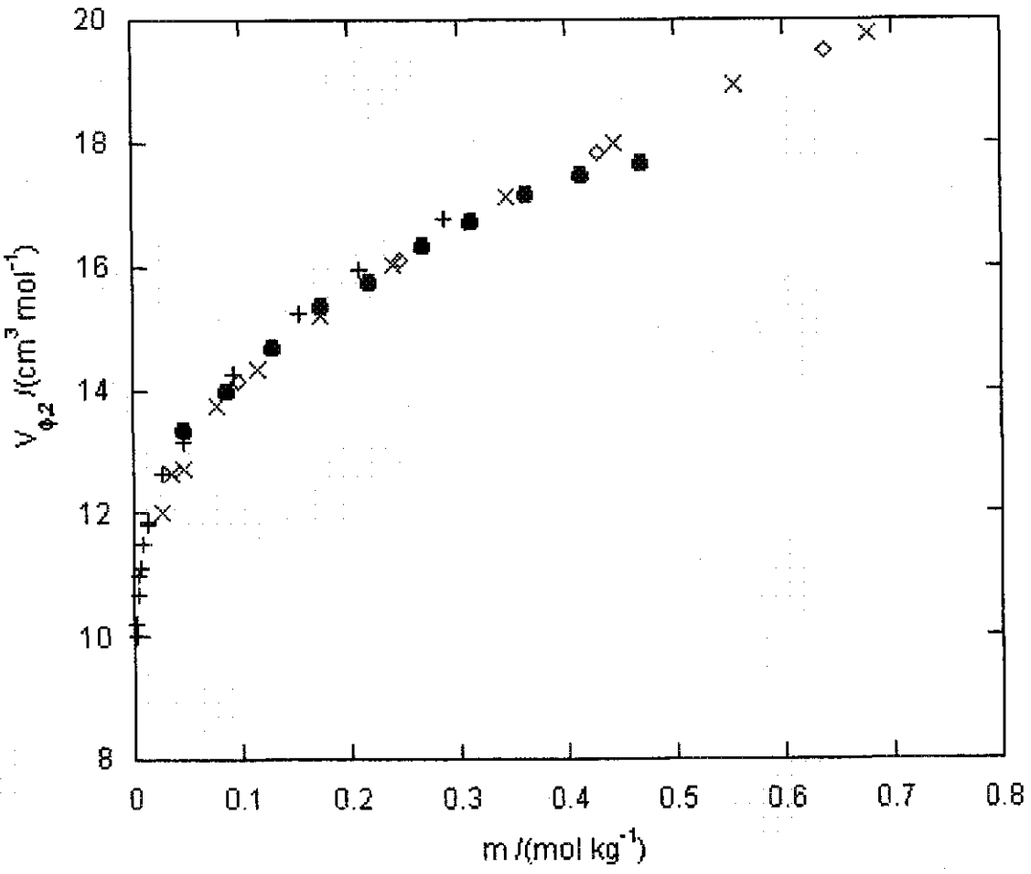

Figure 5.4 Comparison between experimental $C_{p\phi 2}$ values for $YbCl_3$ at T = 298.15K.

Data reported here (•) and those reported by Spedding and Jones (1966a) (X)

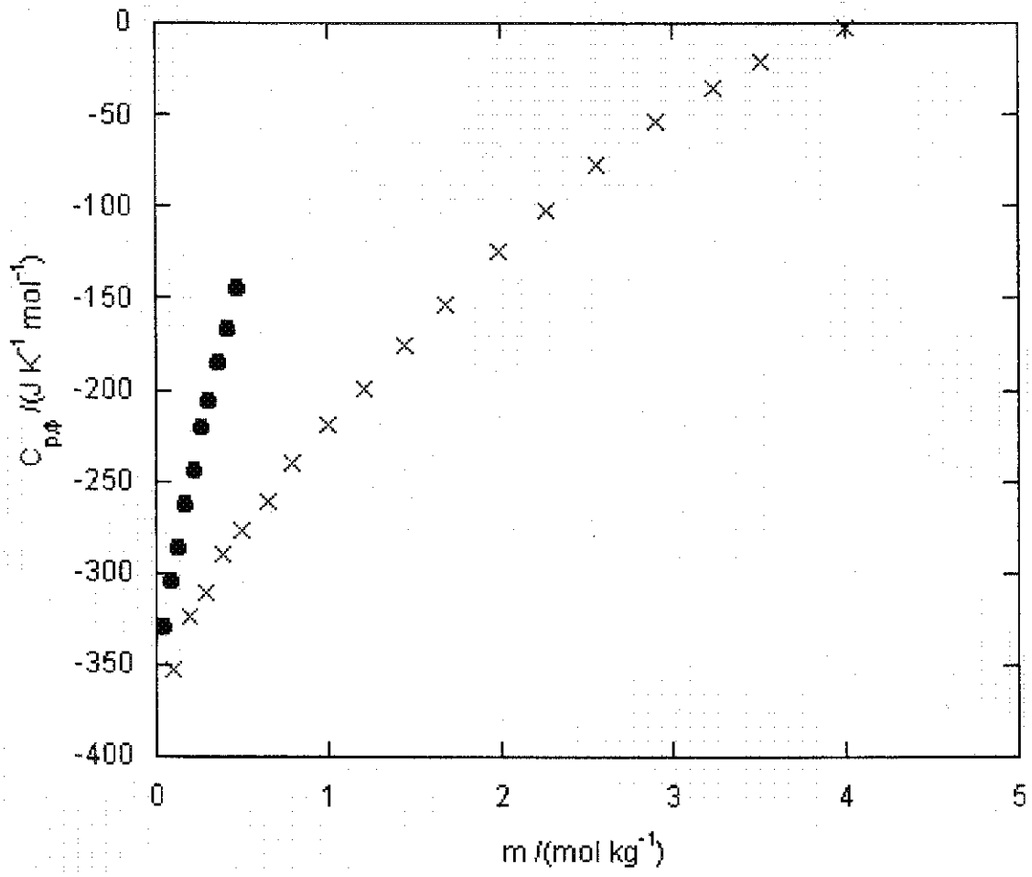

Figure 5.5 Comparison between experimental $V_{\phi 2}$ values for $DyCl_3$ at T = 298.15K .

Data reported here (•), Spedding et al. in (+) 1966b, (X) 1975b, and (◊) Habenschuss and Spedding, 1976

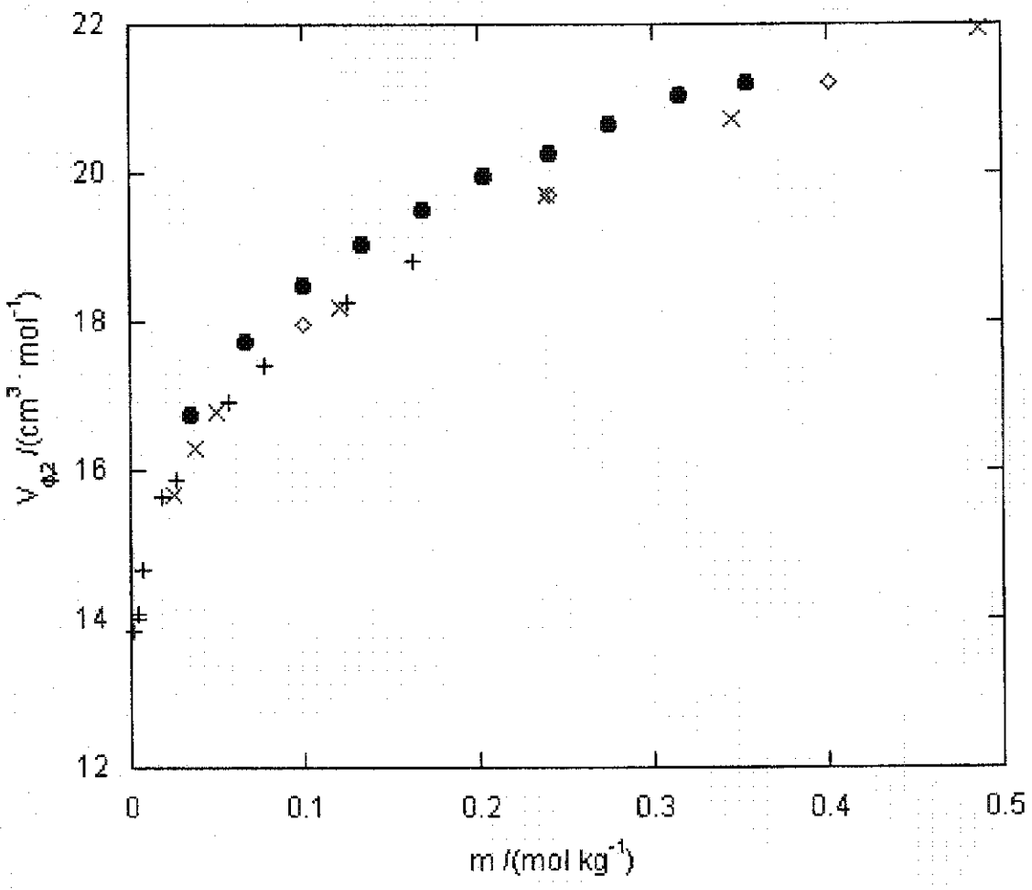

Figure 5.6 Comparison between experimental $C_{p,\phi 2}$ values for $DyCl_3$ at T = 298.15K .

Data reported here (•), Spedding and Jones, 1966a (X)

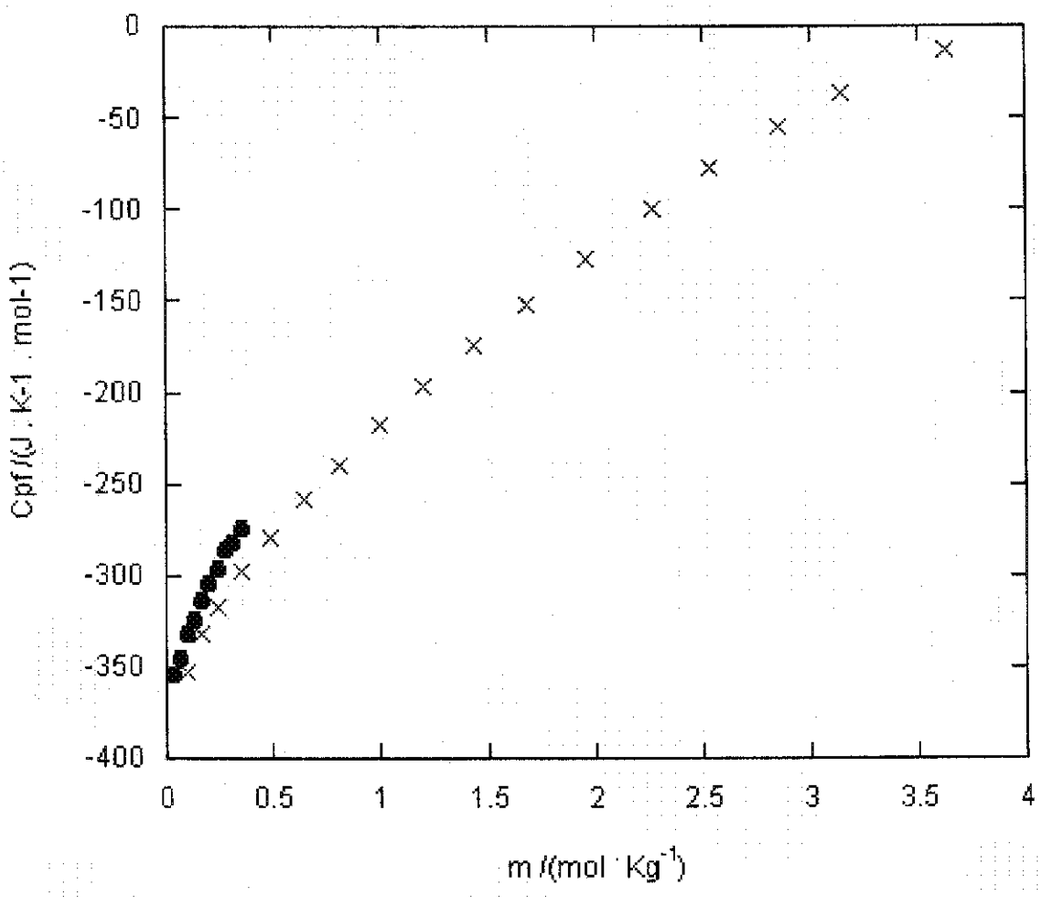

Figure 5.7 Comparison between experimental $V_{\phi 2}$ values for $SmCl_3$ at T = 298.15K.

Data reported here (•), Spedding et al. in (+) 1966b, (X) 1975b, and (◊) Habenschuss and Spedding, 1976

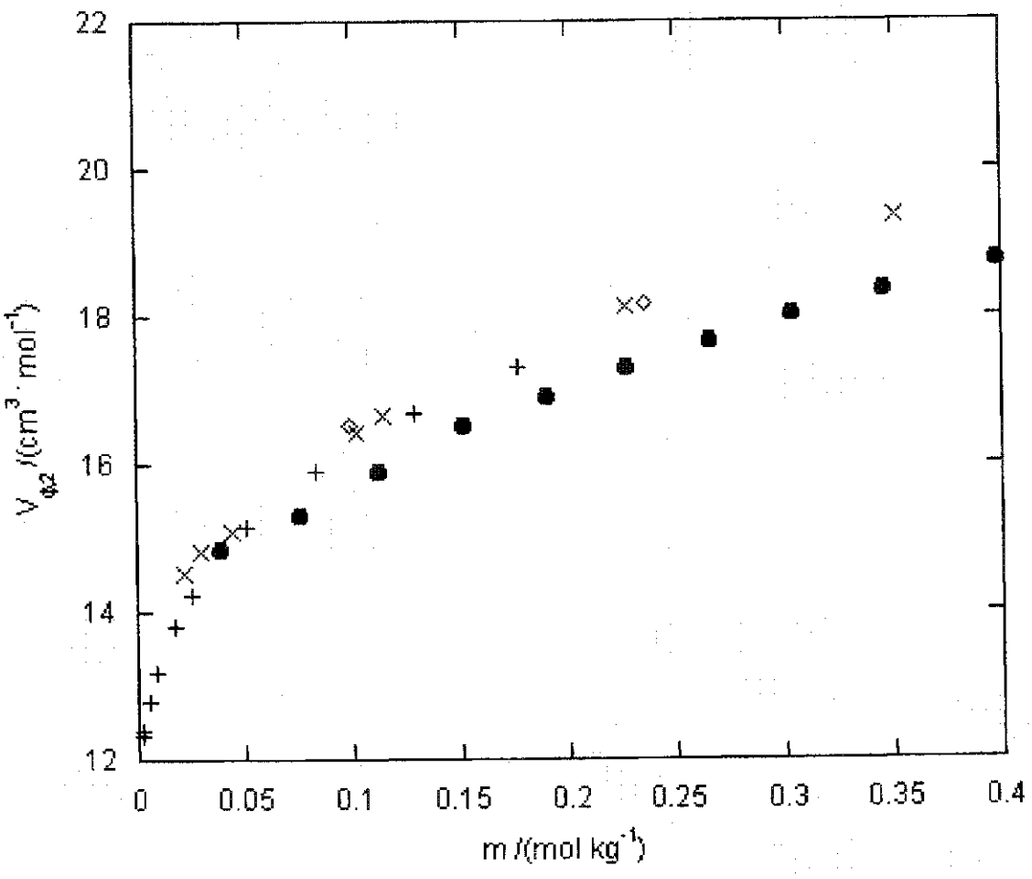

Figure 5.8 Comparison between experimental $C_{p,\phi 2}$ values for $SmCl_3$ at T = 298.15K.

Data reported here (•), Spedding, Walters and Baker (1975c) (X)

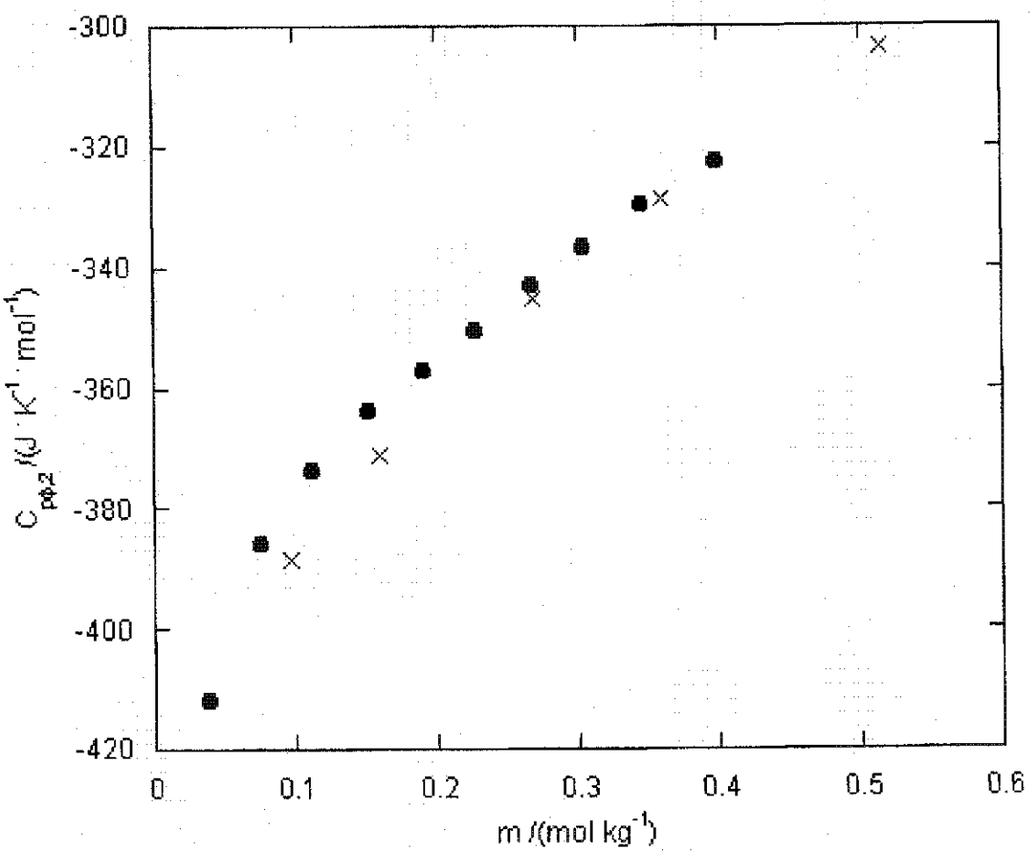

Figure 5.9 Comparison between experimental $V_{\phi 2}$ values for $GdCl_3$ at T = 298.15K.

Data reported here (•), Spedding *et al.* 1966b (+), Spedding *et al.* 1975b (X) and Habenschuss and Spedding, 1976 (◊).

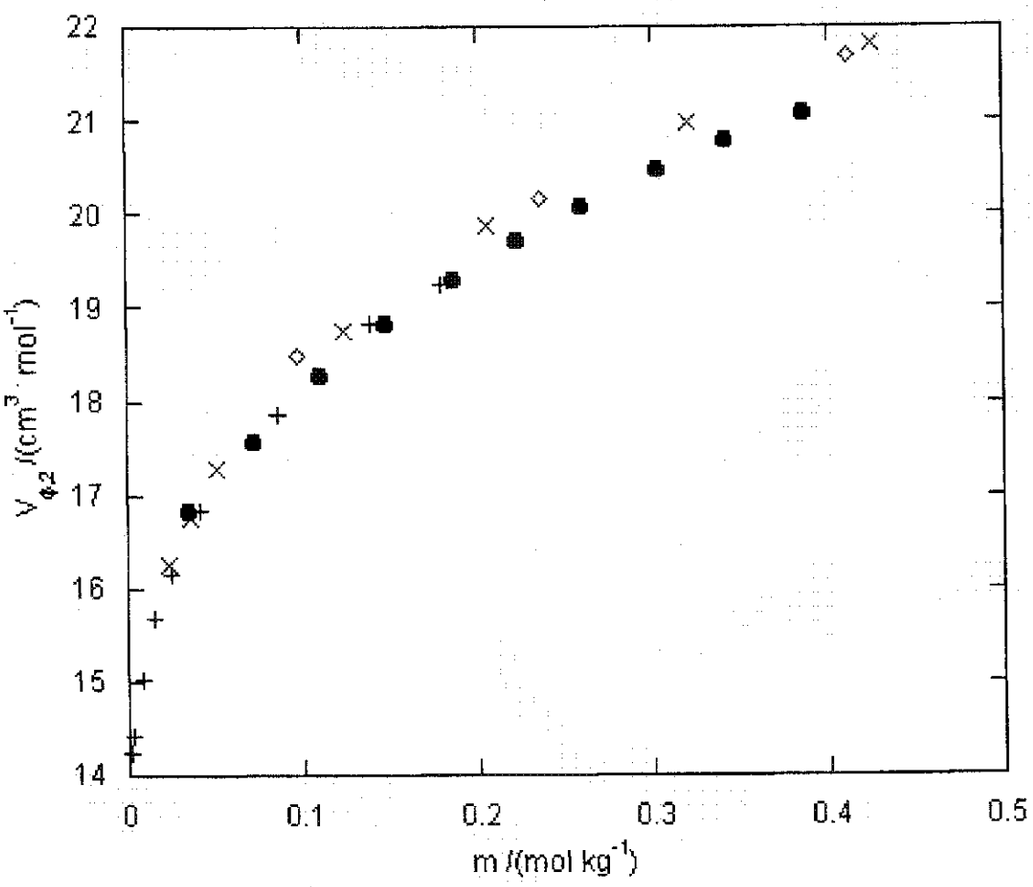

Figure 5.10 Comparison between experimental $C_{p,\phi 2}$ values for $GdCl_3$ at T = 298.15K.

Data reported here (•), Spedding, Walters and Baker, 1975c (X)

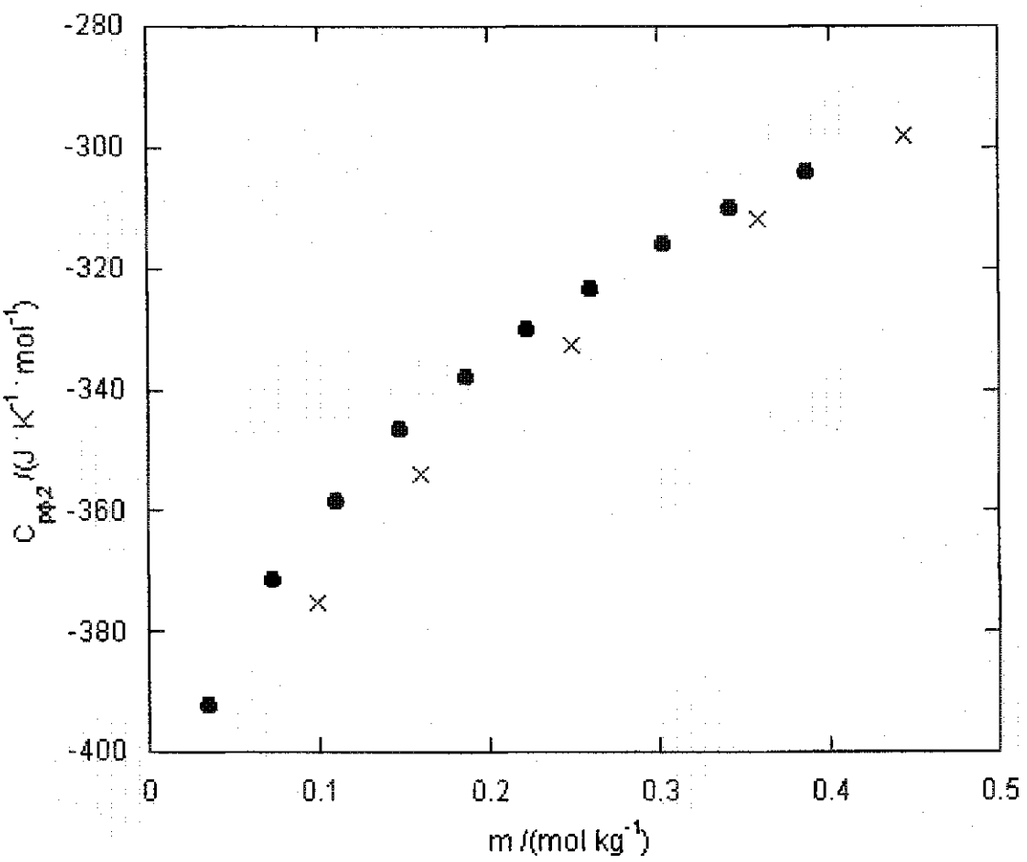

1975b; Habenschuss, 1976; Gildseth, 1975). Experimental apparent molar heat capacities measured at T = 298.15K differ from those reported by Spedding *et al.* (1966a, 1975c) by approximately 7 $JK^{-1}mol^{-1}$. A much greater deviation is observed in the case of ytterbium chloride, with differences of approximately 50 $JK^{-1}mol^{-1}$ at the highest concentration reported in this study. Agreement with the $C_{p,\phi,2}$ values reported by Karapet'yants *et al.* (1975) for aqueous solutions of YCl_3 is good. The apparent molar volumes at T = 298.15 K reported here for YCl_3 are indistinguishable from those reported by Karapet'yants *et al.* (1976).

5.3 Data modeling

The isothermal concentration dependences of the apparent molar volumes of the aqueous trivalent metal chloride salts were modeled using a Pitzer ion interaction equation:

$$V_{\phi,2} - \left\{\frac{6A_V \ln\left(1+b\sqrt{I}\right)}{b}\right\} = V_2^o + RTI\beta^{0V} + 2RTI\beta^{1V} f(I). \qquad (5.1)$$

Similarly, the isothermal concentration dependences of the apparent molar heat capacities were modeled with the equation:

$$C_{p,\phi,2} - \left\{\frac{6A_J \ln\left(1+b\sqrt{I}\right)}{b}\right\} = C_{p.2}^o - RT^2 I\beta^{0J} - 2RT^2 I\beta^{1J} f(I). \qquad (5.2)$$

The coefficients and constants used in these equations have been defined in Chapter 3. Values of the coefficients β^{0V}, β^{1V}, V_2^o, β^{0J}, β^{1J} and $C_{p,2}^o$ were determined using regression analyses and are reported together with standard errors in table 5.6. Table 5.7 compares V_2^o and $C_{p,2}^o$ values obtained at T = 298.15K in this study to those previously reported in the literature. The infinite dilution apparent molar volumes reported here agree well, within experimental uncertainty, with all literature values, deviating less than 2 cm^3mol^{-1}. The deviation between the infinite dilution heat capacities reported here and those reported in the literature reached a maximum of about 60 $JK^{-1}mol^{-1}$.

The temperature and concentration dependences of the apparent molar properties were modeled using modified forms of the Pitzer ion interaction equations. In these equations, the temperature dependences of the β^{0V}, β^{1V}, V_2^o, β^{0J}, β^{1J} and $C_{p,2}^o$ coefficients of equations 5.1 and 5.2 were modeled using equations 5.3 through 5.8.

$$V_2^o = v_1 + \frac{v_2}{T-\Theta} - \omega Q \tag{5.3}$$

$$\beta^{0V} = v_3 + v_4 T \tag{5.4}$$

$$\beta^{1V} = \frac{v_5}{T} + v_6 + v_7 T \tag{5.5}$$

$$C_{p,2}^o = c_1 + \frac{c_2}{(T-\Theta)^2} + \omega TX \tag{5.6}$$

Table 5.6 Estimates of parameters to the Pitzer ion interaction model equations, shown as equations (5.1) and (5.2) within the text, for aqueous solutions of YCl_3, $YbCl_3$, $DyCl_3$, $SmCl_3$ and $GdCl_3$ at T = (288.15, 298.15, 313.15, and 328.15) K and p = 0.1 MPa

T /K	V^o_2 /cm^3 mol^{-1}	$10^4\,\beta^{0V}$ /cm^3 kg mol^{-1} J^{-1}	$10^3\,\beta^{1V}$ /cm^3 kg mol^{-1} J^{-1}	$C_p{}^o{}_2$ /J K^{-1} mol^{-1}	$10^6\,\beta^{0J}$ /kg mol^{-1}K^{-2}	$10^5\,\beta^{1J}$ /kg mol^{-1}K^{-2}
			YCl_3			
288.15	10.90±0.16	1.766±0.215	-1.584±0.289	-466.12±3.84	13.384±1.267	-7.515±2.156
298.15	11.28±0.09	1.742±0.180	-2.648±0.185	-430.80±1.50	8.013±1.022	-15.235±1.053
313.15	11.37±0.19	1.572±0.379	-3.748±0.386	-403.59±1.70	3.717±1.073	-18.723±1.092
328.15	10.45±0.19	1.492±0.241	-4.659±0.321	-409.70±3.24	1.783±1.228	-13.970±1.635
			$YbCl_3$			
288.15	7.895±0.145	1.153±0.308	-0.996±0.317	-438.04±3.04	74.25±2.23	-15.57±2.33
298.15	9.304±0.237	0.581±0.470	-2.222±0.486	-405.91±2.98	55.634±1.969	-16.38±2.077
313.15	8.692±0.134	0.342±0.251	-2.593±0.261	-385.39±4.57	42.511±2.721	-16.755±2.87
328.15	5.951±0.196	-0.553±0.415	-1.827±0.390	-388.09±4.41	28.867±2.821	-13.11±2.70
			$DyCl_3$			
288.15	12.47±0.15	1.593±0.629	-1.571±0.441	-440.60±3.91	42.40±5.58	-24.60±3.91
298.15	12.91±0.08	-0.393±0.311	-0.960±0.225	-412.40±3.90	24.01±4.97	-20.87±3.59
313.15	12.26±0.12	1.714±0.450	-2.142±0.318	-398.28±4.01	13.48±4.80	-16.81±3.39
328.15	10.10±0.26	-0.931±0.674	-1.884±0.560	-413.47±3.27	-8.428±2.609	-3.884±2.168
			$SmCl_3$			
288.15	9.796±0.101	1.005±0.349	-1.405±0.267	-513.00±1.02	10.87±1.21	-3.389±0.942
298.15	11.55±0.17	2.173±0.577	-3.555±0.441	-461.03±2.47	9.421±2.011	-15.02±1.84
313.15	10.74±0.08	0.469±0.250	-2.706±0.192	-431.48±1.41	3.593±1.420	-15.68±1.11
328.15	9.034±0.076	0.667±0.230	-3.276±0.176	-433.33±1.54	4.079±1.404	-13.19±1.10
			$GdCl_3$			
288.15	12.56±0.11	0.760±0.302	-1.443±0.266	-477.20±0.97	12.90±0.89	-7.558±0.794
298.15	13.40±0.10	1.392±0.353	-2.569±0.262	-457.71±0.69	3.655±0.814	-5.606±0.615
313.15	12.73±0.07	-0.304±0.260	-2.314±0.190	-433.35±2.30	-5.581±2.540	-6.433±1.884
328.15	10.21±0.14	-1.407±0.439	-2.001±0.328	-405.13±0.90	2.625±0.870	-19.83±0.66

Table 5.7 A comparison between V_2^o values obtained in this study and those previously reported in the literature at T = 298.15 K and p = 0.1 MPa.

Chloride Salt	V_2^o (current study) /cm^3 mol^{-1}	V_2^o (literature) /cm^3 mol^{-1}	$C_{p,2}^o$ (current study) /J K^{-1} mol^{-1}	$C_{p,2}^o$ (literature) /J K^{-1} mol^{-1}
YCl_3	11.28 ± 0.09	13.354 ± 0.13[b], 13.35[d], 12.5[e], 13.19 ± 0.12[f]	–430.8 ± 1.5	–418.4[c]
$YbCl_3$	9.304 ± 0.237	9.22 ± 0.12[a], 9.433 ± 0.16[b], 8.16[c]	–405.9 ± 3.0	–438.7[g], –436.15[i]
$DyCl_3$	12.91 ± 0.08	12.82 ± 0.04[a], 12.903 ± 0.07[b], 12.16[c], 12.83[d], 12.70 ± 0.06[f]	–412.4 ± 3.9	-450.6[g], –448.52[i]
$SmCl_3$	11.55 ± 0.17	11.42 ± 0.02[a], 11.374 ± 0.08[b], 10.68[c], 11.15 ± 0.04[f]	–461.0 ± 2.5	–519.4[h], –495.63[i]
$GdCl_3$	13.40 ± 0.10	13.30 ± 0.04[a], 13.319 ± 0.07[b], 12.82[c], 13.08 ± 0.04[f]	–457.7 ± 0.7	–492.9[h], –446.62[i]

[a] Spedding et al., 1966b; [b] Spedding *et al.*, 1975b; [c] Habenschuss *et al.*, 1976; [d] Pitzer *et al.*, 1978; [e] Karapet'yants *et al.*, 1976; [f] Marriott *et al.*, 2001; [g] Spedding, 1966a; [h] Spedding et al., 1975c; [i] Criss and Millero, 1999

$$\beta^{0J} = \frac{c_3}{T} + c_4 + c_5 T \tag{5.7}$$

$$\beta^{1J} = \frac{c_6}{T} + c_7 + c_8 T \tag{5.8}$$

Values of the fitting constants v_i (i=1-7) and c_i (i=1-8) were determined through regression analyses and can be found along with their uncertainties in tables 5.8 and 5.9 respectively. Equations 5.3 and 5.6 take the form of the HKF equations of state. The first two terms in each of these equations represent the structural contribution to the apparent molar property at infinite dilution while the third term represents the electrostatic contribution.

5.4 Single ion values

Single ion apparent molar volumes and heat capacities were calculated from the infinite dilution apparent molar properties reported in table 5.6:

$$Y^o_{R^{3+}} = Y^o_{RCl_3} - 3Y^o_{Cl^-} \tag{5.9}$$

$V_2^o(Cl^-)$ and $C^o_{p,2}$ (Cl^-) were calculated from the equations reported by Sharygin and Wood (1997) and Ballerat-Busserolles *et al.* (1999) for aqueous hydrochloric acid and $V_2^o(H^+)$ and $C^o_{p,2}$ (H^+) are equal to zero.

Table 5.8 Estimates of parameters to equations (5.3), (5.4), and (5.5) which model the temperature dependences of $V_{\phi,2}$ values for aqueous solutions of YCl_3, $YbCl_3$, $DyCl_3$, $SmCl_3$ and $GdCl_3$ at p = 0.1 MPa.

Parameter	YCl_3	$YbCl_3$	$DyCl_3$
v_1 /(cm^3 mol^{-1})	37.26 ± 0.61	31.59 ± 0.57	36.11 ± 0.47
v_2 /(cm^3 K mol^{-1})	-483.64 ± 46.00	-270.37 ± 37.18	-316.57 ± 31.43
10^4 v_3 /(kg mol^{-1} MPa^{-1})	7.967 ± 3.189	24.10 ± 4.15	0.5984 ± 0.4663
10^6 v_4 /(kg mol^{-1} K^{-1} MPa^{-1})	-2.067 ± 1.029	-7.749 ± 1.328	–
v_5 /(kg mol^{-1} K MPa^{-1})	38.25 ± 5.17	-0.566 ± 0.194	-66.75 ± 5.33
10 v_6 /(kg mol^{-1} MPa^{-1})	-2.339 ± 0.309	–	4.476 ± 0.336
10^4 v_7 /(kg mol^{-1} K^{-1} MPa^{-1})	3.447 ± 0.464	–	-7.538 ± 0.528

Parameter	$SmCl_3$	$GdCl_3$
v_1 /(cm^3 mol^{-1})	38.60 ± 0.84	34.84 ± 0.74
v_2 /(cm^3 K mol^{-1})	-656.75 ± 62.09	-203.51 ± 58.72
10^4 v_3 /(kg mol^{-1} MPa^{-1})	-19.17 ± 11.21	19.63 ± 8.78
10^6 v_4 /(kg mol^{-1} K^{-1} MPa^{-1})	6.583 ± 3.628	-6.229 ± 2.823
v_5 /(kg mol^{-1} K MPa^{-1})	11.01 ± 2.54	-55.87 ± 6.57
10 v_6 /(kg mol^{-1} MPa^{-1})	-0.3869 ± 0.0825	3.622 ± 0.376
10^4 v_7 /(kg mol^{-1} K^{-1} MPa^{-1})	–	-5.935 ± 0.540

Table 5.9 Estimates of parameters to equations (5.6), (5.7), and (5.8) which model the temperature dependences of $C_{p\phi,2}$ values for aqueous solutions of YCl_3, $YbCl_3$, $DyCl_3$ $SmCl_3$ and $GdCl_3$ at p = 0.1 MPa.

Parameter	YCl_3	$YbCl_3$	$DyCl_3$
c_1 /(J K^{-1} mol^{-1})	-66.47 ± 5.14	-40.79 ± 3.28	-69.69 ± 6.87
10^{-5} c_2 /(J K mol^{-1})	-4.872 ± 0.305	-4.903 ± 0.110	-4.027 ± 0.332
10 c_3 /(kg mol^{-1} K^{-1})	-4.948 ± 1.010	-5.651 ± 0.445	-6.619 ± 2.735
10^3 c_4 /(kg mol^{-1} K^{-2})	3.099 ± 0.656	3.300 ± 0.286	3.962 ± 1.757
10^6 c_5 /(kg mol^{-1} K^{-3})	-4.853 ± 1.060	-4.901 ± 0.460	-5.928 ± 2.815
c_6 /(kg mol^{-1} K^{-1})	-1.504 ± 0.698	0.04825 ± 0.00489	2.418 ± 1.418
10^2 c_7 /(kg mol^{-1} K^{-2})	0.987 ± 0.442	–	-1.440 ± 0.899
10^5 c_8 /(kg mol^{-1} K^{-3})	-1.568 ± 0.698	–	2.175 ± 1.420

Parameter	$SmCl_3$	$GdCl_3$
c_1 /(J K^{-1} mol^{-1})	-74.06 ± 3.51	-65.07 ± 7.01
10^{-5} c_2 /(J K mol^{-1})	-6.545 ± 0.175	-6.152 ± 0.418
10 c_3 /(kg mol^{-1} K^{-1})	-7.408 ± 0.480	6.485 ± 2.611
10^3 c_4 /(kg mol^{-1} K^{-2})	4.758 ± 0.323	-4.306 ± 1.680
10^6 c_5 /(kg mol^{-1} K^{-3})	-7.640 ± 0.546	7.123 ± 2.699
c_6 /(kg mol^{-1} K^{-1})	-0.2002 ± 0.0599	-7.139 ± 1.428
10^2 c_7 /(kg mol^{-1} K^{-2})	0.07653± 0.01936	4.557 ± 0.901
10^5 c_8 /(kg mol^{-1} K^{-3})	–	-7.225 ± 1.421

The single ion apparent molar volume and apparent molar heat capacity values reported here have been compared to those presented by Shock and Helgeson (1988), Pitzer *et al.* (1978), and Marriott *et al.* (2001). Single ion apparent molar volumes and apparent molar heat capacities of the trivalent metal cations investigated here are compared to those in the literature in Table 5.10. Figure 5.11 compares the infinite dilution apparent molar volumes of the trivalent REE cations reported here with the HKF equations of state reported by Shock and Helgeson (1988). Although the difference between the two predictions is only approximately 2 cm^3mol^{-1} the values reported here are based on density measurements performed at lower concentrations than those of Spedding and coworkers on which the equations of Shock and Helgeson are based. Extrapolating to infinite dilutions using low concentration data is more reliable than using high concentration data.

Figures 5.12 and 5.13 show comparisons of the $C^o_{p,2}$ (R^{3+}) presented here to those reported by Shock and Helgeson (1988). The apparent molar heat capacity curves only approach each other at high temperatures, with the differences increasing with decreasing temperature. The deviation is largely due to Shock and Helgeson's use of the lower precision batch calorimeter measurements reported by Spedding and coworkers (1966a, 1975c).

For this study, the $C^o_{p,2}$ (Cl^-) values, obtained from $C^o_{p,2}$ (HCl), reported by Ballerat-Busserolles *et al.* (1999) were used at all temperatures. At $T = 298.15K$ the $C^o_{p,2}$ (Cl^-) reported by Tanger and Helgeson and used by Shock and Helgeson (1988) was -123.2 $JK^{-1}mol^{-1}$ compared with the value of -120.8 $JK^{-1}mol^{-1}$ used in this study. This accounts for a difference between the $C^o_{p,2}$ (R^{3+}) values reported here and those

Table 5.10 A comparison of literature and calculated $V_2^o(R^{3+})$ and $C_{p2}^o(R^{3+})$ values for R^{3+} = (Y^{3+}, Yb^{3+}, Dy^{3+}, Sm^{3+}, and Gd^{3+}) at T = (288.15, 298.15, 313.15, and 328.15) K.

T /K	$V_2^o(R^{3+})$ /cm^3 mol^{-1}		
	Y^{3+}	Yb^{3+}	Dy^{3+}
288.15	-41.4	-44.4	-39.8
298.15	-42.2, –40.21[a]	-44.1, -44.425 (0.3)[a]	-40.5, –40.70 (0.3)[a]
313.15	-42.6	-45.3	-41.7
328.15	-43.0	-47.5	-43.4
	Sm^{3+}	Gd^{3+}	Cl^-
288.15		-39.7	17.439
	-42.5	-40.74b	
298.15		-40.0, -40.495 (0.3)[a],	17.811
	-41.9, -42.25 (0.3)[a]	–41.21[b]	
313.15	-43.2	-41.3, -42.38[b]	17.995
328.15	-44.4	-43.2, -42.13[b]	17.817
T /K	$C_{p2}^o(R^{3+})$ /J K^{-1} mol^{-1}		
	Y^{3+}	Yb^{3+}	Dy^{3+}
288.15	-71.0 (7.8)	-42.9 (8.0)	-45.4(8.4)
298.15	-68.4 (7.6)	-43.5 (8.0)	-50.0 (8.4)
	–70 (10)[a]	–57.2 (5)[a]	–69.6 (10)[a]
313.15	-64.5 (7.6)	-46.3 (8.7)	-59.2(8.4)
328.15	-75.7 (8.3)	-54.1 (8.6)	-79.5(8.4)
	Sm^{3+}	Gd^{3+}	Cl^-
288.15	-117.8 (7.5)	-82.0(7.5)	-131.72
298.15	-98.7 (7.8)	-95.3 (7.5)	-120.79,
	–116.7 (10)[a]	-67.7 (5)[a], -73.6[b]	-126.23[b], –126.32[a]
313.15		-94.3 (7.8)	-113.03
	-92.4 (7.6)	-87.5[b]	-114.76b
328.15		-71.1 (7.5)	-111.33
	-99.3 (7.6)	-87.7[b]	-110.17b

[a] – Spedding et al., 1966a; [b]- Xaio and Tremaine, 1996

Figure 5.11 Comparison of infinite dilution apparent molar volumes of $YbCl_3$.

(●) Equation 5.1, Broken line – Equation 5.3, (X) Habenschuss and Spedding (1976), Solid line – Shock and Helgeson (1988).

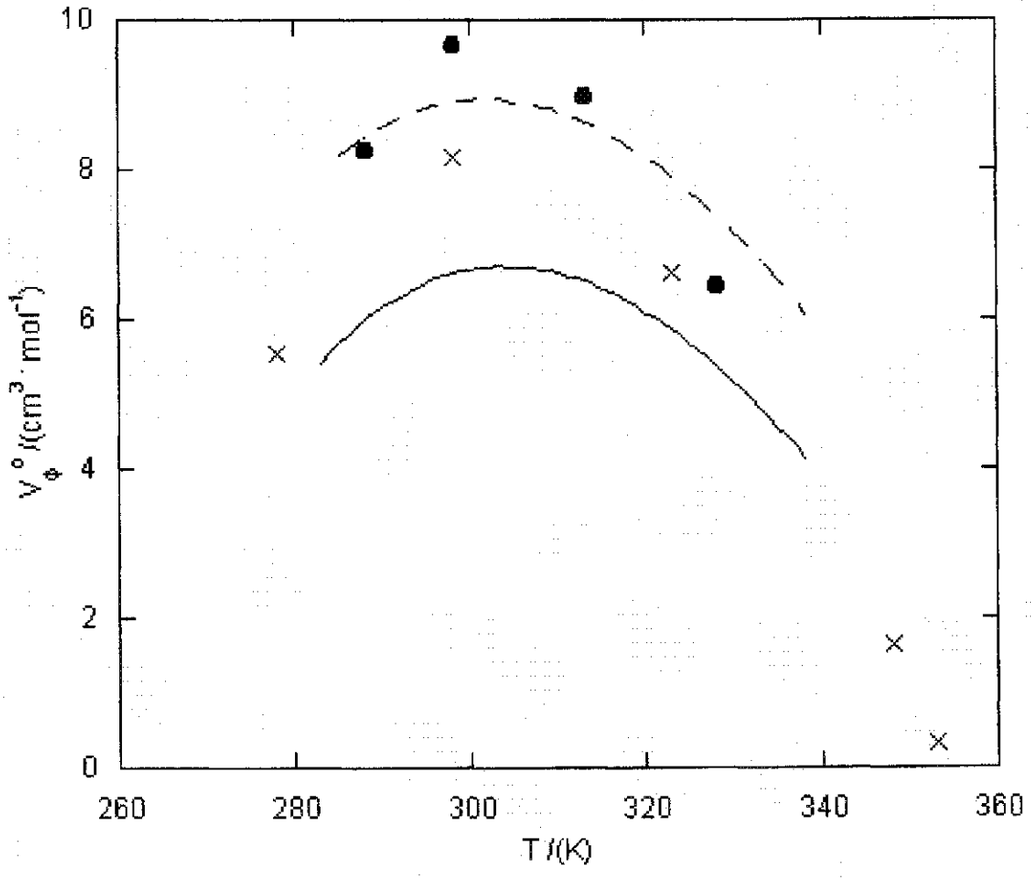

Figure 5.12 Comparison of infinite dilution apparent molar heat capacities of $YbCl_3$.
(●) equation 5.2, broken line – equation 5.6, solid line – Shock and Helgeson (1988)

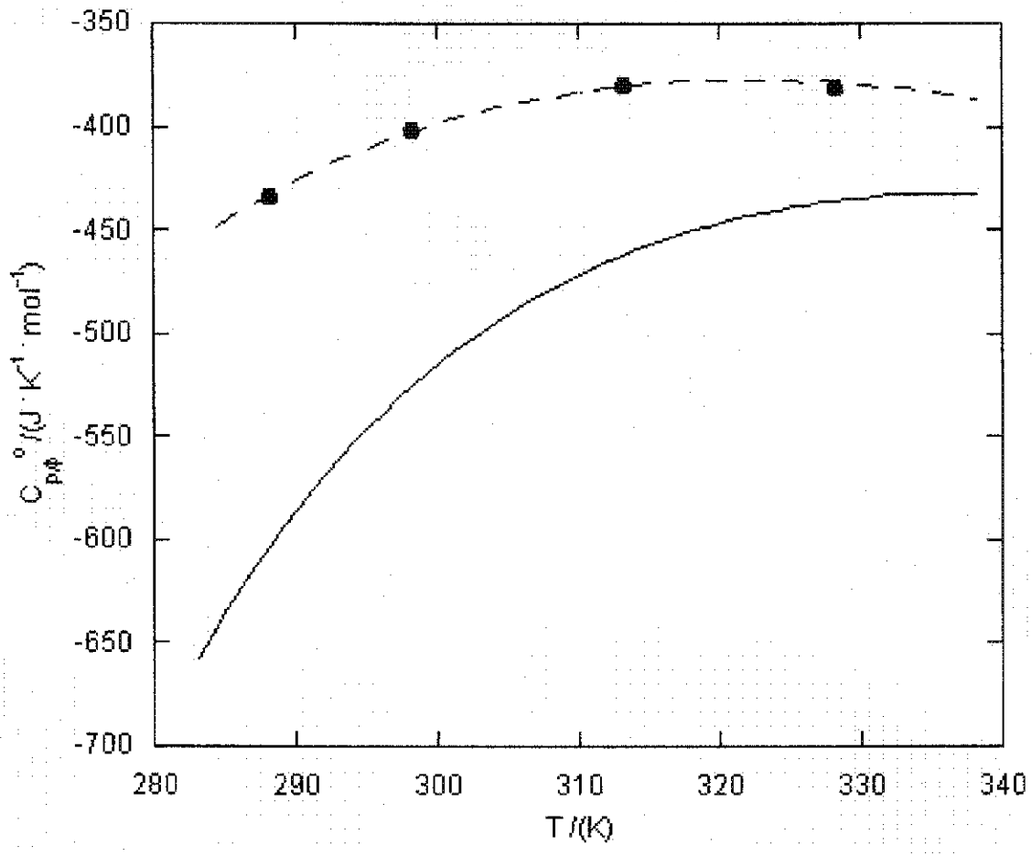

Figure 5.13 Comparison of infinite dilution apparent molar heat capacities of $GdCl_3$.
(●) equation 5.2, broken line – equation 5.6, solid line – Shock and Helgeson (1988).

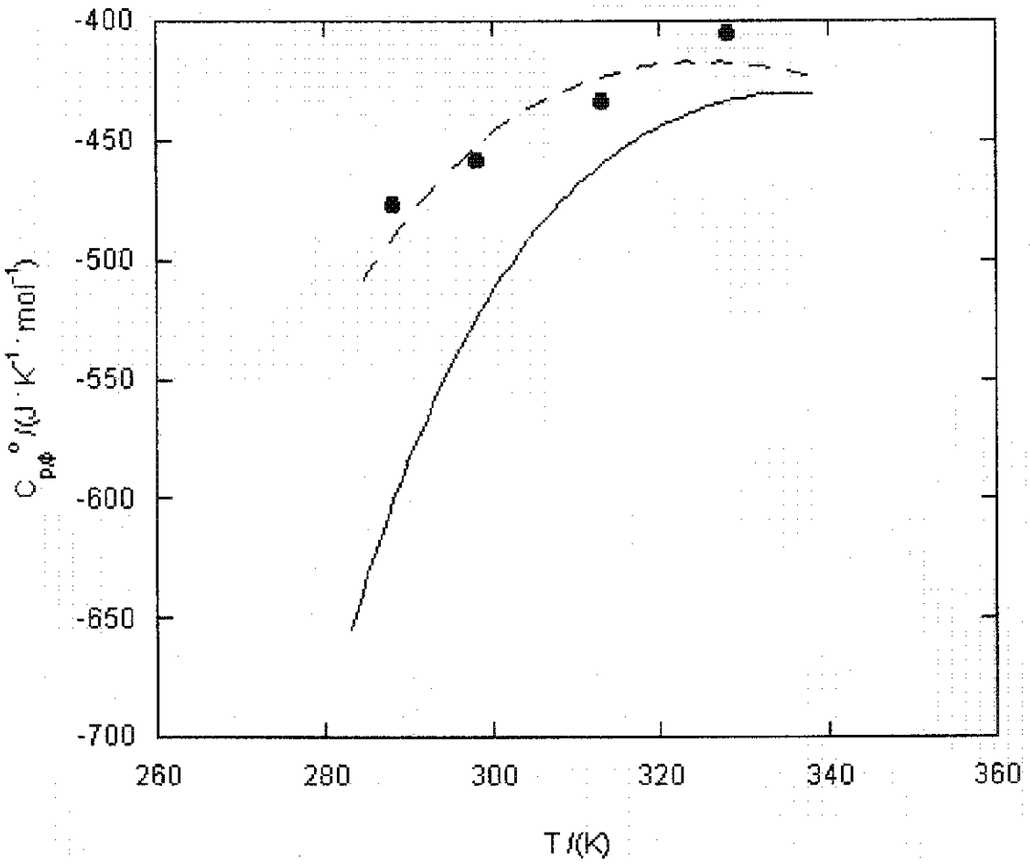

reported by Shock and Helgeson of 7.2 $JK^{-1}mol^{-1}$ due only to the difference in $C^{o}_{p,2}$ (Cl^-). The more recent study reported by Xaio and Tremaine (1996) uses the value of -126.23 $JK^{-1}mol^{-1}$ for $C^{o}_{p,2}$ (Cl^-) at T = 298.15K taken from Tremaine *et al.* (1986) whereas the study by Marriott *et al.* (2001) use the $C^{o}_{p,2}$ (Cl^-) value reported by Criss and Millero (1999) of -126.32 $JK^{-1}mol^{-1}$ at T=298.15K. These values could account for differences of approximately 19 $JK^{-1}mol^{-1}$ between values for $C^{o}_{p,2}$ (R^{3+}) reported in the various studies. A plot of $C^{o}_{p,2}$ (Cl^-) values utilized in this study and those previously reported in the literature versus temperature is shown as figure 5.14.

5.5 Comparison with perchlorate data

The level of complex formation found in aqueous solutions of the chloride salts of trivalent REEs is expected to be observable but not significant, while complex formation in an aqueous solution of a perchlorate salt is thought to be negligible under the conditions encountered in this study. In chloride solutions the dominant complex formed is thought to be $RCl^{2+}_{(aq)}$. A method to illustrate the degree of complex formation is presented by Marriott et al. (2001). The magnitudes of $V_{\phi,2} - V_{\phi,2}^{o}$ and $C_{p\phi,2} - C^{o}_{p,2}$ as a function of the square root of ionic strength are indicative of complex formation within a system. Plotting $V_{\phi,2} - V_{\phi,2}^{o}$ or $C_{p\phi,2} - C^{o}_{p,2}$ versus the square root of ionic strength produces a nearly linear relationship. The slope of the relationship will change with the degree of complex formation. For example Marriott *et al.* (2001) used this procedure successfully to illustrate the high degree of complex

Figure 5.14 Comparison of C_p°(Cl-) in this thesis to the literature.

(●) Ballerat-Busserolles *et al.* (1999), (X) Xiao and Tremaine (1996), (+) Tanger and Helgeson (1988), (◊) Criss and Millero (1999)

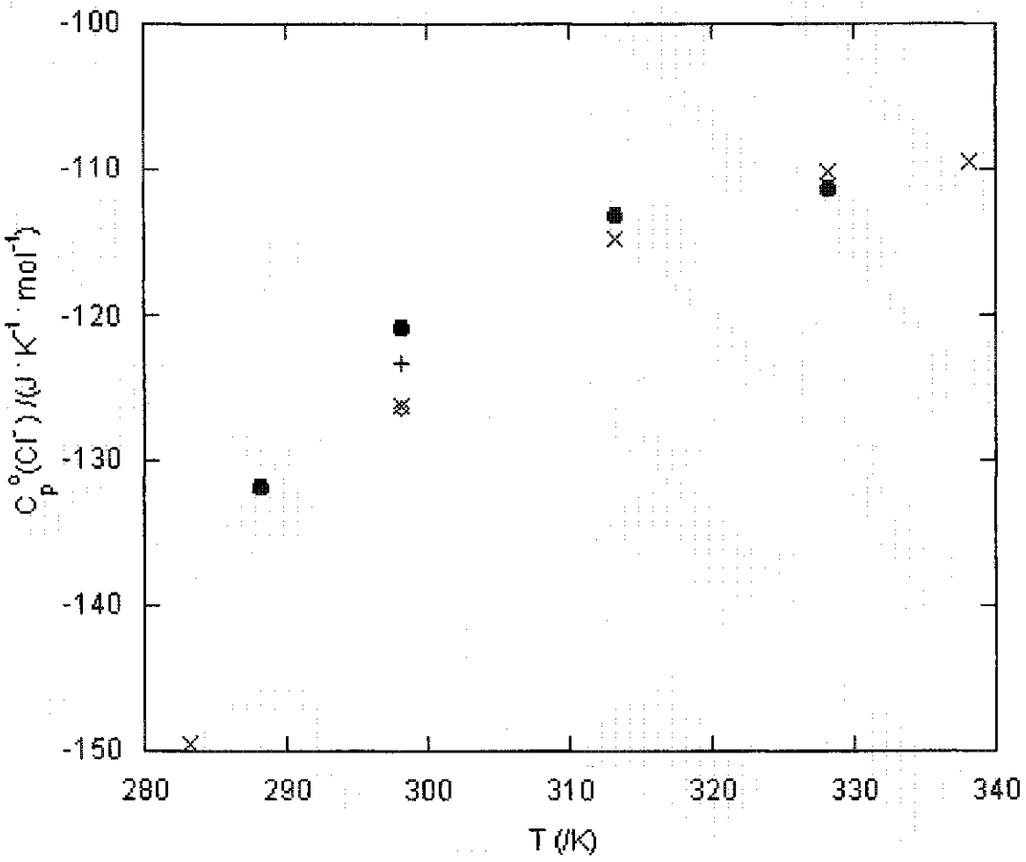

formation in aqueous rare earth sulfate solutions. When compared to the sulfate solutions values for $V_{\phi,2}-V_{\phi,2}^{o}$ and $C_{p,\phi,2}-C_{p,2}^{o}$ for the chloride and perchlorate solutions are dramatically smaller implying a much lower degree of complex formation. From these observations, it was rationalized that, whereas the apparent molar properties of the

perchlorate and the chloride salt solutions could be successfully modeled using equations which emphasize ion interaction, the properties of the sulfates are best modeled using equations which emphasize complex formation.

The method utilized by Marriott *et al.* (2001) was applied to the apparent molar heat capacities and apparent molar volumes reported in Chapter 4 for the perchlorate systems and the $C_{p,\phi,2}$ and $V_{\phi,2}$ values reported for YCl_3, $YbCl_3$, $DyCl_3$, $SmCl_3$ in this chapter. Figures 5.15-5.18 show $V_{\phi,2} - V_{\phi,2}^{o}$ for $SmCl_3$ compared to $V_{\phi,2} - V_{\phi,2}^{o}$ for $Sm(ClO_4)_3$ at the investigated temperatures. Comparing each temperature it can be seen that the degree of complex formation appears to increase with increasing temperature, in the manner predicted by Wood (1990a, 1990b). The comparison plots for the other trivalent metal salts showed similar but less pronounced change in slope with temperature.

A corresponding increase in slope with temperature is not apparent when $C_{p,\phi,2}$-$C_{p,2}^{o}$ values of the trivalent metal chlorides and perchlorates are compared. Conclusions are difficult to draw from the heat capacity comparisons due to the differences in $C_{p,\phi,2}$-$C_{p,2}^{o}$ being comparable in magnitude to the sum of the uncertainties in $C_{p,\phi,2}$ for the chlorides and perchlorates.

When comparing the $C_{p,\phi,2}$-$C_{p,2}^{o}$ and $V_{\phi,2}$–$V_{\phi,2}^{o}$ comparison plots reported here to those of Marriott *et al.* (2001) we see that the deviation of the chloride $C_{p,\phi,2}$-$C_{p,2}^{o}$ and $V_{\phi,2}$–$V_{\phi,2}^{o}$ values from those of the perchlorate salt are insignificant when compared to the deviation of the sulfate from the perchlorate salt. While differences

Figure 5.15 Change in apparent molar volume of SmX_3 at T = 288.15 K with concentration.

• – $Sm(ClO_4)_3$, X – $SmCl_3$.

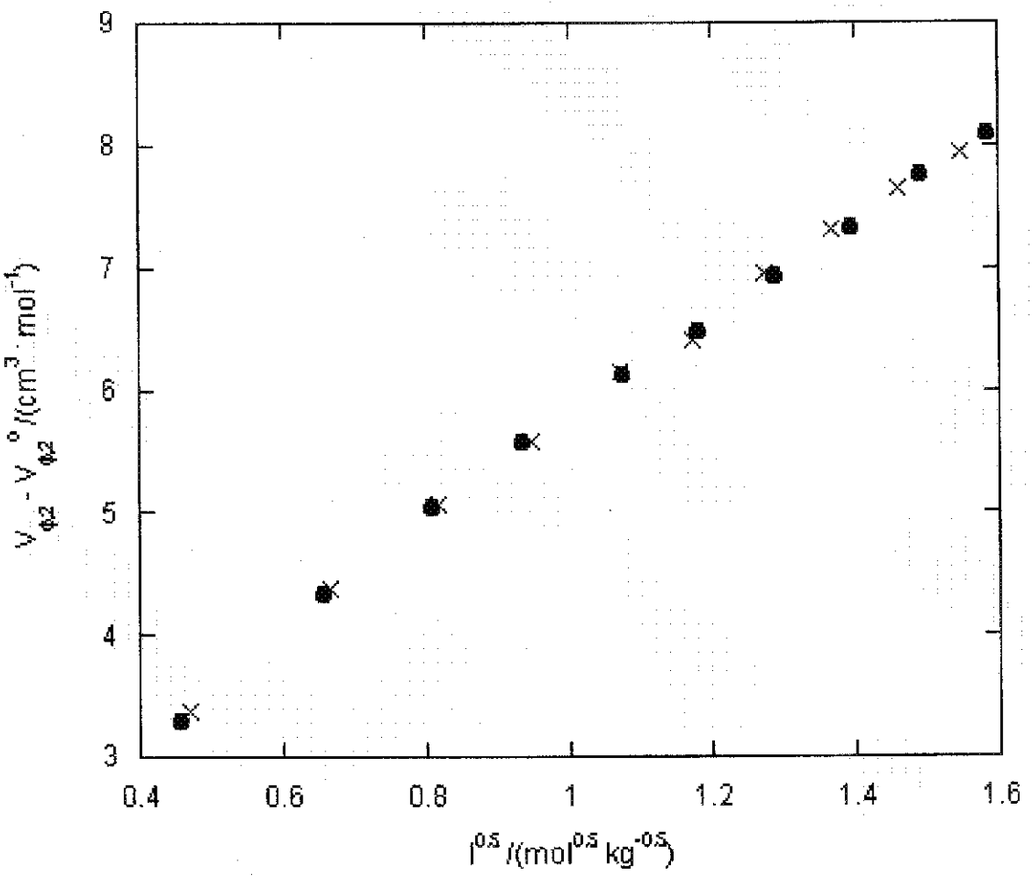

Figure 5.16 Change in apparent molar volume of SmX_3 at T = 298.15 K with concentration.

•– $Sm(ClO_4)_3$, X – $SmCl_3$.

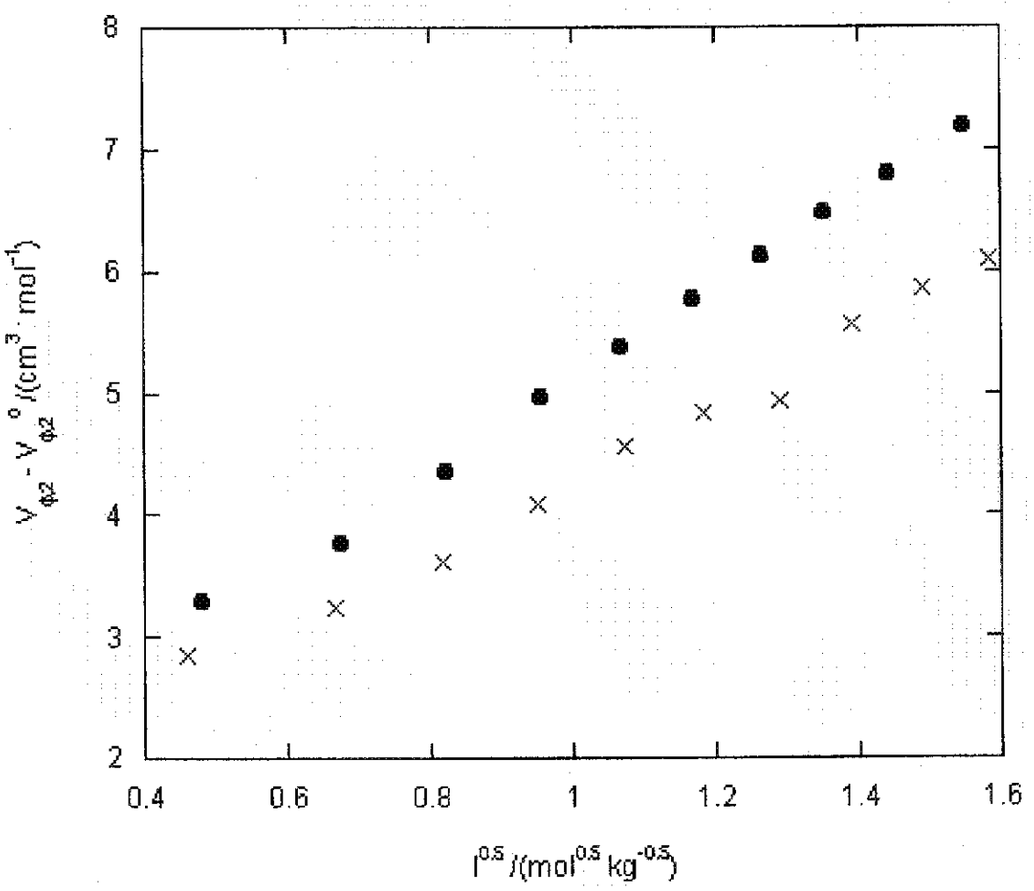

Figure 5.17 Change in apparent molar volume of SmX_3 at T = 313.15 K with concentration.

• – $Sm(ClO_4)_3$, X – $SmCl_3$.

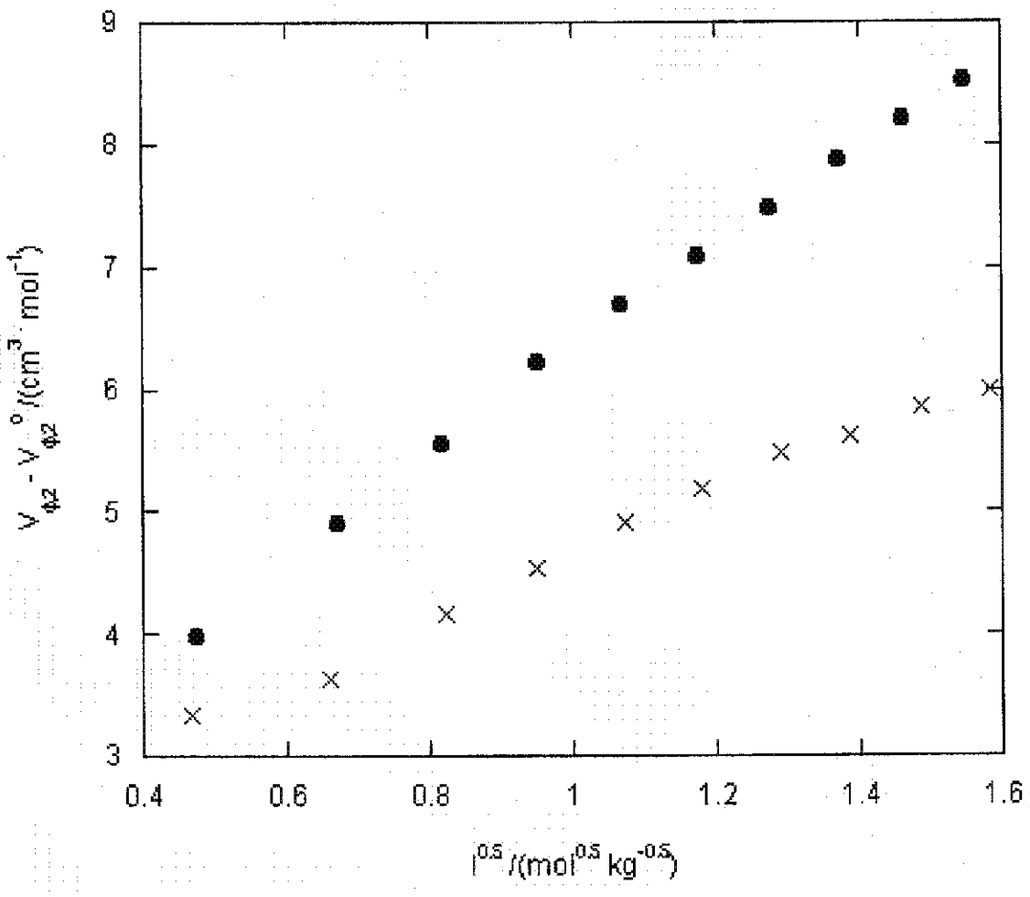

Figure 5.18 Change in apparent molar volume of SmX_3 at T = 328.15 K with concentration.

• – $Sm(ClO_4)_3$, X – $SmCl_3$.

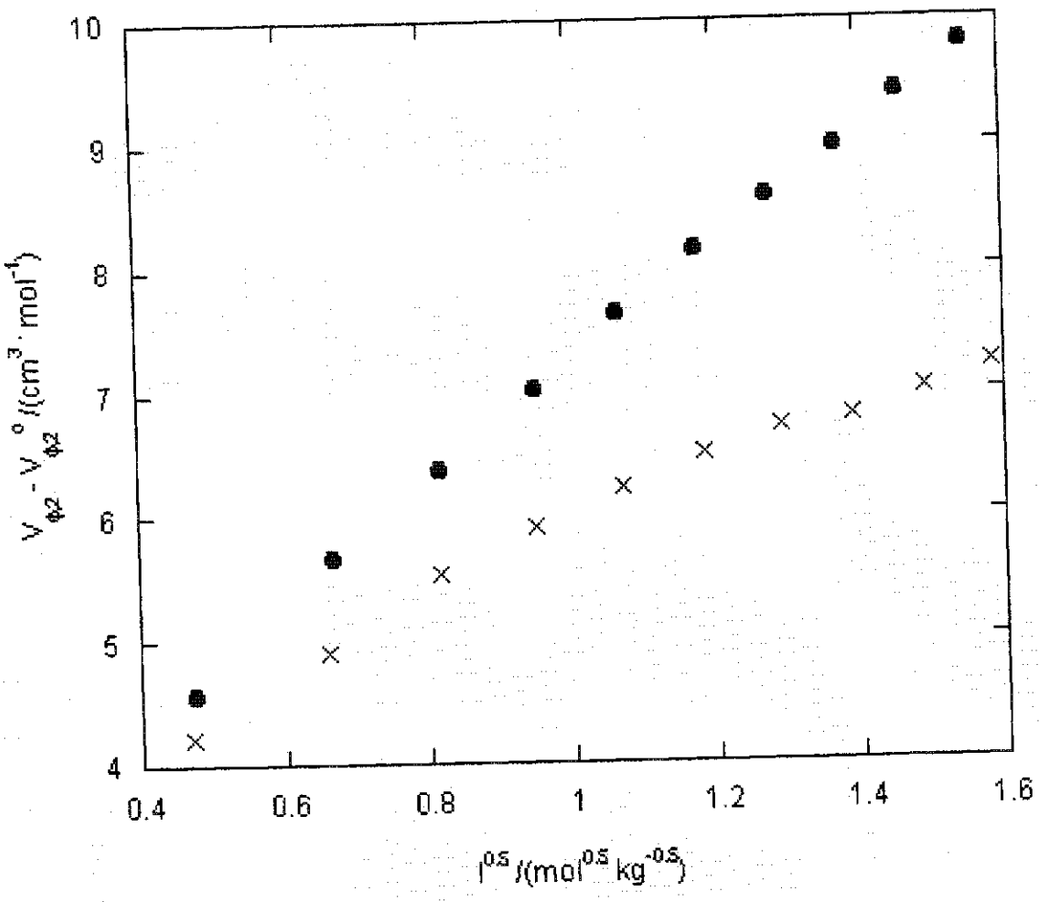

between $V_{\phi 2}$–$V_{\phi 2}^{o}$ of the chloride salts and the perchlorate salts reached a maximum of ~5cm^{3}mol^{-1}, the difference between $V_{\phi 2}$–$V_{\phi 2}^{o}$ of the sulfate salts and the perchlorate salts reached a maximum of approximately 50cm^{3}mol^{-1}. Similarly, the difference in $C_{p,\phi 2}$-$C_{p,2}^{o}$ between the chloride salts and the perchlorate salts only reached a maximum of 50 JK^{-1}mol^{-1}, while the difference in $C_{p\phi 2}$-$C_{p,2}^{o}$ between the sulfate salts and the perchlorate salts may be as large as 1000 JK^{-1}mol^{-1}.

5.6 Conclusions

It has been qualitatively shown that complex formation is present in dilute solutions of trivalent metal chloride salts, however, the degree of complex formation is thought to be very small at all temperatures investigated in this study. Differences between single ion apparent molar properties calculated from the perchlorate salts and those reported in this chapter are generally small, being within the sum of experimental uncertainties. It is recommended that the values derived from the perchlorate measurements be used in all studies requiring single ion values because of the small amount of complex formation found to be present in aqueous solutions of the rare earth chlorides.

6 HIGH TEMPERATURE AND PRESSURE VOLUMETRIC MEASUREMENTS

6.1 Previous measurements

No previous studies reported in the literature have investigated the pressure and temperature dependence of apparent molar volumes of aqueous rare earth perchlorate salt solutions in the temperature and pressure range reported in this chapter. However, theoretical models have been published which permit the estimation of thermodynamic properties for these systems at infinite dilution over extended temperature and pressure ranges (Shock and Helgeson, 1988). Although ytterbium perchlorate was the main focus of the study presented here, no reports of volumetric measurements on perchloric acid at elevated temperatures and pressures could be found in the literature, thus necessitating the measurement of densities for aqueous perchloric acid solutions over the same temperature and pressure range as used in the ytterbium perchlorate investigation.

6.2 Experimental

6.2.1 Solution preparation

Solutions of perchloric acid were prepared by dilution of concentrated perchloric acid (BDH Chemicals). Perchloric acid solution samples were sealed in glass volumetric flasks.

Solutions of acidified ytterbium perchlorate were prepared by dissolving ytterbium oxide in approximately 1.2 M perchloric acid that was heated to approximately T = 353 K. The solution was stirred until the dissolution of the oxide appeared to have

stopped. The solution was then cooled and the pH measured. If the pH had risen above 3, additional 0.1 M perchloric acid was added and the solution was again heated. When no more oxide appeared to dissolve, the solution was allowed to cool and the pH measured. This heating and pH measurement/adjustment cycle was continued until the pH of the solution no longer rose above 3. The solution was then vacuum filtered using a fine sintered glass filter funnel. The final solution was subsequently stored in a sealed glass volumetric flask and was found to be free of colloidal particles.

6.2.2 Standardization of stock solutions

The stock acidified ytterbium perchlorate solution was standardized using titrimetric analysis. The perchloric acid present in the ytterbium perchlorate stock solution was determined by titration with tris(hydroxymethyl)aminomethane (THAM) (99.94±0.01 mol%, obtained from US Department of Commerce, National Bureau of Standards) using xylenol orange as the indicator. To determine the concentration of Yb^{3+} in the stock solution, the solution was titrated with the disodium salt of ethylenediaminetetraacetic acid (EDTA) (obtained from BDH, 99.0-101.0% assay) buffered to pH=5.5 using an acetic acid sodium acetate buffer solution. In this titration, methyl red was used as the indicator. Solutions of EDTA used in the titrations were prepared according to the procedure outlined by Skoog *et al.* (2000). The final Yb^{3+} concentration was calculated as the average of multiple trials.

The concentration of the perchloric acid stock solution was determined using three separate methods. Initially, samples of the perchloric acid stock solution were titrated with THAM in the same manner used for the determination of acid in the stock

ytterbium perchlorate solution. As an additional check on the perchloric acid concentration, both potentiometric and conductimetric titrations were performed. Potentiometric and conductometric titrations provide objective endpoints to titration while visual indicator titrations may be subject to determinant errors related to end-point determination. Unfortunately it was not possible to successfully complete potentiometric or conductometric titrations of the rare earth stock solutions due to the formation of rare earth hydroxide species with increasing pH.

Potentiometric titration involves measuring the change in potential difference across a glass membrane electrode as titrant is added to the analyte. For the titrations performed in this study, a 10.00 mL aliquot of perchloric acid was titrated with 0.1 M sodium hydroxide (standardized against dried KHP (potassium hydrogen phthalate)). Titrations were followed using a glass combination electrode (Fisher, catalogue number 13-620-108) connected to a Fisher Scientific Accumet® pH Meter 915. Plotting measured potential versus volume of sodium hydroxide added gives a typical strong/acid strong base titration curve. Figure 6.1 shows the results of plotting potential versus volume of sodium hydroxide added. Plotting the second derivative of the potential with respect to the volume of sodium hydroxide added, as seen in figure 6.2, allows determination of the equivalence point with enhanced precision. To obtain a plot of the second derivative of the potential, the difference between adjacent potentials (ΔV) was calculated, then the difference between adjacent ΔV values was calculated and plotted.

Figure 6.1 Typical acid-base titration curve.

The vertical line segment represents the equivalence point of the titration.

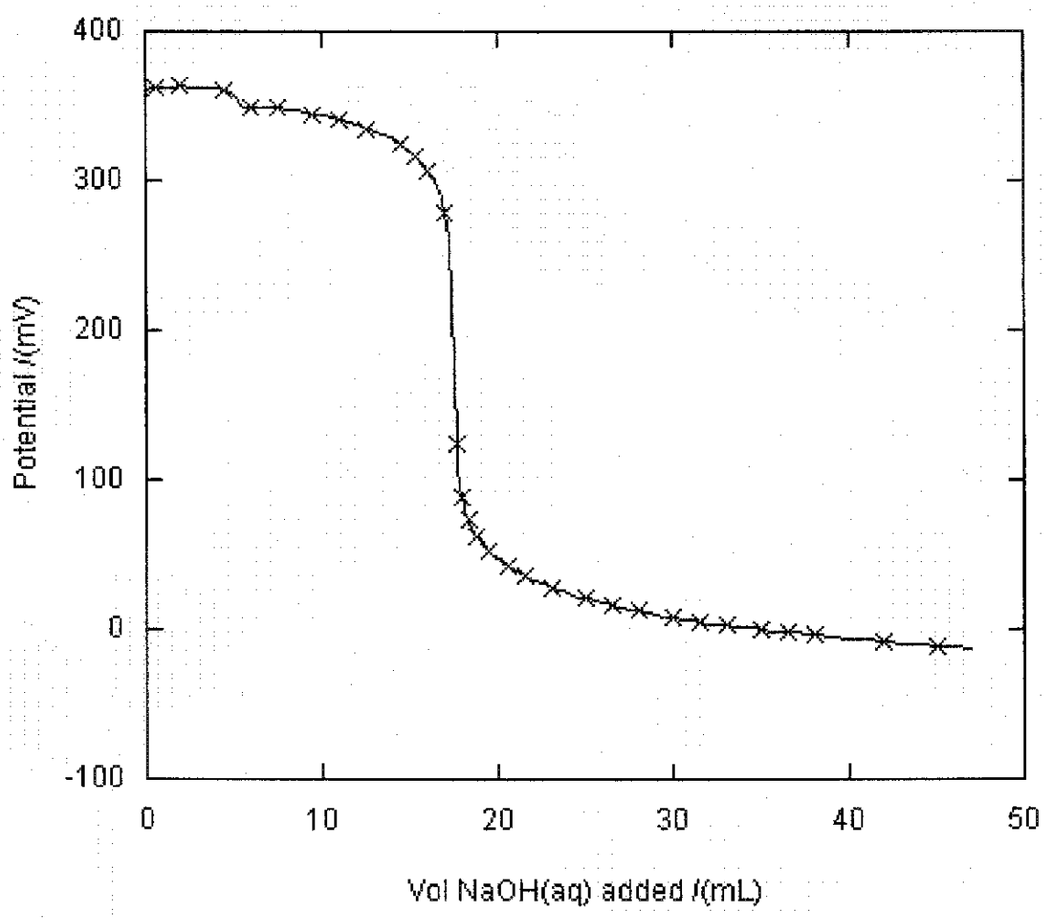

Conductimetric titrations measure the change in conductance of a solution as titrant is added using a resistance cell. The resistance cell consists of two platinum contacts set a fixed distance apart from each other on a glass rod. The contacts are connected to an Industrial Instruments Conductivity Bridge Model RC 16B2 and the glass rod is immersed in an electrolyte ensuring that both contacts are covered by electrolyte. The resistance of the probe does not change over the course of the titration, any change in

Figure 6.2 Typical plot of the second derivative of potential versus volume of titrant added in an acid-base titration.

The vertical line in the centre of the plot indicates the equivalence point of the titration.

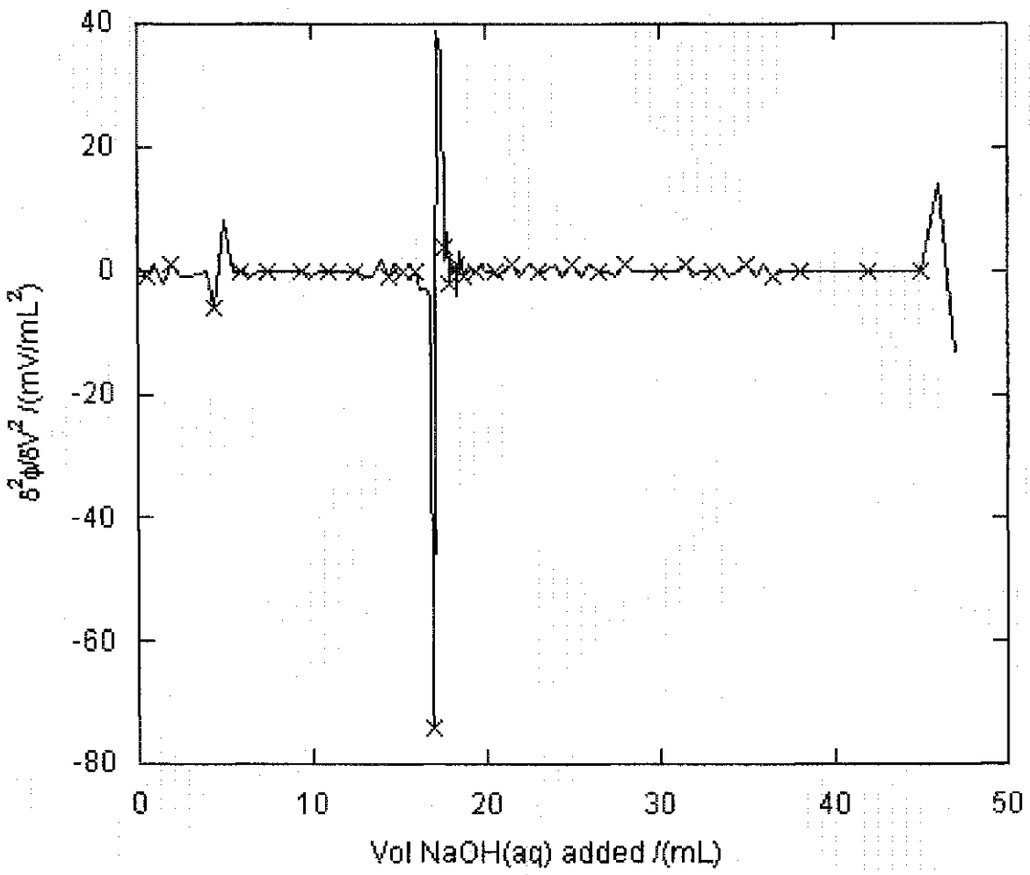

conductance results entirely from a change in conductance of the electrolyte in which the conductivity cell is immersed. In the case of the perchloric acid titrations, 10.00 mL of the perchloric acid stock solution were placed in a tall-form flask and distilled water (~90 mL) was added to ensure that both contacts of the resistance cell were submerged. The initial conductance of the solution was then measured. Sodium hydroxide was added to the perchloric acid solution in 1.00mL aliquots and the conductance of the resulting solution was measured after each addition. The profile of conductance versus volume of

sodium hydroxide added can be seen in figure 6.3. To facilitate the determination of the exact equivalence point of the titration, linear regression was applied to the set of conductance measurements occurring before the equivalence point and also to the conductance data set collected following the equivalence point. The intersection of these two straight lines indicates the equivalence point of titration exactly. Initially, as sodium hydroxide was added to the perchloric acid solution, the sodium hydroxide neutralized the perchloric acid in solution and the conductance of the solution decreased as the concentration of aqueous H^+ decreased. When all of the perchloric acid had been neutralized, excess sodium hydroxide added to the titration flask caused an increase in conductance of the solution.

Volumetric measurements were performed on solutions that were prepared by weight, making use of the molal concentration scale necessary. To convert from calculated molarity to molality, the density of both the perchloric acid and acidified ytterbium perchlorate stock solutions was measured at the temperatures at which titrations were performed. The molal concentration of ytterbium perchlorate, m_2, in an acidified solution can be converted to molal concentrations using the equation:

$$m_2 = \frac{1000c_2}{(1000\rho)-(c_3M_3)-(c_2M_2)}. \qquad (6.1)$$

In equation 6.1 the terms c_2, c_3, M_2 and M_3 are the molar concentrations and molar masses of the rare earth salt and acid, respectively and ρ is the density of the acidified ytterbium perchlorate solution at the temperature at which the titration was performed.

Figure 6.3 Typical plot of conductance versus volume added for a titration of perchloric acid with sodium hydroxide.

Regression analysis of each line gives a value for the equivalence point of the titration. The dashed lines represent the values returned by regression analysis and the intersection of the dashed lines is the equivalence point of the titration.

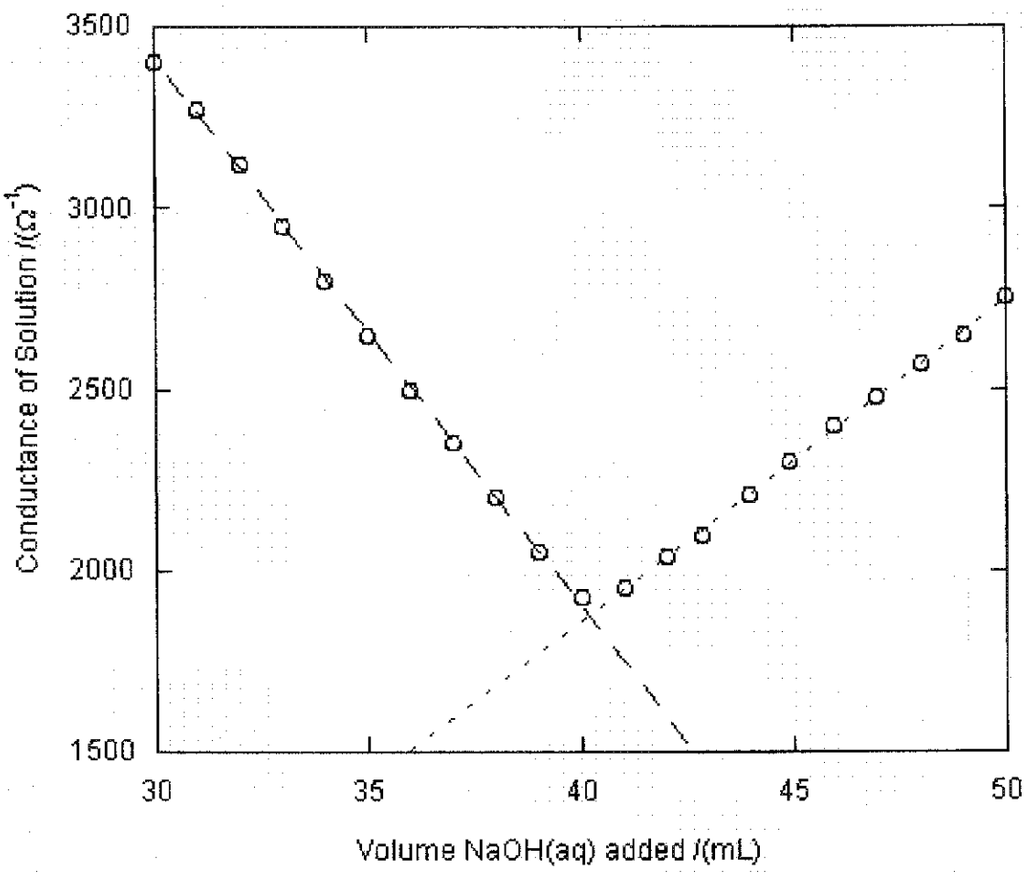

6.2.3 Preparation of sets of solutions

For each set of temperature/pressure conditions at which volumetric measurements were made, 8 to 10 solutions in the concentration range m = (0.01624 to 0.2531 M $Yb(ClO_4)_3$ and 0.02725 to 0.4000 M $HClO_4$) were prepared. Solutions were prepared by mass using a Mettler Toledo AT201 balance by diluting a known mass of

stock solution with a known mass of pure water. The reference solution used in the collection of relative density measurements was a concentrated (approximately 5.0 M) solution of aqueous sodium chloride. The reference NaCl(aq) solutions were prepared by dissolving a known mass of dried NaCl(s) with pure water by mass. All water used was distilled and purified by an Osmonics model Aries High-Purity D.I. Loop that polishes water to a resistance of 18.3MΩ.

6.3 Modeling of experimental data

Solution densities for the aqueous perchloric acid and acidified $Yb(ClO_4)_3$ were measured using a high temperature and pressure vibrating tube densimeter following the procedure described in Chapter 2. The density of the NaCl(aq) reference solution was obtained from Archer's program for the thermodynamic properties of aqueous sodium chloride (Archer, 1992). Experimental apparent molar volumes, $V_{\phi,exp}$, for the acidified perchlorate salt solutions were calculated from experimentally determined solution densities using equation 6.2:

$$V_{\phi,\exp} = \frac{\dfrac{1+(m_2M_2)+(m_3M_3)}{\rho} - \dfrac{1}{\rho^o}}{1000(m_2+m_3)} \qquad (6.2)$$

In equation 6.2, ρ^0 is the density of pure water at the temperature and pressure at which measurements were made, values of which were taken from Archer (1992). The concentration dependences of relative densities and apparent molar volumes of aqueous solutions of perchloric acid and $Yb(ClO_4)_3$ at T = (348.15, 373.15, 398.15 and 423.15) K

and p = (10, 20 and 30) MPa are reported in Tables 6.1-6.4 and 6.5-6.8 respectively along with uncertainties of apparent molar volumes. Uncertainties were calculated using the procedure described in Chapter 2.

6.3.1 Modeling of perchloric acid volumetric data

Apparent molar volumes of solutions of perchloric acid are required to determine the contribution of perchloric acid to the apparent molar volume of the acidified rare earth perchlorate salt solutions. The temperature and pressure range of the perchloric acid data set was expanded by including the volumetric data reported by Hovey (1988) at the p = 0.1MPa and T = (283.15, 298.15, 313.15 and 328.15) K. The latter data (Hovey, 1988) were also used in the calculations presented in Chapter 5. The equation used to model the combined apparent molar volume data sets for aqueous perchloric acid solutions takes the form utilized by Simonson (1994) in the modeling of volumetric data for aqueous sodium chloride solutions. This Pitzer ion-interaction equation takes the form:

$$V_\phi = V_\phi^o + \left(\frac{A_V}{b}\right)\ln\left(1+b\sqrt{\left(\frac{m}{m^o}\right)}\right) + 2RT\left(\frac{m}{m^o}\right)\left(B^V + \left(\frac{m}{m^o}\right)C^V\right), \qquad (6.3)$$

where A_V is the Debye-Huckel limiting slope taken from Archer and Wang (1990), b is a constant equal to 1.2, R is the ideal gas constant, and m^o is a standard concentration equal to 1 mol kg^{-1}. V_ϕ^o is apparent molar volume at infinite dilution and in its expanded form is represented by the equation:

Table 6.1 The densities of pure water, the concentration dependence of relative densities and apparent molar volumes of aqueous solutions of perchloric acid at temperature T = 348.15 K and pressures p = (10, 20 and 30) MPa as well as the uncertainty in each apparent molar volume ($\delta V_{\phi,2}$).

Concentration /mol kg^{-1}	T /K	p /MPa	ρ^o /g cm^{-3}	ρ-ρ^o /g cm^{-3}	$V_{\phi\ exp}$ /cm^3 mol^{-1}	$\delta V_{\phi,2}$ /cm^{3}mol^{-1}
0.0606	347.36	10.00	0.979662	0.003267	46.23	0.12
0.0606	347.38	10.00	0.979652	0.003261	46.34	0.12
0.1178	347.27	10.00	0.979716	0.006051	48.71	0.16
0.1564	347.28	10.00	0.979714	0.008028	48.68	0.89
0.1992	347.33	10.01	0.979688	0.010104	49.19	0.06
0.1992	347.34	10.01	0.979680	0.010108	49.17	0.06
0.2354	347.31	10.01	0.979698	0.011935	49.12	0.07
0.2354	347.27	10.01	0.979721	0.011918	49.19	0.07
0.2742	347.10	10.01	0.979820	0.013913	48.98	0.10
0.3153	347.01	10.01	0.979874	0.015863	49.33	0.22
0.3153	347.07	10.01	0.979840	0.015932	49.10	0.22
0.3545	347.09	10.01	0.979829	0.017846	49.19	0.17
0.3996	347.12	10.01	0.979811	0.020118	49.08	0.13
0.3996	347.12	10.01	0.979810	0.020066	49.21	0.13
0.0384	346.29	20.02	0.984572	0.002075	46.16	2.62
0.0769	346.49	20.03	0.984466	0.004016	47.95	0.83
0.0769	346.53	20.02	0.984441	0.003972	48.54	0.82
0.1170	346.78	20.04	0.984303	0.006046	48.42	0.41
0.1170	346.88	20.03	0.984238	0.006093	48.00	0.41
0.1546	346.85	20.02	0.984256	0.007897	48.94	0.13
0.1546	346.89	20.03	0.984234	0.007881	49.05	0.13
0.2010	346.99	20.02	0.984180	0.010295	48.68	0.84
0.2377	346.90	20.03	0.984227	0.012133	48.77	0.37
0.2377	346.84	20.03	0.984266	0.012064	49.07	0.37
0.2758	346.92	20.03	0.984218	0.013987	49.02	0.26
0.2758	346.92	20.03	0.984218	0.014029	48.87	0.26
0.3056	346.85	20.02	0.984252	0.015477	49.01	0.23
0.3611	346.75	20.04	0.984316	0.018239	49.02	0.08
0.3611	346.81	20.04	0.984283	0.018218	49.09	0.08
0.3996	346.77	20.04	0.984306	0.020179	48.93	0.11
0.3996	346.73	20.04	0.984332	0.020219	48.83	0.11
0.0488	346.48	29.95	0.988617	0.002618	46.61	1.24
0.0488	346.54	29.95	0.988581	0.002677	45.37	1.24
0.0781	346.54	29.92	0.988573	0.004218	46.15	2.80
0.1186	346.79	29.91	0.988423	0.006156	48.18	0.22
0.1186	346.83	29.91	0.988398	0.006182	47.96	0.22
0.1544	346.97	29.94	0.988333	0.007945	48.58	0.21

Table 6.1 Continued

Concentration /mol kg^{-1}	T /K	p /MPa	ρ^o /g cm^{-3}	$\rho-\rho^o$ /g cm^{-3}	$V_{\phi\ exp}$ /cm^3 mol^{-1}	$\delta V_{\phi 2}$ /cm^{3}mol^{-1}
0.1544	347.03	29.93	0.988296	0.007977	48.37	0.21
0.1965	347.31	29.91	0.988129	0.010087	48.58	0.76
0.1965	347.55	29.90	0.987986	0.010236	47.81	0.76
0.2351	347.71	29.93	0.987901	0.012012	48.73	0.07
0.2351	347.75	29.91	0.987872	0.011997	48.80	0.07
0.2766	347.71	29.91	0.987897	0.014123	48.67	0.40
0.2766	347.69	29.93	0.987916	0.014235	48.25	0.40
0.3148	347.68	29.92	0.987917	0.015954	48.97	1.32
0.3581	347.52	29.81	0.987960	0.018134	48.90	0.79
0.3996	347.32	29.82	0.988082	0.020256	48.75	0.48

Table 6.2 The density of pure water, concentration dependence of relative densities and apparent molar volumes of aqueous solutions of perchloric acid at temperature T = 373.15 K and pressures p = (10, 20 and 30) MPa as well as the uncertainty in each apparent molar volume ($\delta V_{\phi,2}$).

Concentration /mol kg^{-1}	T /K	p /MPa	ρ^o /g cm^{-3}	ρ-ρ^o /g cm^{-3}	$V_{\phi\ exp}$ /cm^3 mol^{-1}	$\delta V_{\phi,2}$ /cm^{3}mol^{-1}
0.0432	371.63	10.05	0.964044	0.002222	48.72	1.65
0.0432	371.66	10.05	0.964022	0.002155	50.37	1.65
0.0773	371.77	10.05	0.963946	0.003970	48.71	0.12
0.0773	371.82	10.05	0.963916	0.003964	48.80	0.12
0.1174	371.85	10.06	0.963894	0.005980	49.11	2.02
0.1585	372.00	10.05	0.963785	0.008085	48.90	2.20
0.1967	372.02	10.04	0.963770	0.009817	49.98	1.60
0.2354	372.28	10.05	0.963592	0.011873	49.32	1.25
0.2354	372.31	10.05	0.963565	0.011595	50.60	1.25
0.2751	372.36	10.05	0.963531	0.013665	50.05	1.60
0.3117	372.40	10.05	0.963507	0.015523	49.82	0.31
0.3117	372.44	10.05	0.963478	0.015430	50.14	0.31
0.3535	372.44	10.05	0.963474	0.017575	49.80	0.33
0.3535	372.42	10.05	0.963488	0.017463	50.14	0.33
0.3996	372.50	10.05	0.963435	0.019654	50.25	0.10
0.3996	372.57	10.05	0.963387	0.019622	50.34	0.10
0.0432	371.57	20.01	0.968552	0.002209	49.06	2.32
0.0432	371.64	20.01	0.968512	0.002303	46.73	2.32
0.0773	371.80	20.02	0.968400	0.003955	48.94	0.31
0.0773	371.91	20.02	0.968321	0.003978	48.63	0.31
0.1174	372.14	20.01	0.968162	0.005951	49.40	0.54
0.1174	372.21	20.02	0.968120	0.006011	48.85	0.54
0.1585	372.23	20.03	0.968109	0.007979	49.64	0.01
0.1585	372.25	20.03	0.968092	0.007981	49.63	0.01
0.1967	372.30	20.01	0.968056	0.010001	49.00	1.13
0.2354	372.46	20.00	0.967936	0.011938	49.05	1.24
0.2751	372.48	20.01	0.967926	0.013761	49.70	0.34
0.2751	372.49	20.01	0.967922	0.013672	50.04	0.34
0.3535	372.67	20.02	0.967798	0.017719	49.38	0.23
0.3996	372.92	20.00	0.967622	0.019844	49.76	0.13
0.3996	373.03	20.02	0.967551	0.019796	49.89	0.13
0.0402	371.48	30.05	0.973006	0.002099	47.99	3.21
0.0790	371.77	30.05	0.972940	0.002221	47.95	2.12
0.0790	371.86	30.04	0.972806	0.004121	50.08	2.12
0.1137	372.25	30.04	0.972744	0.003962	47.70	2.06
0.1137	372.36	30.04	0.972475	0.005945	49.79	2.06
0.1553	372.53	30.04	0.972403	0.005721	50.04	0.16

Table 6.2 Continued.

Concentration /mol kg^{-1}	T /K	p /MPa	ρ^o /g cm^{-3}	ρ-ρ^o /g cm^{-3}	$V_{\phi,exp}$ /cm^3 mol^{-1}	$\delta V_{\phi,2}$ /cm^{3}mol^{-1}
0.1553	372.46	30.04	0.972337	0.007742	50.20	0.16
0.1935	372.73	30.04	0.972149	0.009726	49.66	0.36
0.1935	372.75	30.05	0.972139	0.009709	49.75	0.35
0.2353	372.89	30.05	0.972044	0.011700	50.13	0.65
0.2353	372.97	30.04	0.971982	0.011819	49.59	0.65
0.3146	373.33	30.04	0.971740	0.015699	49.72	0.28
0.3146	373.35	30.06	0.971734	0.015613	50.01	0.28
0.3529	373.37	30.04	0.971712	0.017610	49.64	0.33
0.3529	373.27	30.05	0.971781	0.017497	49.98	0.33
0.3996	373.30	30.05	0.971763	0.020103	49.08	0.64
0.3996	373.33	30.05	0.971739	0.019854	49.74	0.64

Table 6.3 The density of pure water, concentration dependence of relative densities and apparent molar volumes of aqueous solutions of perchloric acid at temperature T = 398.15 K and pressures p = (10, 20 and 30) MPa as well as the uncertainty in each apparent molar volume ($\delta V_{\phi,2}$).

Concentration /mol kg^{-1}	T /K	p /MPa	ρ^o /g cm^{-3}	ρ-ρ^o /g cm^{-3}	$V_{\phi\ exp}$ /cm^3 mol^{-1}	$\delta V_{\phi,2}$ /cm^{3}mol^{-1}
0.0392	398.47	10.01	0.943695	0.001940	50.70	4.65
0.0392	398.95	10.01	0.943311	0.002103	46.03	4.65
0.0778	398.76	10.01	0.943460	0.004016	48.30	2.04
0.1170	399.08	10.01	0.943199	0.005746	51.01	0.83
0.1580	399.27	10.01	0.943049	0.007910	49.81	2.36
0.2341	399.32	10.02	0.943007	0.011327	51.51	0.84
0.2740	399.35	10.01	0.942983	0.013212	51.58	0.04
0.2740	399.35	10.01	0.942982	0.013201	51.62	0.04
0.3159	399.29	10.01	0.943026	0.015421	50.81	0.53
0.3159	399.34	10.01	0.942994	0.015275	51.33	0.53
0.3547	399.30	10.01	0.943025	0.017177	51.13	0.32
0.3547	399.26	10.01	0.943051	0.017152	51.21	0.32
0.3996	399.24	10.01	0.943071	0.019474	50.68	0.64
0.3996	399.13	10.00	0.943156	0.019239	51.34	0.64
0.2755	398.50	20.06	0.948785	0.001707	51.82	1.51
0.3138	398.63	20.07	0.948748	0.001556	52.40	0.28
0.3138	398.66	20.08	0.948712	0.003329	52.68	0.28
0.3534	398.72	20.07	0.948709	0.003130	51.74	0.44
0.3534	398.73	20.07	0.948632	0.005566	51.29	0.44
0.3996	398.70	20.07	0.948519	0.005295	51.73	5.80
0.0414	396.86	30.07	0.948478	0.007193	46.63	4.39
0.0414	397.02	30.08	0.948535	0.009198	51.04	4.39
0.0824	397.45	30.08	0.948541	0.008921	50.00	2.23
0.0824	397.53	30.09	0.948621	0.011097	47.75	2.23
0.1229	397.52	30.08	0.948592	0.010983	46.92	3.51
0.1229	397.47	30.08	0.948565	0.013227	50.47	3.51
0.1638	397.47	30.08	0.948466	0.014872	50.19	4.08
0.1993	397.43	30.08	0.948442	0.014795	50.23	14.92
0.2409	397.74	30.14	0.948390	0.016931	50.34	1.07
0.2409	397.78	30.13	0.948385	0.017076	49.72	1.08
0.2815	397.83	30.16	0.948408	0.019101	50.94	1.51
0.3604	397.96	30.08	0.948424	0.016934	50.25	0.38
0.3604	397.88	30.08	0.954557	0.002209	50.65	0.38
0.4030	397.68	30.07	0.954438	0.002043	49.98	0.50
0.4030	397.56	30.07	0.954103	0.004130	50.50	0.50

Table 6.4 The density of pure water, concentration dependence of relative densities and apparent molar volumes of aqueous solutions of perchloric acid at temperature T = 423.15 K and pressures p = (10 and 20) MPa as well as the uncertainty in each apparent molar volume ($\delta V_{\phi,2}$).

Concentration /mol kg^{-1}	T /K	p /MPa	ρ^o /g cm^{-3}	ρ-ρ^o /g cm^{-3}	$V_{\phi\ exp}$ /cm^3 mol^{-1}	$\delta V_{\phi,2}$ /cm^{3}mol^{-1}
0.0397	421.25	10.01	0.924041	0.002424	49.28	12.07
0.0997	421.51	10.01	0.924097	0.002012	49.53	8.16
0.1164	421.54	10.01	0.923859	0.005013	49.64	1.68
0.1164	421.64	10.01	0.923835	0.005841	47.97	1.68
0.1546	421.76	10.01	0.923743	0.006006	47.10	0.50
0.1546	421.65	10.02	0.923634	0.008077	47.07	0.50
0.1959	421.35	10.01	0.923736	0.008081	49.65	0.76
0.1959	421.34	10.01	0.924003	0.009793	49.04	0.76
0.2343	421.15	10.01	0.924014	0.009894	49.24	0.73
0.2343	421.10	10.02	0.924190	0.011776	49.49	0.73
0.2750	421.20	10.02	0.924234	0.011726	49.55	2.09
0.3166	421.09	10.02	0.924146	0.013717	48.49	2.16
0.3996	421.38	10.01	0.924247	0.016055	49.25	1.55
0.1183	421.27	20.01	0.923980	0.019927	51.41	3.73
0.1589	421.08	20.00	0.929393	0.005760	47.97	3.97
0.1960	421.19	20.00	0.929560	0.008195	50.35	0.62
0.1960	421.26	20.01	0.929457	0.009684	49.79	0.63
0.2371	421.67	20.00	0.929405	0.009780	47.57	2.40
0.2753	421.89	20.01	0.929039	0.012265	48.64	4.08
0.3106	421.50	20.01	0.928846	0.013960	46.27	2.14
0.3996	421.34	20.01	0.929187	0.016370	45.23	0.39
0.3996	421.26	20.01	0.929333	0.021338	45.64	0.39

Table 6.5 The density of pure water, concentration dependence of relative densities and apparent molar volumes of aqueous solutions of $Yb(ClO_4)_3$ at T = 348.15 K and p = (10, 20 and 30) MPa as well as the uncertainty in each apparent molar volume ($\delta V_{\phi 2}$).

m_2 /mol kg^{-1}	m_3 /mol kg^{-1}	T /K	p /MPa	ρ^o /g cm^{-3}	ρ-ρ^o /g cm^{-3}	$V_{\phi\ exp}$ /cm^3 mol^{-1}	$V_{\phi 2}$ /cm^{3}mol^{-1}	$\delta V_{\phi 2}$ /cm^{3}mol^{-1}
0.0231	0.000343	347.90	10.04	0.979361	0.008402	101.15	101.93	1.15
0.0548	0.000815	347.77	10.04	0.979438	0.019845	101.85	102.63	0.84
0.0548	0.000815	347.73	10.03	0.979460	0.019891	101.00	101.78	0.84
0.0849	0.001262	347.70	10.04	0.979461	0.030533	103.06	103.87	0.87
0.0849	0.001262	347.69	10.04	0.979485	0.030603	102.25	103.04	0.87
0.1192	0.001772	347.92	10.04	0.979350	0.042684	103.47	104.28	0.06
0.1192	0.001772	348.03	10.04	0.979285	0.042680	103.48	104.29	0.06
0.1499	0.002228	348.08	10.03	0.979252	0.053433	103.98	104.80	0.49
0.1499	0.002228	348.10	10.04	0.979246	0.053486	103.63	104.44	0.50
0.1890	0.002809	348.11	10.05	0.979244	0.067194	103.37	104.18	0.48
0.1890	0.002809	348.06	10.03	0.979265	0.067147	103.62	104.43	0.48
0.2163	0.003215	348.11	10.05	0.979242	0.076481	104.41	105.24	0.15
0.2163	0.003215	348.13	10.04	0.979223	0.076518	104.24	105.06	0.15
0.2531	0.003761	348.06	10.05	0.979270	0.089092	104.57	105.39	0.60
0.2531	0.003761	348.03	10.04	0.979288	0.088992	104.96	105.79	0.60
0.0242	0.000360	347.53	20.04	0.983864	0.008809	102.48	103.28	4.32
0.0486	0.000723	347.54	20.04	0.983858	0.017641	102.39	103.19	0.21
0.0486	0.000723	347.54	20.04	0.983859	0.017646	102.30	103.09	0.21
0.0751	0.001116	347.65	20.04	0.983797	0.027091	103.47	104.29	0.43
0.0751	0.001116	347.61	20.05	0.983822	0.027058	103.91	104.73	0.43
0.1046	0.001554	347.54	20.06	0.983869	0.037588	103.73	104.54	0.23
0.1046	0.001554	347.48	20.05	0.983902	0.037568	103.93	104.74	0.23
0.1382	0.002053	347.57	20.05	0.983846	0.049514	103.57	104.39	0.23
0.1382	0.002053	347.60	20.05	0.983830	0.049509	103.60	104.42	0.23
0.1776	0.002639	347.50	20.06	0.983896	0.063176	104.70	105.53	0.41
0.1776	0.002639	347.46	20.06	0.983914	0.063220	104.46	105.29	0.41
0.2227	0.003309	347.61	20.06	0.983831	0.078781	105.02	105.86	0.09
0.2227	0.003309	347.76	20.04	0.983732	0.078795	104.94	105.77	0.09
0.2531	0.003761	347.65	20.04	0.983796	0.089348	104.68	105.51	0.12
0.2531	0.003761	347.56	20.04	0.983849	0.089340	104.72	105.55	0.12
0.0242	0.000360	346.80	30.03	0.988467	0.008821	103.21	104.03	0.78
0.0242	0.000360	346.77	30.01	0.988476	0.008838	102.50	103.31	0.78
0.0486	0.000723	346.71	30.02	0.988512	0.017682	102.77	103.58	0.48
0.0486	0.000723	346.73	30.03	0.988507	0.017690	102.62	103.43	0.48
0.0751	0.001116	346.71	30.02	0.988514	0.027178	103.55	104.36	0.26
0.0751	0.001116	346.67	30.01	0.988535	0.027175	103.59	104.41	0.26
0.1046	0.001554	346.80	30.02	0.988465	0.037626	104.54	105.37	1.06
0.1046	0.001554	347.15	30.01	0.988257	0.037716	103.64	104.46	1.06
0.1382	0.002053	347.27	30.02	0.988192	0.049587	104.15	104.97	0.58
0.1382	0.002053	347.43	30.01	0.988097	0.049669	103.54	104.36	0.58

Table 6.5 Continued.

m_2 /mol kg^{-1}	m_3 /mol kg^{-1}	T /K	p /MPa	ρ^o /g cm^{-3}	ρ-ρ^o /g cm^{-3}	$V_{\phi,exp}$ /cm^3 mol^{-1}	$V_{\phi,2}$ /cm^{3}mol^{-1}	$\delta V_{\phi,2}$ /cm^{3}mol^{-1}
0.1776	0.002639	347.73	30.02	0.987929	0.063365	104.65	105.48	0.49
0.1776	0.002639	347.83	30.02	0.987870	0.063460	104.12	104.94	0.49
0.2227	0.003309	347.40	30.01	0.988117	0.079040	104.93	105.76	0.33
0.2227	0.003309	347.34	30.01	0.988150	0.079018	105.03	105.87	0.32
0.2531	0.003761	347.12	30.03	0.988283	0.089529	105.05	105.89	0.47
0.2531	0.003761	347.05	30.02	0.988319	0.089637	104.66	105.49	0.47

Table 6.6 The density of pure water, concentration dependence of relative densities and apparent molar volumes of aqueous solutions of $Yb(ClO_4)_3$ at $T = 373.15$ K and $p =$ (10, 20 and 30) MPa as well as the uncertainty in each apparent molar volume ($\delta V_{\phi 2}$).

m_2 /mol kg^{-1}	m_3 /mol kg^{-1}	T /K	p /MPa	ρ^o /g cm^{-3}	ρ-ρ^o /g cm^{-3}	$V_{\phi\ exp}$ /cm^3 mol^{-1}	$V_{\phi 2}$ /cm^{3}mol^{-1}	$\delta V_{\phi 2}$ /cm^{3}mol^{-1}
0.0225	0.000334	372.44	10.05	0.963476	0.008021	104.33	105.14	0.42
0.0225	0.000334	372.35	10.05	0.963539	0.008028	104.02	104.83	0.42
0.0536	0.000797	372.61	10.06	0.963362	0.019073	103.91	104.70	2.90
0.0813	0.001208	372.33	10.05	0.963552	0.028835	103.97	104.76	0.87
0.0813	0.001208	372.32	10.05	0.963565	0.028765	104.86	105.66	0.87
0.1121	0.001666	372.53	10.06	0.963415	0.039706	103.31	104.07	0.92
0.1121	0.001666	372.55	10.06	0.963400	0.039603	104.25	105.03	0.92
0.1416	0.002105	372.65	10.05	0.963325	0.049810	104.86	105.64	0.23
0.1416	0.002105	372.78	10.16	0.963289	0.049842	104.62	105.40	0.23
0.1793	0.002665	372.92	10.06	0.963141	0.062821	104.76	105.53	0.61
0.1793	0.002665	372.92	10.05	0.963135	0.062812	104.80	105.58	0.61
0.2064	0.003068	372.67	10.06	0.963321	0.072015	105.38	106.15	1.03
0.2064	0.003068	372.61	10.05	0.963358	0.071880	106.05	106.83	1.03
0.2531	0.003761	372.57	10.06	0.963384	0.087948	105.11	105.86	0.30
0.2531	0.003761	372.44	10.06	0.963481	0.087999	104.93	105.69	0.30
0.0225	0.000334	372.95	20.06	0.967621	0.008077	102.88	103.67	3.31
0.0536	0.000797	372.88	20.06	0.967674	0.019218	102.30	103.06	2.45
0.0536	0.000797	372.78	20.06	0.967743	0.019095	104.68	105.48	2.45
0.0813	0.001208	372.58	20.07	0.967884	0.028789	105.73	106.53	3.36
0.0813	0.001208	372.50	20.06	0.967939	0.029051	102.43	103.18	3.36
0.1121	0.001666	372.35	20.06	0.968038	0.039875	103.00	103.75	1.17
0.1121	0.001666	372.33	20.05	0.968052	0.039760	104.05	104.82	1.17
0.1416	0.002105	372.41	20.05	0.967998	0.050125	103.83	104.58	0.44
0.1416	0.002105	372.47	20.06	0.967956	0.050129	103.79	104.54	0.44
0.1793	0.002665	372.72	20.04	0.967772	0.062933	105.32	106.09	1.02
0.1793	0.002665	372.71	20.04	0.967781	0.063104	104.37	105.12	1.02
0.2064	0.003068	372.53	20.04	0.967908	0.072175	105.76	106.53	0.64
0.2064	0.003068	372.48	20.03	0.967934	0.072282	105.25	106.01	0.64
0.2531	0.003761	372.23	20.06	0.968118	0.088162	105.44	106.19	0.80
0.2531	0.003761	372.09	20.02	0.968204	0.088108	105.68	106.43	0.80
0.0231	0.000343	372.29	30.07	0.972459	0.008310	103.37	104.17	2.19
0.0231	0.000343	372.40	30.06	0.972383	0.008358	101.20	101.97	2.19
0.0548	0.000815	372.41	30.06	0.972373	0.019597	104.55	105.36	1.84
0.0548	0.000815	372.46	30.04	0.972334	0.019691	102.79	103.58	1.84
0.0849	0.001262	372.43	30.04	0.972352	0.030240	104.68	105.48	1.21
0.0849	0.001262	372.56	30.06	0.972274	0.030141	105.85	106.67	1.21
0.1192	0.001772	372.69	30.06	0.972188	0.042289	104.94	105.73	0.73
0.1192	0.001772	372.74	30.07	0.972159	0.042373	104.21	105.00	0.73
0.1499	0.002228	372.72	30.07	0.972166	0.052861	105.98	106.79	1.03
0.1499	0.002228	372.77	30.07	0.972133	0.053013	104.95	105.74	1.03

Table 6.6 Continued.

m_2 /mol kg^{-1}	m_3 /mol kg^{-1}	T /K	p /MPa	ρ^o /g cm^{-3}	ρ-ρ^o /g cm^{-3}	$V_{\phi,exp}$ /cm^3 mol^{-1}	$V_{\phi,2}$ /cm^{3}mol^{-1}	$\delta V_{\phi,2}$ /cm^{3}mol^{-1}
0.1890	0.002809	373.06	30.08	0.971938	0.066379	105.80	106.60	0.85
0.1890	0.002809	373.09	30.09	0.971921	0.066535	104.98	105.76	0.85
0.2163	0.003215	373.08	30.09	0.971932	0.075857	105.44	106.23	0.19
0.2163	0.003215	373.04	30.09	0.971954	0.075815	105.64	106.43	0.19
0.2531	0.003761	373.02	30.09	0.971972	0.088330	105.74	106.51	0.22
0.2531	0.003761	372.94	30.09	0.972024	0.088298	105.87	106.65	0.22

Table 6.7 The density of pure water, concentration dependence of relative densities and apparent molar volumes of aqueous solutions of $Yb(ClO_4)_3$ at $T = 398.15$ K and $p =$ (10, 20 and 30) MPa as well as the uncertainty in each apparent molar volume ($\delta V_{\phi,2}$).

m_2 /mol kg^{-1}	m_3 /mol kg^{-1}	T /K	p /MPa	ρ^o /g cm^{-3}	ρ-ρ^o /g cm^{-3}	$V_{\phi\ exp}$ /cm^3 mol^{-1}	$V_{\phi,2}$ /cm^{3}mol^{-1}	$\delta V_{\phi,2}$ /cm^{3}mol^{-1}
0.0300	0.000446	398.38	10.03	0.943785	0.010675	99.25	99.98	3.62
0.0300	0.000446	398.50	10.03	0.943682	0.010773	95.60	96.28	3.62
0.0489	0.000726	398.66	10.12	0.943597	0.017408	97.77	98.47	3.50
0.0489	0.000726	398.75	10.03	0.943478	0.017250	101.26	102.01	3.50
0.0733	0.001090	398.92	10.03	0.943345	0.025868	100.51	101.24	1.73
0.0733	0.001090	398.98	10.04	0.943303	0.025987	98.74	99.45	1.73
0.0960	0.001426	398.91	10.04	0.943353	0.033804	100.35	101.07	1.21
0.0960	0.001426	398.87	10.03	0.943380	0.033912	99.15	99.85	1.21
0.1210	0.001799	398.92	10.03	0.943346	0.042442	101.13	101.86	0.78
0.1210	0.001799	398.99	10.03	0.943290	0.042530	100.33	101.05	0.78
0.1443	0.002144	399.03	10.02	0.943251	0.050609	100.15	100.86	0.16
0.1443	0.002144	399.03	10.11	0.943295	0.050587	100.33	101.04	0.16
0.1697	0.002522	399.07	10.04	0.943221	0.059225	101.16	101.87	2.16
0.1697	0.002522	399.09	10.03	0.943201	0.059593	98.85	99.54	2.16
0.1919	0.002852	399.08	10.04	0.943212	0.066412	103.35	104.10	2.52
0.1919	0.002852	398.97	10.04	0.943304	0.066888	100.76	101.47	2.52
0.2215	0.003292	398.82	10.03	0.943424	0.076775	101.83	102.55	0.94
0.2215	0.003292	398.74	10.02	0.943487	0.076970	100.93	101.63	0.94
0.2531	0.003761	398.47	10.02	0.943703	0.087762	100.69	101.38	0.53
0.2531	0.003761	398.30	10.02	0.943846	0.087826	100.46	101.15	0.53
0.0245	0.000364	397.89	20.06	0.949045	0.008754	98.69	99.42	8.11
0.0453	0.000673	398.03	20.05	0.948932	0.016150	99.17	99.90	1.39
0.0453	0.000673	398.06	20.06	0.948913	0.016206	97.81	98.52	1.39
0.0708	0.001052	398.17	20.07	0.948832	0.025138	99.60	100.33	1.73
0.0708	0.001052	398.23	20.07	0.948782	0.025025	101.29	102.04	1.73
0.0951	0.001414	398.42	20.07	0.948629	0.033640	100.46	101.20	0.35
0.0951	0.001414	398.44	20.05	0.948606	0.033654	100.29	101.02	0.35
0.1201	0.001785	398.34	20.06	0.948690	0.042259	101.47	102.21	0.60
0.1201	0.001785	398.44	20.06	0.948607	0.042328	100.83	101.57	0.60
0.1473	0.002190	398.54	20.05	0.948523	0.051535	102.59	103.35	0.89
0.1473	0.002190	398.63	20.05	0.948453	0.051661	101.67	102.41	0.89
0.1685	0.002504	398.71	20.05	0.948390	0.058892	102.08	102.83	0.14
0.1685	0.002504	398.70	20.04	0.948395	0.058871	102.21	102.96	0.14
0.1984	0.002949	398.69	20.04	0.948405	0.068962	103.08	103.84	0.77
0.1984	0.002949	398.66	20.03	0.948420	0.069121	102.25	103.00	0.77
0.2220	0.003299	398.57	20.05	0.948501	0.077038	102.80	103.56	0.18
0.2220	0.003299	398.56	20.06	0.948517	0.077011	102.94	103.69	0.18
0.2531	0.003761	398.66	20.06	0.948437	0.087631	102.50	103.25	0.35
0.2531	0.003761	398.65	20.04	0.948430	0.087685	102.28	103.02	0.35
0.0464	0.000690	398.31	30.04	0.953564	0.008188	94.23	100.02	6.21
0.0750	0.001115	398.56	30.05	0.953222	0.026830	98.24	98.95	7.80

Table 6.7 Continued

m_2 /mol kg^{-1}	m_3 /mol kg^{-1}	T /K	p /MPa	ρ^o /g cm^{-3}	ρ-ρ^o /g cm^{-3}	$V_{\phi,exp}$ /cm^3 mol^{-1}	$V_{\phi,2}$ /cm^{3}mol^{-1}	$\delta V_{\phi,2}$ /cm^{3}mol^{-1}
0.0939	0.001395	398.64	30.05	0.953164	0.033244	101.27	102.03	2.90
0.0939	0.001395	398.63	30.04	0.953170	0.033509	98.30	99.01	2.90
0.1193	0.001773	398.58	30.05	0.953213	0.042143	101.30	102.05	11.97
0.1428	0.002123	398.56	30.05	0.953226	0.050544	99.76	100.49	2.27
0.1428	0.002123	398.55	30.05	0.953229	0.050218	102.15	102.92	2.27
0.1717	0.002552	398.57	30.06	0.953220	0.060252	101.81	102.57	4.83
0.2001	0.002974	398.62	30.05	0.953175	0.069731	103.40	104.18	1.58
0.2001	0.002974	398.62	30.04	0.953175	0.069996	102.03	102.80	1.58
0.2224	0.003306	398.59	30.06	0.953206	0.077402	103.06	103.84	1.01
0.2224	0.003306	398.59	30.05	0.953205	0.077639	101.97	102.73	1.01
0.2531	0.003761	398.58	30.05	0.953209	0.087761	103.24	104.02	0.40
0.2531	0.003761	398.55	30.06	0.953239	0.087653	103.68	104.47	0.40

Table 6.8 The density of pure water, concentration dependence of relative densities and apparent molar volumes of aqueous solutions of $Yb(ClO_4)_3$ at $T = 423.15$ K and $p =$ (10, 20 and 30) MPa as well as the uncertainty in each apparent molar volume ($\delta V_{\phi,2}$).

m_2 /mol kg^{-1}	m_3 /mol kg^{-1}	T /K	p /MPa	ρ^o /g cm^{-3}	ρ-ρ^o /g cm^{-3}	$V_{\phi,exp}$ /cm^3 mol^{-1}	$V_{\phi,2}$ /cm^{3}mol^{-1}	$\delta V_{\phi,2}$ /cm^{3}mol^{-1}
0.0235	0.000349	421.83	10.05	0.923590	0.008367	92.01	92.64	0.82
0.0235	0.000349	421.94	10.18	0.923476	0.008351	92.76	93.40	0.82
0.0474	0.000705	421.79	10.05	0.923625	0.016716	95.56	96.25	1.92
0.0474	0.000705	421.76	10.05	0.923657	0.016796	93.64	94.30	1.92
0.0710	0.001055	421.66	10.05	0.923744	0.024998	95.09	95.23	1.74
0.0710	0.001055	421.56	10.05	0.923840	0.025104	93.44	94.11	1.74
0.0936	0.001391	421.23	10.05	0.924132	0.032838	95.99	96.70	0.76
0.0936	0.001391	421.20	10.06	0.924161	0.032772	96.78	97.51	0.76
0.1193	0.001773	421.55	10.05	0.923845	0.041800	95.52	96.24	0.33
0.1193	0.001773	421.52	10.05	0.923869	0.041818	95.36	96.08	0.33
0.1452	0.002158	421.68	10.05	0.923729	0.050677	96.11	96.85	0.28
0.1452	0.002158	421.60	10.05	0.923800	0.050664	96.23	96.97	0.28
0.1726	0.002565	421.57	10.04	0.923822	0.059930	97.18	97.95	2.25
0.2008	0.002984	421.59	10.05	0.923809	0.069486	97.53	98.32	0.19
0.2008	0.002984	421.57	10.05	0.923824	0.069453	97.71	98.51	0.19
0.2248	0.003342	421.38	10.05	0.924000	0.077640	97.56	98.37	0.17
0.2248	0.003342	420.65	10.05	0.924661	0.077601	97.95	98.75	0.17
0.2531	0.003761	420.88	10.05	0.924446	0.086868	98.96	99.79	0.46
0.2531	0.003761	420.97	10.05	0.924366	0.086988	98.42	99.25	0.46
0.0253	0.000376	421.48	20.00	0.929200	0.009069	91.88	92.52	4.35
0.0253	0.000376	421.47	20.01	0.929221	0.008972	96.23	96.93	4.36
0.0490	0.000728	421.28	20.00	0.929384	0.017281	97.27	98.00	2.23
0.0490	0.000728	421.32	20.01	0.929351	0.017379	95.01	95.71	2.23
0.0718	0.001067	421.34	20.02	0.929342	0.025409	95.14	95.85	2.62
0.0718	0.001067	420.74	20.02	0.929866	0.025237	97.98	98.73	2.62
0.0959	0.001425	421.49	20.01	0.929195	0.033781	95.92	96.66	0.94
0.0959	0.001425	421.45	20.01	0.929232	0.033722	96.61	97.37	0.94
0.1198	0.001781	421.06	20.02	0.929588	0.041878	98.27	99.06	0.73
0.1198	0.001781	421.08	20.00	0.929557	0.041936	97.72	98.50	0.73
0.1432	0.002128	421.15	20.01	0.929500	0.050105	96.96	97.75	0.18
0.1432	0.002128	421.04	20.03	0.929605	0.050126	96.83	97.62	0.18
0.1702	0.002530	420.92	20.03	0.929718	0.059313	97.71	98.52	1.48
0.1702	0.002530	420.90	20.01	0.929726	0.059072	99.25	100.09	1.48
0.1994	0.002964	420.93	20.01	0.929693	0.069213	98.22	99.07	1.59
0.1994	0.002964	420.83	20.00	0.929777	0.068934	99.76	100.62	1.59
0.2260	0.003359	420.89	20.01	0.929734	0.078056	99.20	100.08	0.57
0.2260	0.003359	420.92	20.00	0.929697	0.078136	98.81	99.68	0.57
0.2531	0.003761	420.68	20.00	0.929915	0.087113	99.51	100.41	0.27
0.2531	0.003761	420.72	20.01	0.929878	0.087062	99.71	100.62	0.27
0.0437	0.000650	421.63	30.02	0.934218	0.015570	95.02	95.74	0.70
0.0437	0.000650	421.59	30.02	0.934250	0.015545	95.67	96.40	0.70

Table 6.8 Continued

m_2 /mol kg^{-1}	m_3 /mol kg^{-1}	T /K	p /MPa	ρ^o /g cm^{-3}	$\rho-\rho^o$ /g cm^{-3}	$V_{\phi,exp}$ /cm^3 mol^{-1}	$V_{\phi,2}$ /cm^{3}mol^{-1}	$\delta V_{\phi,2}$ /cm^{3}mol^{-1}
0.0700	0.001040	421.45	30.03	0.934383	0.024752	96.90	97.66	-0.64
0.0700	0.001040	421.33	30.02	0.934480	0.024711	97.58	98.35	-0.64
0.0946	0.001407	421.19	30.02	0.934595	0.033397	97.00	97.78	-0.38
0.0946	0.001407	421.17	30.02	0.934614	0.033381	97.19	97.97	-0.38
0.1215	0.001805	420.90	30.02	0.934842	0.042586	98.68	99.51	-0.22
0.1215	0.001805	420.83	30.02	0.934904	0.042564	98.90	99.74	-0.22
0.1427	0.002121	420.74	30.03	0.934989	0.049963	98.40	99.24	-0.46
0.1427	0.002121	420.92	30.03	0.934833	0.049899	98.84	99.69	-0.46
0.1760	0.002616	421.27	30.03	0.934535	0.061252	99.39	100.29	-0.42
0.1760	0.002616	421.28	30.03	0.934523	0.061241	99.46	100.36	-0.42
0.1984	0.002949	421.12	30.03	0.934658	0.068733	100.45	101.39	-0.34
0.1984	0.002949	421.19	30.03	0.934602	0.068788	100.14	101.07	-0.34
0.2209	0.003283	421.26	30.04	0.934542	0.076388	100.25	101.21	-0.40
0.2209	0.003283	421.36	30.04	0.934462	0.076449	99.93	100.89	-0.40
0.2531	0.003761	421.22	30.04	0.934578	0.087319	99.98	100.96	-0.26
0.2531	0.003761	421.04	30.03	0.934733	0.087311	100.05	101.03	-0.26

$$V_\phi^o = v_1 + \beta_T p^o \left(v_2 + \left(\frac{v_3}{T_x} \right) + \frac{v_4 T}{T^o} \right), \tag{6.4}$$

where β_T is the isothermal compressibility of the solvent, p^o is equal to 1 MPa, T^o is equal to 1 K and T_x is equal to (T/T^o)-227.

The second virial coefficient B^V shown in equation 6.3 may also be expanded to give:

$$B^V = v_5 + v_6 \frac{T}{T^o} + v_7 \left(\frac{T}{T^o} \right)^2 + \frac{v_8}{T_x} + v_9 \left(\frac{T}{T^o} \right)^2 \frac{p}{p^o}, \tag{6.5}$$

where v_i (i = 1-9) are fitting parameters. Values of the fitting parameters were determined using regression analysis and are reported along with their standard errors in Table 6.9. Contributions from the third virial coefficient, C^V, were found to be statistically insignificant over the range of concentrations investigated in this study.

Figure 6.4 plots the difference between each observed data point and the corresponding value calculated by the model presented above. The random scatter of data points serves to illustrate that there is no dependence of the magnitude of the residuals on the molality of perchloric acid.

6.3.2 Modeling of ytterbium perchlorate volumetric data

Apparent molar volumes for the aqueous $Yb(ClO_4)_3$ solutions were calculated using Young's rule. Young's rule for apparent molar volumes is written in the form:

Table 6.9 Estimates of parameters to equations 6.4 and 6.5 which model the temperature and pressure dependences of $V_{\phi,2}$ values for aqueous solutions of perchloric acid.

Fitting Parameter	Value	Standard Error
ν_1 (/cm^3 mol^{-1})	44.05	3.20
ν_2 (/cm^3 mol^{-1})	25865.59	10439.21
ν_3 (/cm^3 mol^{-1})	-22.1×10^5	4.4×10^5
ν_4 (/cm^3 mol^{-1})	-109.51	43.53
10-6 ν_5 (/cm^3 J^{-1})	-0.0162	0.004895
10-6 ν_6 (/cm^3 J^{-1})	-3.7×10^6	0.71×10^6
10-6 ν_7 (/cm^3 J^{-1})	22.3×10^{-5}	5.5×10^{-5}
10-6 ν_8 (/cm^3 J^{-1})	2.81	0.66
10-6 ν_9 (/cm^3 J^{-1})	-5.00×10^{-8}	3.05×10^{-8}

$$V_{\phi,\exp} = V_{\phi,2}\left(\frac{m_2}{(m_2+m_3)}\right) + V_{\phi,3}\left(\frac{m_3}{(m_2+m_3)}\right) + \delta, \qquad (6.6)$$

where $V_{\phi,2}$, $V_{\phi,3}$, m_2, and m_3 are the apparent molar volumes and concentrations of ytterbium perchlorate and perchloric acid respectively. Apparent molar volumes of aqueous perchloric acid were calculated at each required concentration using equations 6.3-6.5. δ represents an excess mixing term that has been assumed to be equal to zero in any solution in which the concentration of one species is much greater than the concentration of the other.

In a similar manner to the modeling procedures presented in Chapters 4 and 5, Pitzer ion interaction theory was used as the basis for modeling the temperature, pressure and concentration dependence of the apparent molar volume of aqueous $Yb(ClO_4)_3$ solutions. The apparent molar volumes of $Yb(ClO_4)_3$ at p = 0.1 MPa and T = (288.15,

Figure 6.4 Plot of observed $V_{\phi,2}$ – calculated $V_{\phi,2}$ versus the square root of the perchloric acid molality.

The dashed lines represent 1.96 standard deviations from the mean residual of 0. (O) Hovey (1988), (X) This Chapter.

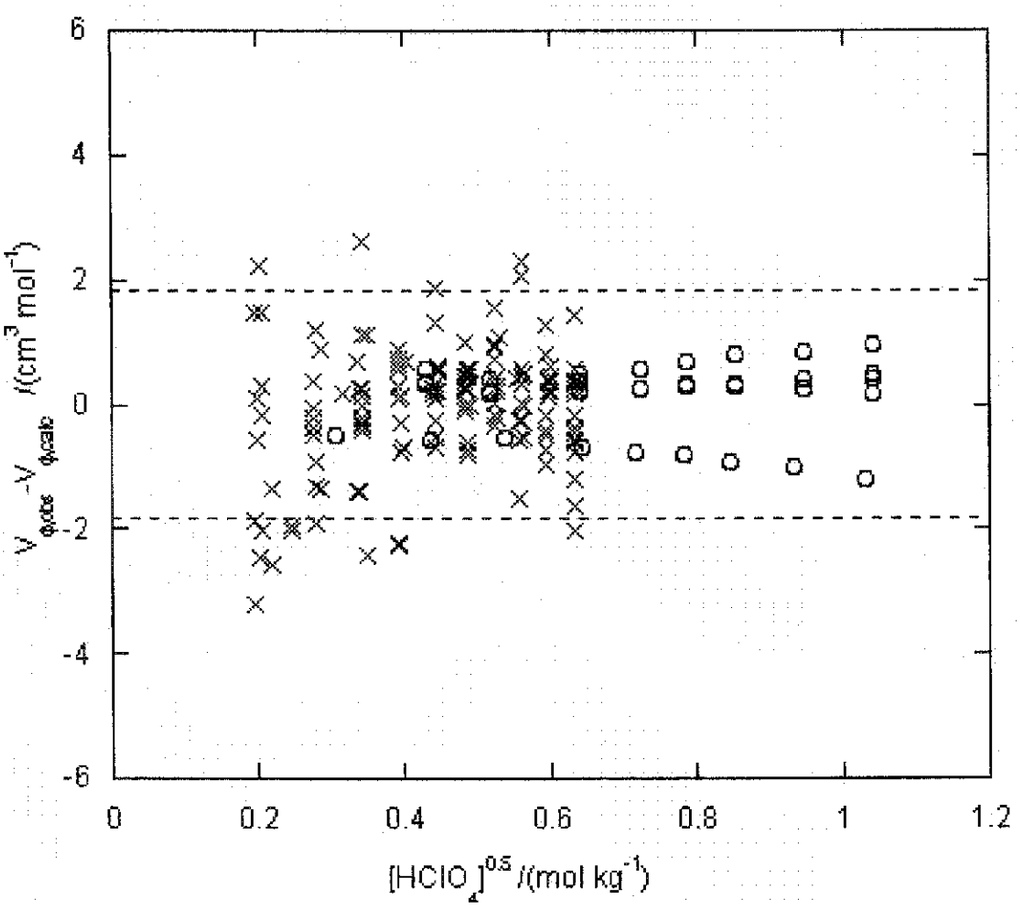

298.15, 313.15 and 328.15) K presented in Chapter 4 were appended to the data set presented in this chapter to increase the number of degrees of freedom within the modeling analysis.

The Pitzer equation used in Chapter 4, equation 4.6, and several variations thereof, were used to model the set of apparent molar volumes of aqueous solutions of

$Yb(ClO_4)_3$. The best form of Pitzer equation was selected by examination of the standard error of the predicted values and also by inspection of calculated residuals. The equation that was found to best model the apparent molar volumes of aqueous solutions of $Yb(ClO_4)_3$ takes the form:

$$V_{\phi,2} - \left(\frac{6A_V \ln\left(1 + b\sqrt{I}\right)}{b} \right) = V_\phi^\circ + 6m_2R(T - 355.5)\beta^0$$

$$+ 12m_2R(T - 355.5)f(I)\beta^1, \qquad (6.7)$$

where V_ϕ^o, β^0 and β^1 may be expanded to give:

$$V_\phi^o = \nu_1 + \frac{\nu_2}{p + \Psi} + \frac{\nu_3}{T - \Theta} - \omega Q, \qquad (6.8)$$

$$\beta^0 = \nu_4(p - 15.00)(T - 355.5) \qquad (6.9)$$

and;

$$\beta^1 = \frac{\nu_5}{(T - 355.5)} + \nu_6 + \nu_7(T - 355.5). \qquad (6.10)$$

In these equations, ω is the effective Born coefficient that is specific to $Yb(ClO_4)_3$ for which a value was calculated from the single ion compilation reported by Shock and Helgeson (1988). The terms Ψ and Θ are solvent dependent parameters equal to 260

MPa and 228 K respectively. The constants T = 355.50 K and p = 15.00 MPa were selected as the midpoints of our investigated temperature and pressure ranges. Values for the v_i (i = 1-7) fitting parameters were determined using regression analysis and are reported along with standard errors in table 6.10.

Figure 6.5 presents the difference between the observed apparent molar volumes of aqueous solutions of $Yb(ClO_4)_3$ and those predicted by equations 6.7-6.10 versus the square root of $Yb(ClO_4)_3$ molality. With few exceptions, all residuals have absolute magnitudes less than 2 cm^3mol^{-1}.

6.4 Comparison of infinite dilution values with HKF predictions

The HKF equations of state reported by Shock and Helgeson (1988) used available data to predict infinite dilution apparent molar properties over a wide range of temperatures and pressures. A comparison between the infinite dilution apparent molar volumes of aqueous perchloric acid predicted by the model presented here to the HKF equations of state reported by Shock and Helgeson can be seen in Figures 6.6-6.9. The infinite dilution apparent molar volumes produced by the model reported in this chapter and those reported by Shock and Helgeson agree within 1 cm^3mol^{-1}. This confirms the quality of the apparent molar volume fit presented here due to the quality of the data upon which Shock and Helgeson based their equations of state. Figures 6.10-6.13 compare the infinite dilution apparent molar volumes of ytterbium perchlorate produced by the model presented here to the values predicted by Shock and Helgeson's HKF equations of state. The discrepancy between the infinite dilution apparent molar volumes presented by

Table 6.10 Estimates of parameters to equations 6.9, 6.10 and 6.11 which model the temperature and pressure dependences of $V_{\phi,2}$ values for aqueous solutions $Yb(ClO_4)_3$.

Fitting Parameter	Value	Standard Error
ν_1 (/cm^3 mol^{-1})	140.74	2.53
ν_2 (/cm^3 mol^{-1} MPa)	-1121.05	715.62
ν_3 (/cm^3 mol^{-1} K)	-2279.87	70.04
10^3 ν_4 (/kg mol^{-1} MPa^{-2})	-2.31	0.10
ν_5 (/kg mol^{-1}KMPa^{-1})	-0.03423	0.002726
ν_6 (/kg mol^{-1} MPa^{-1})	-0.00029	0.00003
10^4 ν_7 (/kg mol^{-1} K^{-1} MPa^{-1})	6.11×10^{-7}	4.98×10^{-7}

Figure 6.5 Plot of observed $V_{\phi,2}$ – calculated $V_{\phi,2}$ versus the square root of the $Yb(ClO_4)_3$ molality.

The dashed lines represent 1.96 standard deviations from the mean residual of 0. (O) Chapter 4 Data, (X) This Chapter

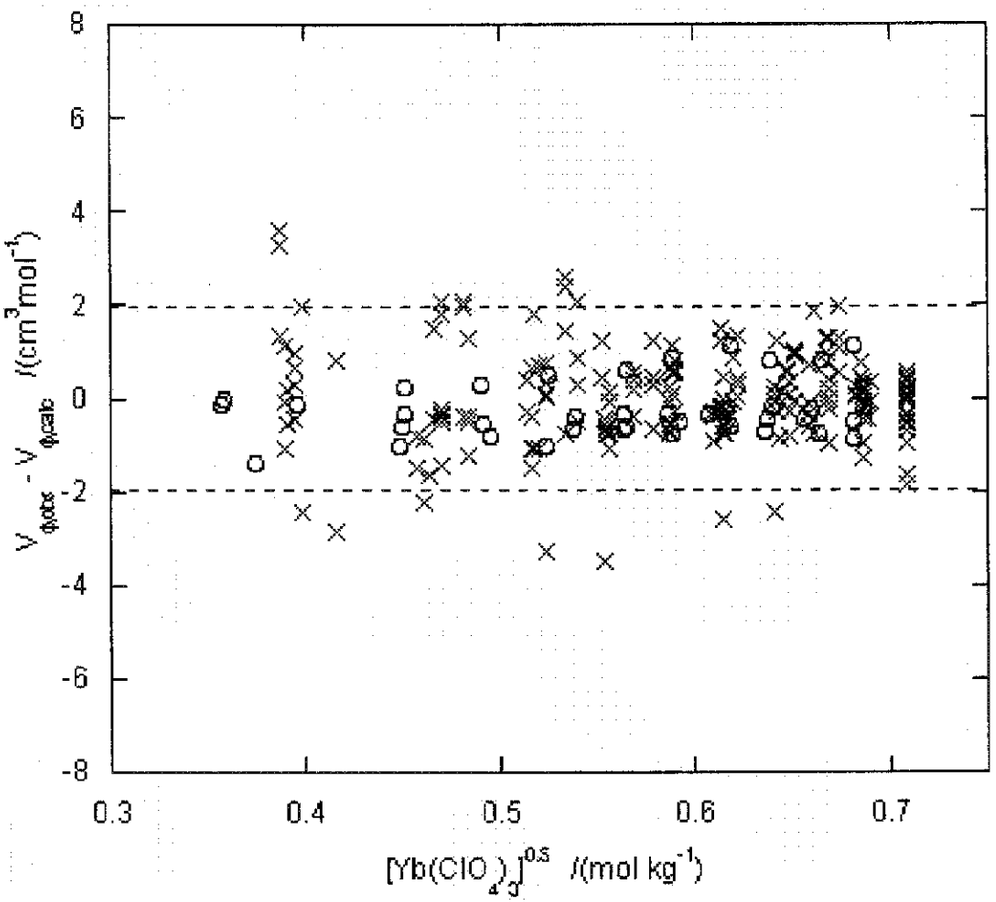

Figure 6.6 Temperature dependence of apparent molar volume at infinite dilution of aqueous perchloric acid at pressure p = 0.1 MPa.

Shock and Helgeson (- - - - - -), values reported in this chapter (_____).

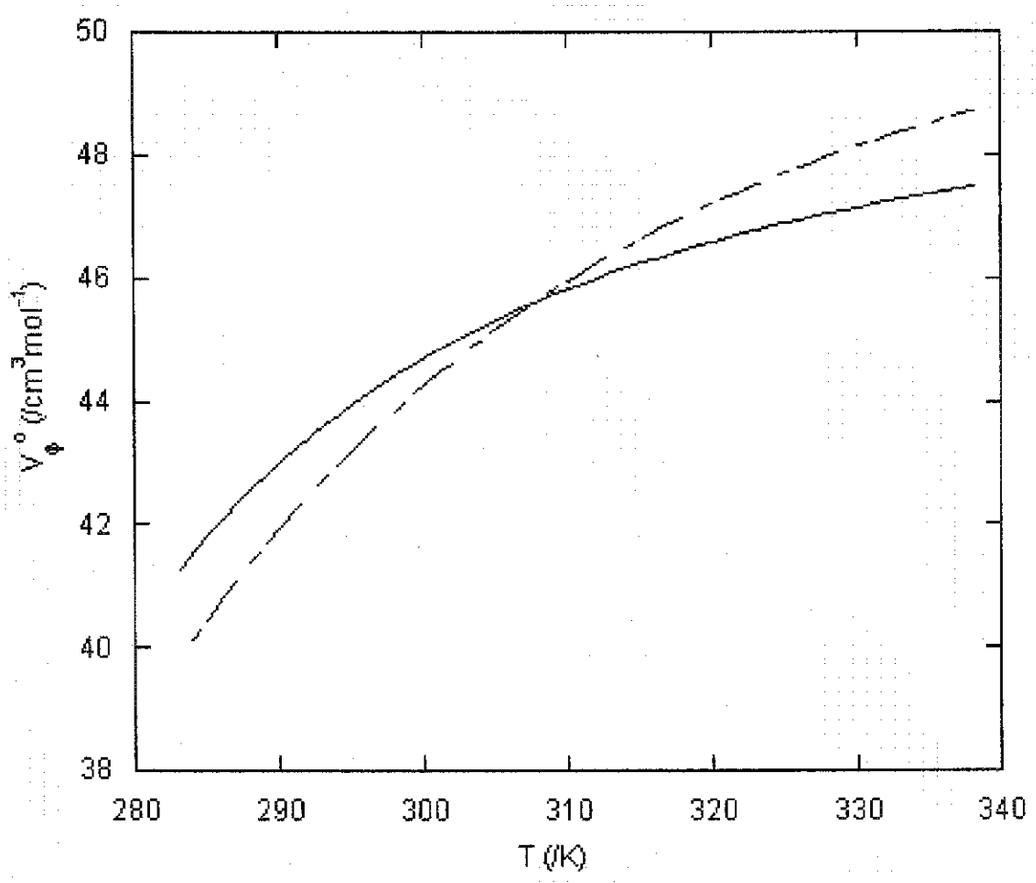

Figure 6.7 Temperature dependence of apparent molar volume at infinite dilution of aqueous perchloric acid at pressure p = 10 MPa.

Shock and Helgeson (- - - - - - - -), values reported in this chapter (_____).

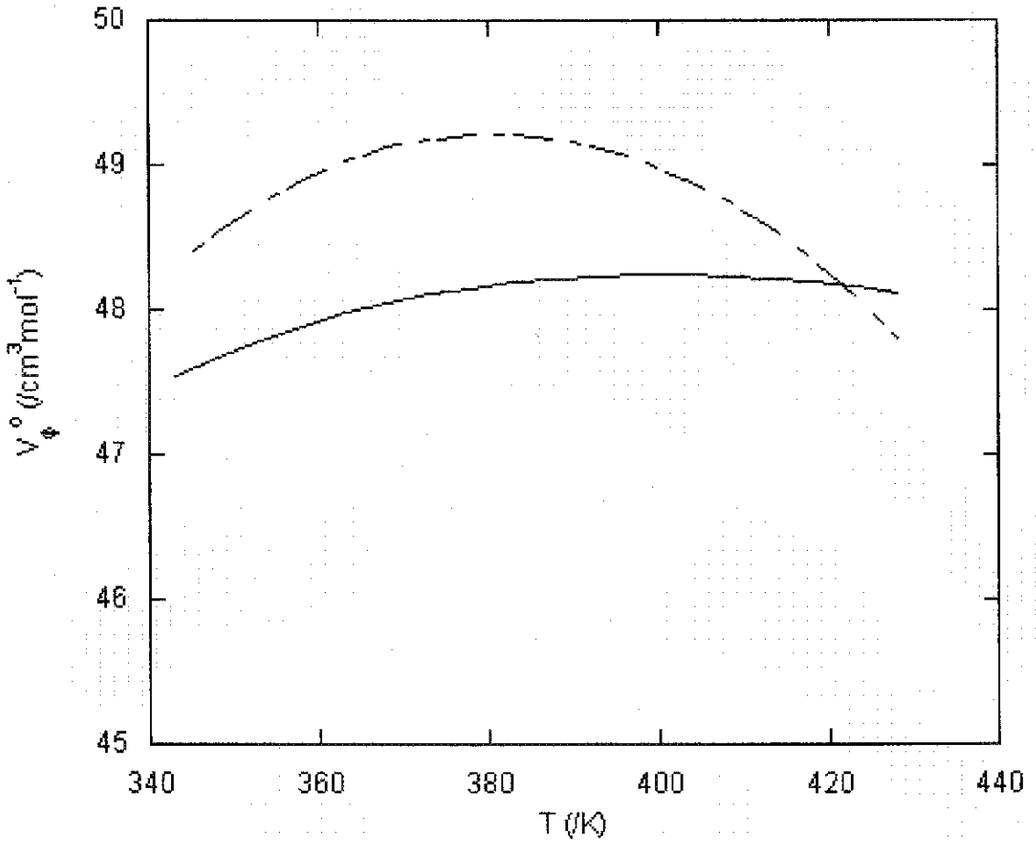

Figure 6.8 Temperature dependence of apparent molar volume at infinite dilution of aqueous perchloric acid at pressure p = 20 MPa.

Shock and Helgeson (- - - - - - -), values reported in this chapter (_____).

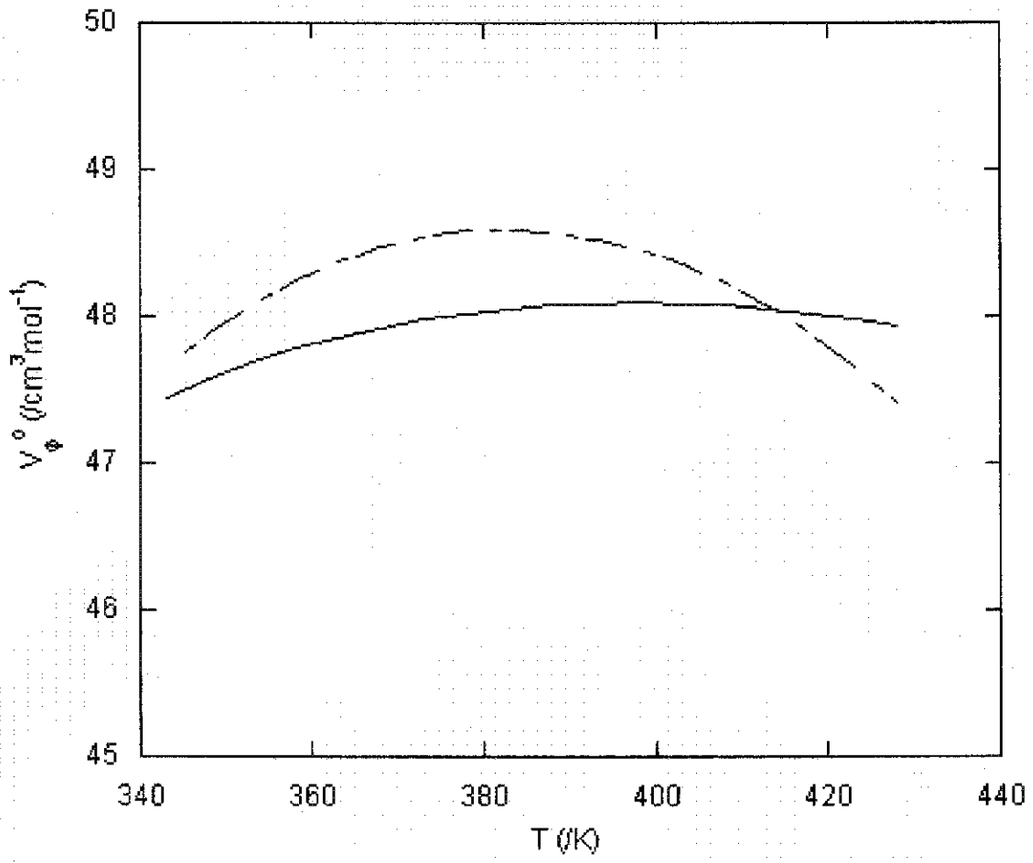

Figure 6.9 Temperature dependence of apparent molar volume at infinite dilution of aqueous perchloric acid at pressure p = 30 MPa.

Shock and Helgeson (- - - - - - -), values reported in this chapter (_____).

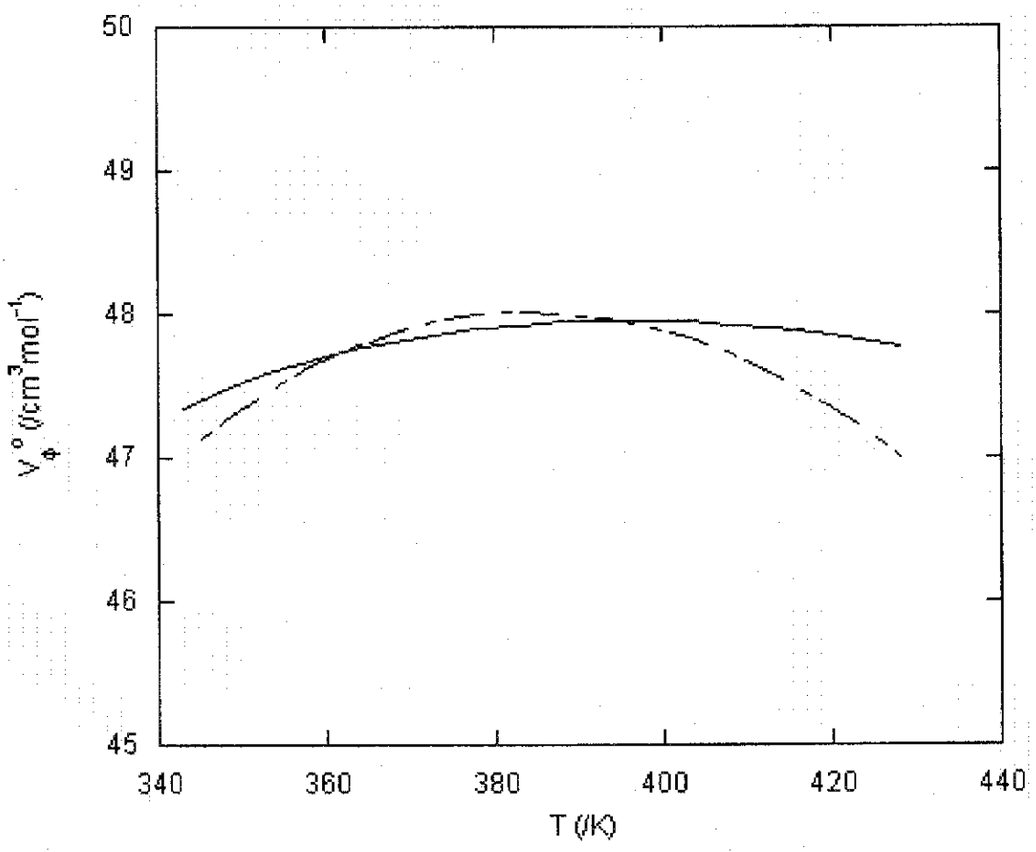

Figure 6.10 Temperature dependence of apparent molar volume at infinite dilution of $Yb(ClO_4)_3$ at pressure p = 0.1 MPa.

Shock and Helgeson (- - - - - - -), values reported in this chapter (_____).

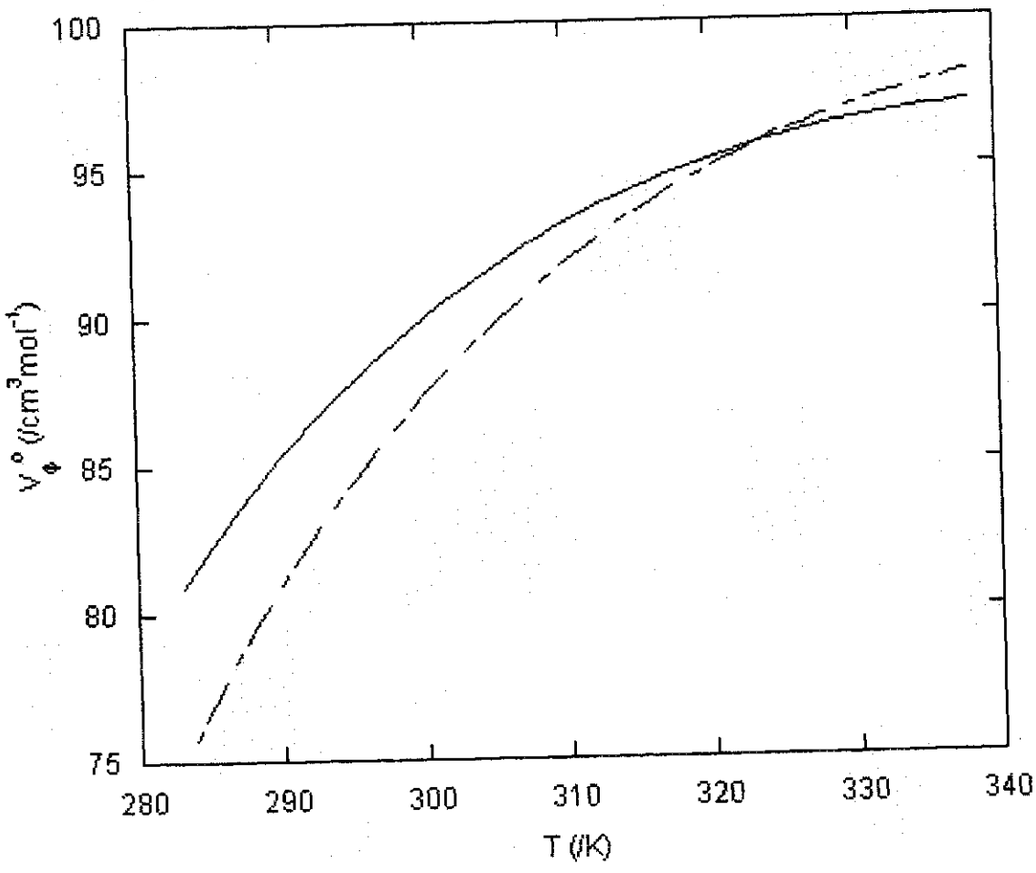

Figure 6.11 Temperature dependence of apparent molar volume at infinite dilution of $Yb(ClO_4)_3$ at pressure p = 10 MPa.

Shock and Helgeson (- - - - - - - -), values reported in this chapter (_____).

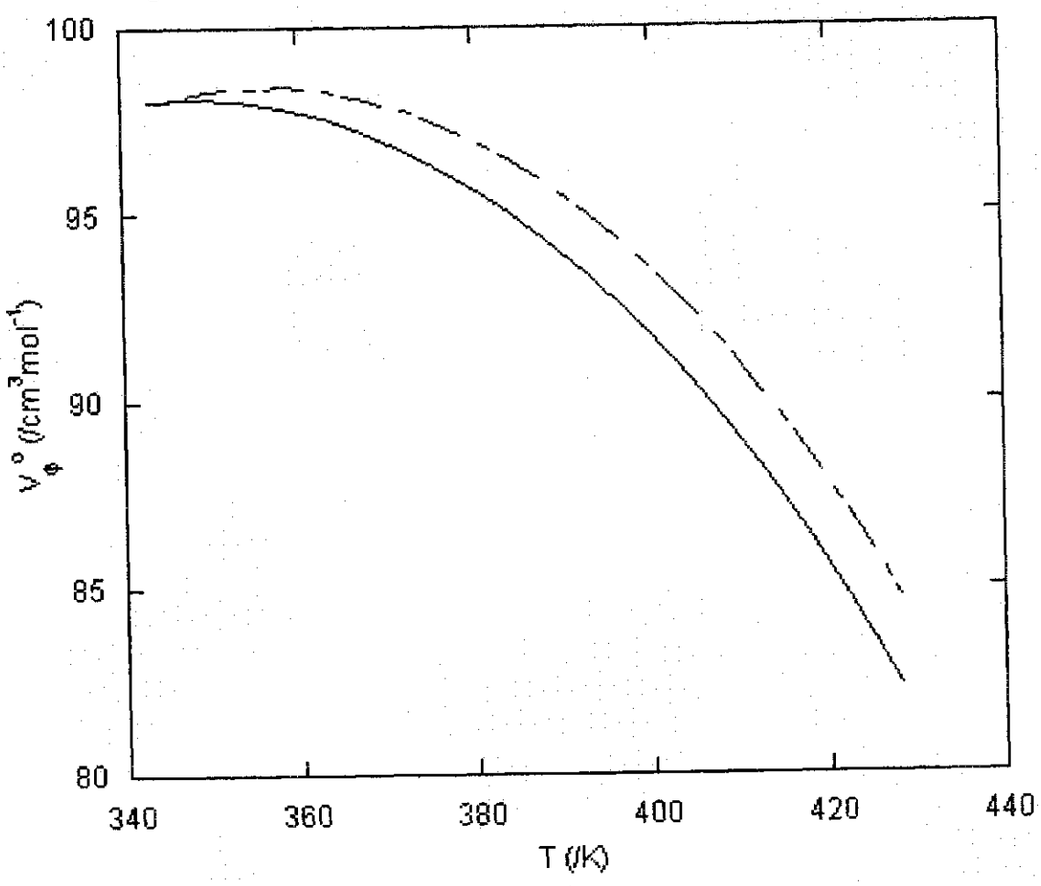

Figure 6.12 Temperature dependence of apparent molar volume at infinite dilution of $Yb(ClO_4)_3$ at pressure p = 20 MPa.

Shock and Helgeson (- - - - - -), values reported in this chapter (_____).

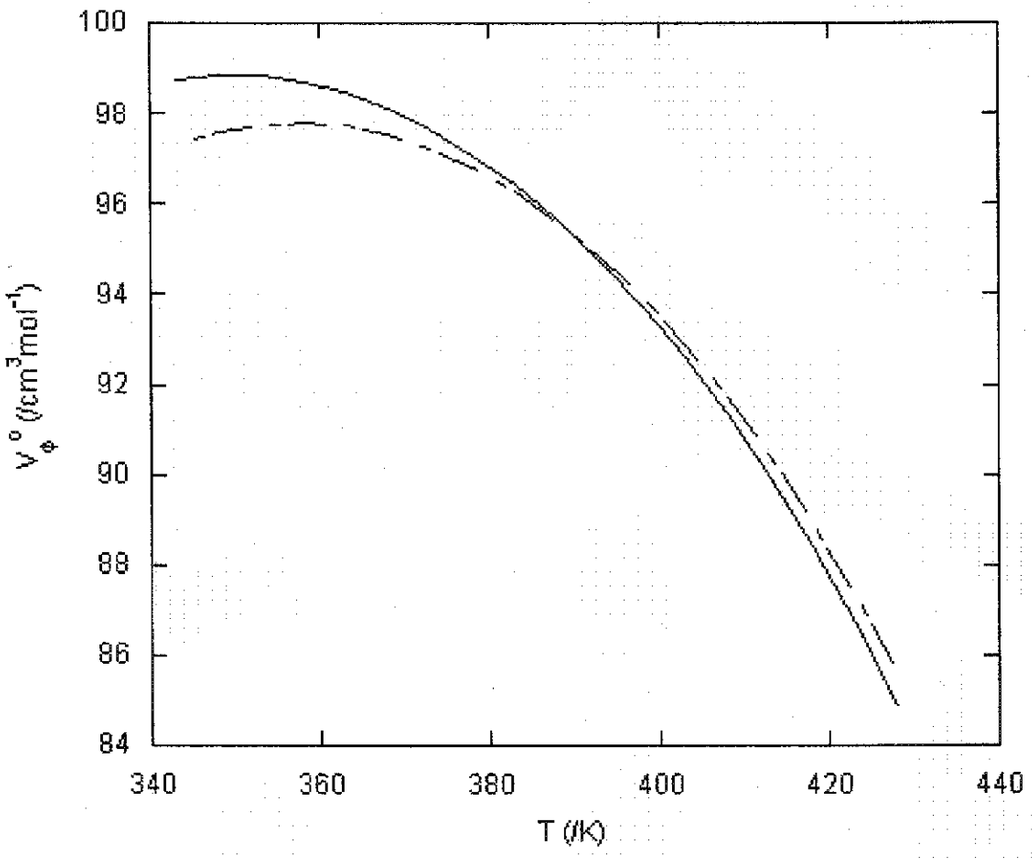

Figure 6.13 Temperature dependence of apparent molar volume at infinite dilution of $Yb(ClO_4)_3$ at pressure p = 30 MPa.

Shock and Helgeson (- - - - - - - -), values reported in this chapter (_____).

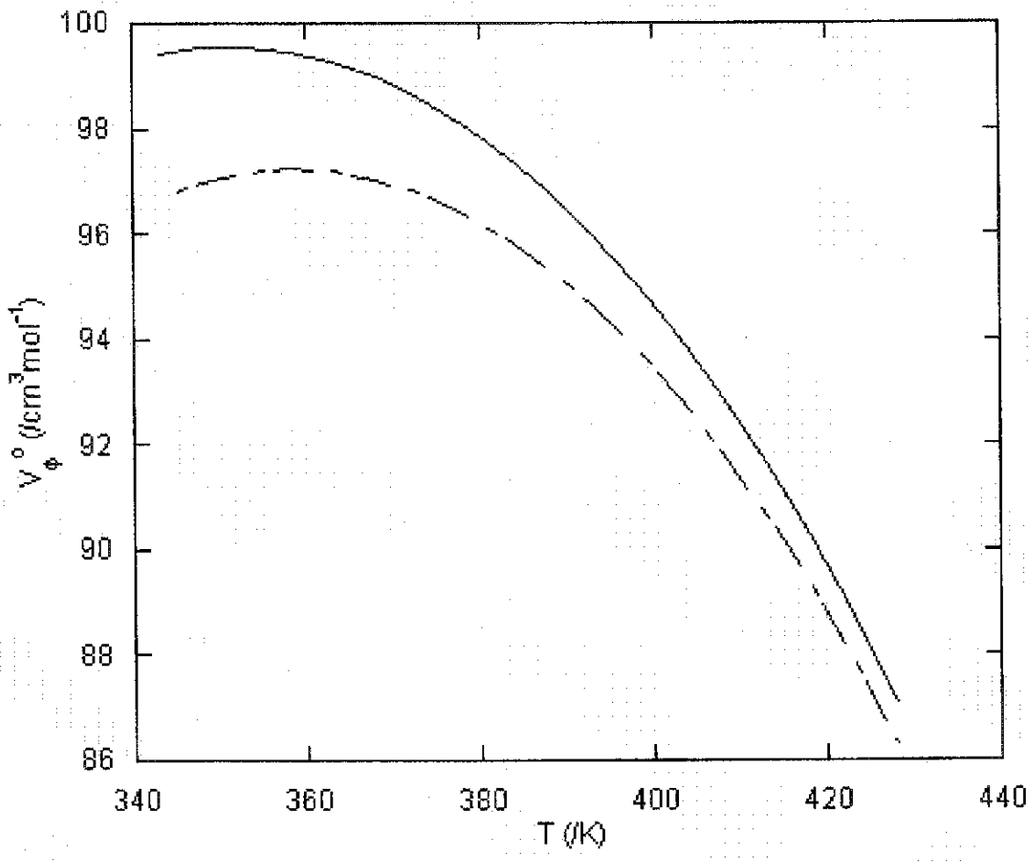

Shock and Helgeson and those presented in this chapter do not exceed 5 cm^3 mol^{-1} and for most temperature and pressure conditions, the difference between the two values is much smaller.

6.5 Conclusions

The greatest difficulty associated with measurement of apparent molar volumes of acidified solutions of trivalent metal salts at elevated temperatures and pressures is producing volumetric data for solutions of pure perchloric acid at elevated temperatures and pressures. Corrosion by perchloric acid of the stainless steel tubing in the high temperature and pressure densimeter caused many serious leaks. The presence of trace metal perchlorates in the high temperature and pressure densimeter during measurement of aqueous perchloric acid is the most obvious cause of the relatively high uncertainty of the apparent molar volume values. The low concentration of perchloric in relation to the concentration of ytterbium perchlorate results in a correction term which has a much smaller uncertainty that the uncertainty in the property of the ytterbium perchlorate itself.

Despite these difficulties, two models have been presented in this chapter, one modeling the concentration, temperature and pressure dependences of the apparent molar volumes of $Yb(ClO_4)_3(aq)$ over a larger temperature and pressure surface than investigated previously. The second model reported the concentration, temperature and pressure dependences of perchloric acid over the same temperature and pressure surface and is instrumental in the modeling of not only $Yb(ClO_4)_3(aq)$ but of any further trivalent metal perchlorate at elevated temperatures and pressures.

References:

Archer D.G. (1992) Thermodynamic properties of the sodium chloride + water system. II. Thermodynamic properties of NaCl(aq), NaCl2H2O(cr), and phase equilibria. *J. Phys. Chem. Ref. Data* **21**, 793-829.

Archer D.G. and Wang P. (1990) The Dielectric Constant of Water and Debye-Hückel Limiting Law Slopes. *J. Phys. Chem. Ref. Data* **19**, 371-411.

Babakulov, N.; Latysheva, V.A. (1974) Heat Capacities of Aqueous Solutions of Group III Metal Perchlorates. *Russ. J. Phys. Chem.*, **48**, 587-589.

Ballerat-Busserolles, K.; Ford, T.D.; Call, T.G.; Woolley, E.M. (1999) Apparent molar volumes and heat capacities of aqueous acetic acid and sodium acetate at temperatures from T=278.15 K to T = 393.15 K at the pressure 0.3_5 MPa. *J. Chem. Thermodynamics*, **31**, 741-762

Criss, C.M.; Millero, F.J. (1999) Modeling Heat Capacities of High Valence-Type Electrolyte Solutions with Pitzer's Equations. *J. Solution Chem.* **28**, 849-864

Debye, P. and Hückel, E. (1923) The theory of electrolytes. I. Lowering the freezing point and related phenomena. *Physik. Z.* **24**, 185-206.

Debye, P. and Hückel, E. (1924) Remarks on a theorem on the cataphorical migration velocity of suspended particles. *Physik. Z.* **25**, 49-52.

Gildseth, W.M.; Habenschuss, A.; Spedding, F.A. (1975). Densities and Thermal Expansion of Some Aqueous Rare Earth Chloride Solutions Between 5° and 80°C. I. $LaCl_3$, $PrCl_3$, and $NdCl_3$ *J. Chem. Eng. Data*, **20**, 292-309

Habenschuss, A.; Spedding, F.A. (1976) Densities and Thermal Expansion of Some Aqueous Rare Earth Chloride Solutions Between 5° and 80°C. II. $SmCl_3$, $GdCl_3$, $DyCl_3$, $ErCl_3$, and $YbCl_3$. *J. Chem. Eng. Data*, **21**, 95-113

Helgeson, H.C. and Kirkham, D.H. (1976) Theoretical prediction of the thermodynamic properties of aqueous electrolytes at high pressures and temperatures: III. Equation of state for aqueous species at infinite dilution. *Am. J. Sci.* **276**, 97-240

Helgeson, H.C., Kirkham, D.H. and Flowers, G.C. (1981) Theoretical prediction of the thermodynamic properties of aqueous electrolytes at high pressures and temperatures: IV. Calculation of activity coefficients, osmotic coefficients and apparent molal and standard and relative partial molal properties to 600oC and 5kb. *Am. J. Sci.* **281**, 1249-1275.

Hovey, J.K. (1988) *Thermodynamics of aqueous solutions*. Ph.D. Thesis, The University of Alberta, Edmonton, Alberta, Canada.

Johnson, J.W. and Norton, D. (1991) Critical phenomena in hydrothermal systems: State, thermodynamic, electrostatic, and transport properties of H_2O in the critical region. *Am. J. Sci.* **291**, 541-648

Karapet'yants, M.Kh.; Vasilev, V.A.; Novikov, S.N. (1976) The Heat Capacities and Densities of Aqueous Yttrium (III) Chloride Solutions at 25°C. *Russian Journal of Phys. Chem.* **50**, 622-623

Kawa, M; Frechet, J.M.J., (1998) Self-Assembled Lanthanide-Cored Dendrimer Complexes: Enhancement of the Luminecsence Properties of Lanthanide Ions through Site-Isolation and Antenna Effects, *Chem. Mater.*, **10**, 286-296

Kell, G.S. (1967) Precise Representation of Volume Properties of Water at One Atmosphere. *J. Chem. Eng. Data.* 12, 66-69.

Pitzer, K.S. and Brewer, L. (1961) Revised edition of Termodynamics by G.N. Lewis and M. Randall, 2nd ed. McGraw-Hill, New York.

Marriott, R.A.; Hakin, A.W.; Rard, J.A. (2001) Apparent molar heat capacities and apparent molar volumes of $Y_2(SO_4)_3$(aq), $La_2(SO_4)_3$(aq), $Pr_2(SO_4)_3$(aq), $Nd_2(SO_4)3$(aq), $Eu_2(SO_4)_3$(aq), $Dy_2(SO_4)_3$(aq), $Ho_2(SO_4)_3$(aq) and $Lu_2(SO_4)_3$(aq) at T = 298.15K and p = 0.1 MPa, *J. Chem. Thermodynamics*, **33**, 643-687.

Nesterenko, P.N. and Jones P. (1997) First isocratic separation of fourteen lanthanides and yttrium by high-performance chelation ion chromatography, *Anal. Commun.*, **34**, 7-8

Pitzer, K.S. ed. (1991) Activity Coefficients in Electrolyte Solutions, Vol. 2, CRC Press, Boca Raton.

Pitzer, K.S.; Peterson, J.R.; Silvester, L.F. (1978) Thermodynamics of Electrolytes. IX. Rare Earth Chlorides, Nitrates, and Perchlorates. *J. Solution Chemistry*, **7**, 45-56

Robinson, R.A. and Stokes, R.H. (1959) Electrolyte Solutions. Butterworths, London

Sabot, J.-L.; Maestro, P. (1995) *Kirk-Othmer Encyclopedia of Chemical Technology: 4th edition, Vol. 14* Howe-Grant, M.: editor. Wiley-Interscience: New York.

Serway, R.A. (1996) Physics for Scientists and Engineers, Fourth Edition, Saunders College Publishing, Philadelphia.

Sharygin, A.V.; Wood, R.H. (1997) Volumes and heat capacities of aqueous solutions of hydrochloric acid at temperatures from 298.15 K to 623 K and pressures to 28 MPa. *J. Chem. Thermodynamics*, **29**, 125-148

Shock E.L.; Helgeson, H.C. (1988) Calculation of the thermodynamic and transport properties of aqueous species at high pressures and temperatures: Correlation algorithms for ionic species and equation of state predictions to 5kb and 1000°C. *Geochimica et Cosmochimica Acta,* , **52**, 2009-2036.

Simonson J.M., Oakes C.S., and Bodnar R.J. (1994) Densities of NaCl(aq) to the temperature 523 K at pressures to 40 MPa measured with a new vibrating-tube densitometer. *J. Chem. Thermodynamics* **26**, 345-359.

Skoog, D.A.; West, D.M.; Holler, F.J.;Crouch, S.R. (2000) In *Analytical Chemistry: An Introduction: 7th Edition*, Sunders College Publishing, Harcourt Inc., 742.

Spedding, F.H.; Baker, J.L.; Walters, J.P. (1979) Apparent and Partial Molal Heat Capacities of Aqueous Rare Earth Nitrate Solutions at 25°C. *J. Chem. Eng. Data*, **24**, 298-305

Spedding, F.H.; Shiers, L.E.; Brown, M.A.; Derer, J.L.; Swanson, D.L.; Habenschuss, A. (1975e) Densities and Apparent Molal Volumes of Some Aqueous Rare Earth Solutions at 25oC. II. Rare Earth Perchlorates. *J. Chem. Eng. Data* **20**, 81-88.

Spedding, F.H.; Baker, J.L.; Walters, J.P. (1975d) Apparent and Partial Molal Heat Capacities of Aqueous Rare Earth Perchlorate Solutions. *J. Chem. Eng. Data*, **20**, 189-195

Spedding, F.H.; Baker, J.L.; Walters, J.P. J. (1975a) Apparent and Partial molar Heat Capacities of Aqueous Rare Earth Perchlorate Solutions at 25°C. *Chem. Eng. Data*, **20**, 199-195.

Spedding, F.H.; Jones K.C. (1966a) Heat Capacities of Aqueous Rare Earth Chloride Solutions at 25°. *J. Phys. Chem.*, **70**, 2450-2455

Spedding, F.H.; Pikal, M.J.; Ayers, B.O. (1966b) Apparent Molal Volumes of Some Aqueous Rare Earth Chloride and Nitrate Solutions at 25°. *J. Phys. Chem.*, **70**, 2440-2449

Spedding, F.H.; Saeger, V.W.; Gray, K.A.; Boneau, P.K.; Brown, M.A.; DeKock, C.W.; Baker, J.L.; Shiers, L.E.; Weber, H.O.; Habenschuss, A. (1975b). Densities and Apparent Molal Volumes of Some Aqueous Rare Earth Solutions at 25oC. I. Rare Earth Chlorides *J. Chem. Eng. Data*, **20**, 72-81

Spedding, F.H.; Walters, J.P.; Baker, J.L. (1975c) Apparent and Partial Molal Heat Capacities of Some Aqueous Rare Earth Chloride Solutions at 25oC *J. Chem. Eng. Data*, **20**, 438-443

Stimson, H.F. (1955) Heat Units and Temperature Scales for Calorimetry. *Am. J. Phys.* **23**, 614-622.

Tanger, J.C. and Helgeson, H.C.(1988), Calculation of the thermodynamics and transport properties of aqueous species at high pressures and temperatures. Revised equations of state for the standard partial molar properties of ions and electrolytes. *Am. J. Sci.* **288**, 19-98

Tremaine, P.R.; Sway, K.; Barbero J.A. (1986) The apparent molar heat capacity of aqueous hydrochloric acid from 10°C to 140°C. *J. Solution Chem.*, **15**, 1-22

Wood, S.A. (1990a) The aqueous geochemistry of the rare-earth elements and yttrium. 1. Review of the available low-temperature data for inorganic complexes and the inorganic REE speciation of natural waters. *Chemical Geology*, **82**, 159-186

Wood, S.A. (1990b) The aqueous geochemistry of the rare-earth elements and yttrium. 2. Theoretical predictions of speciation in hydrothermal solutions to 350°C at saturation water vapor pressure. *Chemical Geology*, **88**, 99-125

Xaio, C.; Tremaine, P.R. (1996) Apparent molar heat capacities and volumes of $LaCl_3(aq)$, $La(ClO_4)_3(aq)$, and $Gd(ClO_4)_3(aq)$ between the temperatures 283 K and 338 K *J. Chem. Thermodynamics*, **28**, 43-66

Xaio, C.; Tremaine, P.R. (1997) The thermodynamics of aqueous trivalent rare earth elements. Apparent molar heat capacities and volumes of $Nd(ClO_4)_{3(aq)}$, $Eu(ClO_4)_{3(aq)}$, $Er(ClO_4)_{3(aq)}$, and $Yb(ClO_4)_{3(aq)}$ from the temperatures 283 K to 328 K. *J. Chem. Thermodynamics*, **29**, 827-852.